Generalizations of Threshold Graph Dynamical Systems

Christopher James Kuhlman

Thesis submitted to the Faculty of the
Virginia Polytechnic Institute and State University
in partial fulfillment of the requirements for the degree of

Master of Science
in
Mathematics

Henning S. Mortveit, Chair
Jeffrey T. Borggaard
William J. Floyd

May 2, 2013
Blacksburg, Virginia

Keywords: Social Behavior, Contagion Processes, Graph Dynamical Systems,
Network Dynamics

Generalizations of Threshold Graph Dynamical Systems

Christopher James Kuhlman

(ABSTRACT)

Dynamics of social processes in populations, such as the spread of emotions, influence, language, mass movements, and warfare (often referred to individually and collectively as contagions), are increasingly studied because of their social, political, and economic impacts. Discrete dynamical systems (discrete in time and discrete in agent states) are often used to quantify contagion propagation in populations that are cast as graphs, where vertices represent agents and edges represent agent interactions. We refer to such formulations as graph dynamical systems. For social applications, threshold models are used extensively for agent state transition rules (i.e., for vertex functions). In its simplest form, each agent can be in one of two states (state 0 (1) means that an agent does not (does) possess a contagion), and an agent contracts a contagion if at least a threshold number of its distance-1 neighbors already possess it. The transition to state 0 is not permitted. In this study, we extend threshold models in three ways. First, we allow transitions to states 0 and 1, and we study the long-term dynamics of these bithreshold systems, wherein there are two distinct thresholds for each vertex; one governing each of the transitions to states 0 and 1. Second, we extend the model from a binary vertex state set to an arbitrary number r of states, and allow transitions between every pair of states. Third, we analyze a recent hierarchical model from the literature where inputs to vertex functions take into account subgraphs induced on the distance-1 neighbors of a vertex. We state, prove, and analyze conditions characterizing long-term dynamics of all of these models.

Acknowledgments

I thank the professors on my committee for their time, consideration, and suggestions. In particular, Professor Henning S. Mortveit, my committee chair, spent much time with me and I thank him for his patience and guidance. He helped me a lot.

I thank several professors from whom a learned a great deal in the classroom, teachers in the noblest sense of the word: Jeffrey T. Borggaard, Leslie Kay, and Henning S. Mortveit (Virginia Tech); Chao-Kun Cheng and William J. Terrell (Virginia Commonwealth University); and Donald E. Carlson, John P. D'Angelo, and E. Graham Evans Jr. (University of Illinois–Urbana). While all of these professors helped me beyond the classroom, I gratefully note that Professor Leslie Kay spent an inordinate number of hours patiently and kindly helping me with her class.

I thank Professor S. S. Ravi, University at Albany–SUNY, for teaching me the importance of theory and guiding me in Computer Science. I thank my Computer Science advisor, Professor Madhav V. Marathe, for the same and for supporting this path of study, even though it took away from other work.

I thank Mr. Donald Weed and Ms. Patty Soriano for their friendship.

I thank my parents and my wife's parents for giving my kids, Nora Claire and Finnegan Thomas, the love and attention which otherwise would have been lacking. I thank Nora and Finnegan for their patience and understanding. I thank my siblings Kathy, Mark, and Karen for their encouragement and interest.

I thank my wife Helen Renee for her help, encouragement, and patience in this process. In addition to helping me, she gave of herself, and then some, to see that our kids did not go without.

Contents

List of Figures

Chapter 1

Introduction

A *contagion* is any entity or phenomenon that can be transmitted through a population. Examples of contagions for human populations are information [47], disease [37], and influence [34]. Our motivations come from the social sciences, where contagion processes include participation in mass movements [17], civil unrest [22], and revolutions [1]; the spread of warfare [10, 23]; language evolution [49]; rumor spread [40]; and technology adoption [14]. However, many other fields such as biology [38], ecology [12], and economics [20] make use of contagion processes. A recent survey is [72].

Contagion dynamics are studied because of their potential social, political, and economic impacts. The 1992 Los Angeles riots are estimated to have caused $1 billion in damage, 54 deaths, and many injuries [75]. Bragg [9] argues that the English language survived the incursion of Latin because the Black Death of 1348-1350 disproportionately hit urban centers and monestaries, the source of Latin's usage. He states, "Though the Black Death was a catastrophe, it set in train a series of social upheavals which would speed the English language along the road to full restoration as the recognized language of the natives." Events such as the 2011 Arab Spring can lead to significant widespread change [1, 76].

There is ample evidence for contagion processes. Schelling [64] mentions mundane applications of contagion processes, such as individuals following a leader who crosses a street against a traffic light. Health workers, in multiple studies (e.g., [48,65]), have infused safety procedures into communities of drug users, through opinion leaders who then pass on the information, to reduce overdoses or the spread of HIV. These intervention approaches are demonstrated to be effective. Emotions are known to

propagate among individuals [33]. Financial crises across countries can be explained in terms of contagion processes [53]. The 2011 protests in Spain, due to austerity measures, have been explained in terms of contagion processes [30], as has the process of joining Facebook [71] and viral marketing [47].

The basic setup for our studies is illustrated in Figure 1.1. There is a collection of agents (green means the agent possesses the contagion; red means it does not) whose interactions are indicated by dashed lines. Thus, for example, the green agent at the upper left does not directly interact with the red one at the lower right. Through these interactions, contagions are transmitted. Hence, the agent in green can only pass the contagion to its two distance-1 neighbors. The contagion dynamics process is discrete in time and discrete in the finite number of states which an agent may occupy. Each agent is assigned a function that describes its behavior, where, in many formulations, the inputs to the function are the state of the agent and those of its distance-1 neighbors. It is by altering the functions that the discrete dynamical system is specialized for a particular application. Throughout this work, we take the functions to be deterministic.

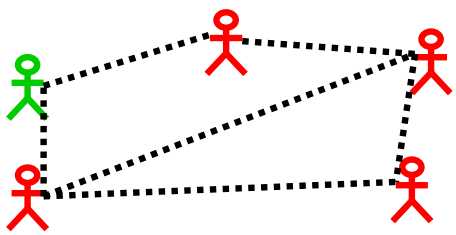

Figure 1.1: A five-agent system where pairwise interactions are indicated by dashed lines. The green (red) color of an agent indicates that it possesses (does not possess) the contagion.

Overwhelmingly in the social sciences context (e.g., [14,31,64]), and to an appreciable extent in the data mining literature (e.g., [15,41]), agents may be in one of two states: state 0 (red state) means that an agent does not possess a contagion and state 1 (green state) means that an agent does possess the contagion. Moreover, it is very often the case that a single transition, from state 0 to state 1, is permitted. These are called *progressive* systems [41]. This sole transition models incipient behavior, such as the

choice to join a mob action [31]. An example of dynamics in a 7-agent system, where an agent contracts a contagion if at least two of its neighbors possess it, is given in Figure 1.2. This is referred to as a *threshold* model, where, here, threshold $k = 2$. In this example, at each time, all agents execute their functions and update their states in parallel; this is the *parallel* update model. (Another option is for the agents to update their states in a predefined sequence, the *sequential* update method.) With three agents initially in state 1, six agents possess it by time $t = 3$, at which time no further transitions are possible. For the given initial system state (i.e., the sequence of vertex states at $t = 0$) and parallel update scheme, the limit cycle is a fixed point. Our goal here is to understand *all* state transitions, and therefore all limit cycles, for a given graph, vertex state set, set of vertex functions, and update scheme. In this Introduction, we are using terms informally to capture some basic ideas; all terms are defined formally in later chapters.

Another variant of the basic threshold model is a two vertex state set, as above, but now both transitions $0 \to 1$ and $1 \to 0$ are permitted. A vertex in state 0 transitions to state 1 as described above, for a given threshold k. A vertex in state 1 transitions to 0 if the number of neighbors in state 1, plus one (for the vertex itself), is strictly less than k.

Our work focuses on three generalizations of the basic threshold model. First, we introduce and study a *bithreshold* contagion dynamics model where vertices can transition back-and-forth between states 0 and 1, and there are separate thresholds for the transitions $0 \to 1$ (up-threshold) and $1 \to 0$ (down-threshold). Second, we investigate a new *multithreshold* contagion model in which there are r states (0 through $r - 1$), and each transition $i \to j$ between two states $i, j \in \{0, 1, \ldots, r - 1\}$ is characterized by a corresponding threshold. Finally, we study a recent *hierarchical* model from the literature that introduces hierarchical structural dependencies among interacting agents, beyond distance-1 neighborhoods as used in Figure 1.2. Our main findings for each topic are summarized next.

Bithreshold model. We show that for parallel systems, the only permissible limit cycles are fixed points and 2-cycles, irrespective of threshold values. These results coincide with the classical case described above where a single threshold controls both transitions ($0 \to 1$ and $1 \to 0$). For sequential systems, the behavior is quite different. If the difference between the down- and up-thresholds is less than two, then limit cycles may only be fixed points. However, if the difference is two or more, then longer limit cycles are possible. Hence, the threshold difference of 2 is a bifurcation point, where a transition may occur from fixed point limit sets to limit sets with arbitrarily long cycles. We prove that graph dynamical systems (GDSs) exist that

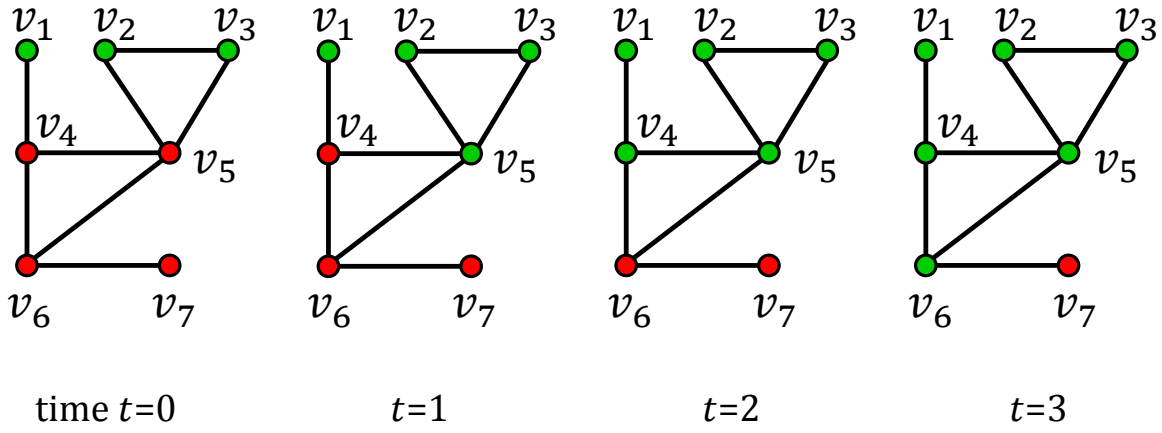

Figure 1.2: Discrete dynamics of contagion spread through a 7-agent system. Each agent transitions from state 0 (red) to state 1 (green) when at least a threshold $k = 2$ number of its neighbors possess the contagion. The sole permissible state transition is $0 \to 1$. The initial system state consists of three agents with a contagion. The dynamics halt after $t = 3$, producing a fixed point limit cycle.

exhibit these behaviors. To our knowledge, this bifurcation phenomenon is another novel aspect of this work.

Multithreshold model. The multithreshold model is a generalization of the bithreshold model. We provide constructive proofs of sufficient conditions for which the only limit cycles are fixed points, for any value of r, the sequential update scheme, and different classes of state transitions. We provide a procedure for determining these conditions in the general case. We use the case $r = 3$ and two classes of state transitions to show that the boundary conditions for fixed points can be tight; i.e., if any one condition of the set is violated, then arbitrarily long limit cycles can be generated. In this sense, as above, a bifurcation phenomenon is proven. Moreover, we recover well-known fixed point conditions for restrictions of our results.

Hierarchical model. We introduce a hierarchical dynamics model based on a recent model of the behavior of individuals joining Facebook [71]. The Facebook model was generated by mining online social network data. We generalize the experimentally-determined model, and show that the more general hierarchical model produces maps that are equal when switching two consecutive vertices in two otherwise identical permutations, if the two vertices do not form an edge in a graph X. This behavior is also found in standard or classic dynamics models. We identify the absence of triangles in a graph X as a sufficient condition to ensure that a hierarchical model and its corresponding classical model are equal. We also demonstrate a property of Nor models that holds for hierarchical and classic models. Finally, we present the conditions under which a Boolean sequential hierarchical model map will generate only fixed points as limit sets. This work is ongoing.

We developed a computational framework to analyze GDSs and we used this software to analyze all of the GDSs of this study. It will be reported on in future work.

While our results are useful in their own right, they are also useful for verification and validation (V&V) and simulation of population dynamics. Verification is the process of ensuring that a model is implemented correctly. Validation is the comparison of model output to known or measured system behavior to confirm that the two are sufficiently close, based on some predefined criterion. For example, our parallel bithreshold results can be used to verify that simulation results contain only fixed points and 2-cycles as limit cycles. We have indeed made these and other comparisons in simulation studies as parts of other works.

From a simulation standpoint, theory and modeling complement each other. An impact of theory on modeling was just described. Simulation can also augment

theory, for while it has been proved that parallel update may produce limits cycles of maximum length two, it does not provide the limit cycles themselves. For many practical problems, it is important to determine the character of limit cycles, often on very large graphs (e.g., those with tens or hundreds of millions of vertices). For example, in a 2-cycle, and in the context of modeling a revolution, it is meaningful as to whether a population oscillates between 20% and 30% of the agents rebelling, or between 80% and 90%, or between 10% and 90%.

Thesis organization. Chapter 2 contains our bithreshold work. Chapter 3 describes our multithreshold study. Our hierarchical model is presented in Chapter 4. We conclude in Chapter 5.

Author contributions. For Chapter 2, the author contributed five propositions. Chapters 3 and 4 were produced by student and advisor.

Chapter 2

Bithreshold Systems

2.1 Introduction

A standard Boolean *threshold function* $\boldsymbol{t}_{k,m}\colon \{0,1\}^m \longrightarrow \{0,1\}$ is defined by

$$\boldsymbol{t}_{k,m}(x_1,\ldots,x_m) = \begin{cases} 1, & \text{if } \sigma(x_1,\ldots,x_m) \geq k \quad \text{and} \\ 0, & \text{otherwise,} \end{cases} \tag{2.1}$$

where $\sigma(x_1,\ldots,x_m) = \big|\{1 \leq i \leq m \mid x_i = 1\}\big|$. This class of functions is a common choice in modeling biological systems [38, 39], and social behaviors (e.g., joining a strike or revolt, adopting a new technology or contraceptives, spread of rumors and stress, and collective action), see, e.g., [11, 14, 31, 41, 52, 74].

A *bithreshold function* is a function $\boldsymbol{t}_{i,k^\uparrow,k_\downarrow,m}\colon \{0,1\}^m \longrightarrow \{0,1\}$ defined by

$$\boldsymbol{t}_{i,k^\uparrow,k_\downarrow,m}(x_1,\ldots,x_m) = \begin{cases} \boldsymbol{t}_{k^\uparrow,m}, & \text{if } x_i = 0, \\ \boldsymbol{t}_{k_\downarrow,m}, & \text{if } x_i = 1\ . \end{cases} \tag{2.2}$$

Here i denotes a designated argument – later it will be the vertex or cell index. We call $k^\uparrow$ the *up-threshold* and $k_\downarrow$ the *down-threshold*. When $k^\uparrow = k_\downarrow$ the bithreshold function coincides with a standard threshold function. Note that unlike the standard threshold function in (2.1) which is symmetric, the bithreshold function is *quasi-symmetric* (or outer-symmetric) – with the exception of index i, it only depends on its arguments through their sum.

In this paper we consider synchronous and asynchronous *graph dynamical systems* (GDSs), see [51, 58], of the form $\mathbf{F}\colon \{0,1\}^n \longrightarrow \{0,1\}^n$ induced by bithreshold functions. These are natural extensions of threshold GDSs and capture threshold phenomena exhibiting hysteresis properties. Bithreshold systems are also prevalent in social systems where each individual can change back-and-forth between two states; Schelling states: "Numerous social phenomena display cyclic behavior ...", see [64, p. 86]. Among his examples is whether pick-up volleyball games will continue through an academic semester or die (e.g., individuals regularly choosing to play or not play). One can also look at public health concerns such as obesity, where an individual's back-and-forth decisions to diet or not—which are peer influenced [16], and therefore can be at least partially described by thresholds—are so commonplace that it has a name: "yo-yo dieting" [3]. When $k^{\uparrow} > k_{\downarrow}$, a vertex that transitions from state 0 to state 1 is more likely to remain in state 1 than what would be the case in a standard threshold GDS. For the state transitions from 1 to 0 the situation is analogous. This suggests that the cost to change back to state 0 is great or that a change to state 0 will occur only if the conditions that gave rise to the $0 \to 1$ transition significantly diminish. A company that acquires and later divests itself of a competitor is such an example. Examples where $k_{\downarrow} \geq k^{\uparrow}$ are commonplace. For example, [64] states that he often witnesses people who start to cross the street against traffic lights, but will return to the curb if they observe an insufficient number of others following behind. Overshooting, whereby a group of individuals take some action, and within a short time period, a subset of these pull back from it, is also of interest to the sociology community [7] and is characterized by $k_{\downarrow} \geq k^{\uparrow}$.

It is convenient to introduce the quantity $\Delta = k_{\downarrow} - k^{\uparrow}$. The first of our main results (Theorem 2) characterizes limit cycle structure of synchronous bithreshold GDS (also known as as Boolean networks). Building on the proof for threshold functions in [26], we prove that only fixed points and periodic orbits of length 2 can occur for each possible combination of $k^{\uparrow}$ and $k_{\downarrow}$. Since we re-use parts of their proof, and also since their proof only appears in French, a condensed English translation is included in the appendix on page 25. The situation is very different for asynchronous bithreshold GDSs where a vertex permutation is used for the update sequence. Our second main result states that when $\Delta < 2$, only fixed points can occur as limit cycles. However, for $\Delta \geq 2$ there are graphs for which arbitrary length periodic orbits can be generated. The case $\Delta = 2$ is identified using a potential function argument and represents a (2-parameter) *bifurcation* in a discrete system, a phenomenon that to our knowledge is novel. We also include a series of results for bithreshold dynamics on special graph classes. These offer examples of asynchronous bithreshold GDSs with long periodic orbits, and may also serve as building blocks in construction and

modeling of bithreshold systems with given cycle structures.

Organization. We introduce necessary definitions and terminology for graph dynamical systems in Section 2.2. The two main theorems are presented in Section 2.3. Our collection of results on dynamics for graph classes like trees and cycle graphs follow in Section 2.4 before we conclude in Section 2.5. Section 2.6 contains an appendix for this chapter.

2.2 Background and Terminology

In the following we let X denote an undirected graph with vertex set $\mathrm{v}[X] = \{1, 2, \ldots, n\}$ and edge set $\mathrm{e}[X]$. To each vertex v we assign a state $x_v \in K = \{0, 1\}$ and refer to this as the *vertex state*. Next, we let $n[v]$ denote the sequence of vertices in the 1-neighborhood of v sorted in increasing order and write

$$x[v] = (x_{n[v](1)}, x_{n[v](2)}, \ldots, x_{n[v](d(v)+1)})$$

for the corresponding sequence of vertex states. Here $d(v)$ denotes the degree of v. We call $x = (x_1, x_2, \ldots, x_n)$ the *system state* and $x[v]$ the *restricted state*. The dynamics of vertex states is governed by a list of *vertex functions* $(f_v)_v$ where each $f_v \colon K^{d(v)+1} \longrightarrow K$ maps as

$$x_v(t+1) = f_v\big(x(t)[v]\big) \ .$$

In other words, the state of vertex v at time $t+1$ is given by f_v evaluated at the restricted state $x[v]$ at time t. An *update mechanism* governs how the list of vertex functions assemble to a *graph dynamical system* map (see e.g. [51, 58])

$$\mathbf{F} \colon K^n \longrightarrow K^n$$

sending the system state at time t to that at time $t+1$.

For the update mechanism we will here use *synchronous* and *asynchronous* schemes. In the former case we obtain Boolean networks where

$$\mathbf{F}(x_1, \ldots, x_n) = (f_1(x[1]), \ldots, f_n(x[n])) \ .$$

This sub-class of graph dynamical systems is sometimes referred to as *generalized cellular automata*. In the latter case we will consider permutation update sequences.

For this we first introduce the notion of *X-local functions*. Here the X-local function $F_v\colon K^n \longrightarrow K^n$ is given by

$$F_v(x_1, \ldots, x_n) = (x_1, x_2, \ldots, f_v(x[v]), \ldots, x_n) \ .$$

Using $\pi = (\pi_1, \ldots, \pi_n) \in S_X$ (the set of all permutations of $\mathrm{v}[X]$) as an update sequence, the corresponding asynchronous (or sequential) graph dynamical system map $\mathbf{F}_\pi\colon K^n \longrightarrow K^n$ is given by

$$\mathbf{F}_\pi = F_{\pi(n)} \circ F_{\pi(n-1)} \circ \cdots \circ F_{\pi(1)} \ . \tag{2.3}$$

We also refer to this class of asynchronous systems as (permutation) *sequential dynamical systems* (SDSs). The X-local functions are convenient when working with the asynchronous case. In this chapter we will consider graph dynamical systems induced by bithreshold functions, that is, systems where each vertex function is given as

$$f_v = f_{v,k^{\uparrow}{}_v,k_{\downarrow_v}} := \boldsymbol{t}_{v,k^{\uparrow}{}_v,k_{\downarrow_v},d(v)+1} \ .$$

The phase space of the GDS map $\mathbf{F}\colon K^n \longrightarrow K^n$ is the directed graph with vertex set K^n and edge set $\{\big(x, \mathbf{F}(x)\big) \mid x \in K^n\}$. A state x for which there exists a positive integer p such that $\mathbf{F}^p(x) = x$ is a *periodic point*, and the smallest such integer p is the *period* of x. If $p = 1$ we call x a *fixed point* for $\mathbf{F}$. A state that is not periodic is a *transient state*. Classically, the *omega-limit set* of x, denoted by $\omega(x)$, is the set of accumulation points of the sequence $\{\mathbf{F}^k(x)\}_{k\geq 0}$. In the finite case, the omega-limit set is the unique periodic orbit reached from x under $\mathbf{F}$.

Example 1. *To illustrate the above concepts, take $X = \mathrm{Circ}_4$ as the graph (shown in Figure 2.1), and choose thresholds $k^{\uparrow} = 1$ and $k_{\downarrow} = 3$. For the synchronous case we have for example $\mathbf{F}(1,0,0,1) = (0,1,1,0)$. Using the update sequence $\pi = (1,2,3,4)$ we obtain $\mathbf{F}_\pi(1,0,0,1) = (0,0,1,0)$. The phase spaces of $\mathbf{F}_\pi$ and $\mathbf{F}$ are shown in Figure 2.1. Notice that $\mathbf{F}_\pi$ has cycles of length 3, while the maximal cycle length of $\mathbf{F}$ is 2.*

We remark that graph dynamical systems generalize concepts such as cellular automata and Boolean networks, and can describe a wide range of distributed, nonlinear phenomena.

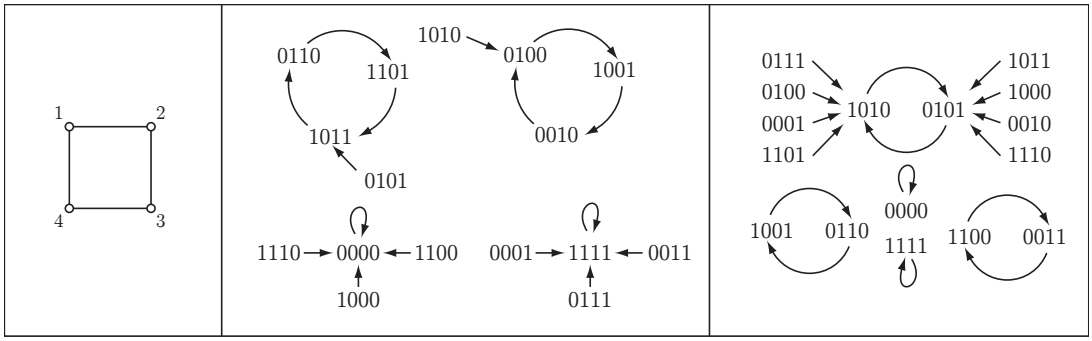

Figure 2.1: The graph $X = \mathrm{Circ}_4$ (left), and the phase spaces of $\mathbf{F}_\pi$ (middle) with $\pi = (1, 2, 3, 4)$ and $\mathbf{F}$ (right) for Example 1.

2.3 ω-Limit Set Structure of Bithreshold GDS

This section contains the two main results on dynamics of synchronous and asynchronous bithreshold GDSs.

2.3.1 Synchronous Bithreshold GDSs

Let $K = \{0, 1\}$ as before, let $A = (a_{ij})$ be a real-valued symmetric matrix, let $(k^{\uparrow}{}_i)_{i=1}^n$ and $(k_{\downarrow_i})_{i=1}^n$ be vertex-indexed sequences of up- and down-thresholds, and define the function $\mathbf{F} = (f_1, \ldots, f_n) \colon K^n \longrightarrow K^n$ by

$$f_i(x_1, \ldots, x_n) = \begin{cases} 1 & \text{if } x_i = 0 \text{ and } \sum_{j=1}^{n} a_{ij} x_j \geq k_i^{\uparrow} \\ 0 & \text{if } x_i = 1 \text{ and } \sum_{j=1}^{n} a_{ij} x_j < k_{\downarrow_i} \\ x_i & \text{otherwise.} \end{cases} \tag{2.4}$$

The following theorem is a generalization of Theorem 14 (see appendix) to the case of bithreshold functions.

Theorem 2. *If* $\mathbf{F}$ *is the synchronous GDS map over the complete graph of order* n *with vertex functions as in Equation* (2.4)*, then for all* $x \in K^n$*, there exists* $s \in \mathbb{N}$ *such that* $\mathbf{F}^{s+2}(x) = \mathbf{F}^s(x)$*.*

The proof builds on the arguments of the proof from [26] for standard threshold functions (see page 25 of the appendix). Note that we can use Lemma 15 in its orig-

inal form, but for Lemma 16 changes are needed to adapt for bithreshold functions. The position is marked [**Cross-reference for bithreshold systems**] in the proof of Lemma 16 on page 27. Before starting the proof of the theorem above, we first introduce the notion of *bands* and give a result on their structural properties. This is essential in the extension of the original result.

As in the proof of [26] in the appendix, let $z_i \in S$ and assume that $\gamma_i \geq 3$ (the period of the i^{th} component of z). We set

$$\operatorname{supp}(z_i) = \big\{l \in \{0, 1, 2, \ldots, T-1\} : z_l = 1\big\};$$

and use their partition $\mathcal{C} = \{C_0, C_1, C_2, \ldots, C_p\}$. By the assumption $\gamma_i \geq 3$, we are guaranteed that $p \geq 1$. The bithreshold functions require a more careful structural analysis of the elements of $\mathcal{C}$ than in the case of standard threshold functions. We say that $C \in \mathcal{C}$ is of *type ab* if $C = (l, l+2, l+4, \ldots, k)$ and $z_{l-1} = a$ and $z_{k+1} = b$ where all indices are modulo T. Here we write $m_{ab} = m_{ab}(\mathcal{C})$ for the number of elements of $\mathcal{C}$ of type ab.

We claim that $m_{01} = m_{10}$. Before we prove this, observe first that the sequence $\big(z_i(0), z_i(1), \ldots, z_i(T-1)\big)$ can be split into contiguous (modulo T) sub-sequences (*bands*) whose states contain only isolated 0s, where the end points have state 1, and where bands are separated by sub-sequences of lengths ≥ 2 whose state consist entirely of 0s. By the construction of $\mathcal{C}$, each element $C \in \mathcal{C}$ must be fully contained in a single band. Our claim above is now a direct consequence of the following lemma:

Lemma 3. *A band either (i) contains no element C of type* 01 *or* 10*, or (ii) contains precisely one element C of type* 01 *and precisely one element C' of type* 10*.*

Proof. Fix a band B and let $C \in \mathcal{C}$ be the partition containing the first element of B. There are now two possibilities. In the first case, C also contains the final element of B. Then C has type 00, and any other partition element contained in B is necessarily of type 11. In the second case, C terminates before the end of B. The configuration at the end of C must then be as

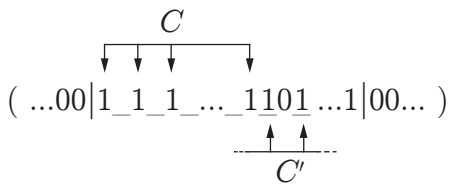

and C is of type 01. The element C' containing the index after the last element of C either goes all the way to the end of B, in which case it is of type 10, or it terminates before that, in which case the situation is as in the diagram above and C' is of type 11. By repeated application of this argument, the band B is eventually exhausted with an element C'' of type 10. All other elements of $\mathcal{C}$ within B not included in the sequence of partitions C, C' and so on, must be of type 11, and the proof is complete. □

Corollary 4. $m_{01}(\mathcal{C}) = m_{10}(\mathcal{C})$

(Theorem 2). **Claim:** If $\gamma_i \geq 3$ for $z_i \in S$ then $\sum_{j=1}^{n} L(z_i, z_j) < 0$.

We can write

$$\sum_{i=1}^{n} L(z_i, z_j) = \sum_{k=0}^{p} \Big(\sum_{j=1}^{n} a_{ij} \sum_{l \in C_k} \big(z_j(l+1) - z_j(l-1) \big) \Big) = \sum_{k=0}^{p} \Psi_{ik} \ ,$$

where

$$\Psi_{ik} = \sum_{j=1}^{n} a_{ij} \sum_{l \in C_k} \big(z_j(l+1) - z_j(l-1) \big) = \sum_{j=1}^{n} a_{ij} z_j(l_k + 2q_k + 1) - \sum_{j=1}^{n} a_{ij} z_j(l_k - 1) \ .$$

We need to consider Ψ_{ik} for the four types of partition elements. As in the original proof, note that $\Psi_{i0} = 0$.

$\underline{C_k \textbf{ is of type } 00\textbf{:}}$ in this case $z_i(l_k - 1) = 0$, $z_i(l_k) = 1$, $z_i(l_k + 2q_k + 1) = 0$ and $z_i(l_k + 2q_k + 2) = 0$, which is only possible if

$$\sum_{j=1}^{n} a_{ij} z_j(l_k - 1) \geq k_i^{\uparrow} \quad \text{and} \quad \sum_{j=1}^{n} a_{ij} z_j(l_k + 2q_k + 1) < k_i^{\uparrow} \ ,$$

which implies that $\Psi_{ik} < 0$.

$\underline{C_k \textbf{ is of type } 11\textbf{:}}$ this case is completely analogous to the 00 case, and again we conclude that $\Psi_{ik} < 0$.

$\underline{C_k \textbf{ is of type } 10\textbf{:}}$ here $z_i(l_k - 1) = 1$, $z_i(l_k) = 1$, $z_i(l_k + 2q_k + 1) = 0$ and $z_i(l_k + 2q_k + 2) = 0$. This implies that

$$\sum_{j=1} a_{ij} z_j(l_k - 1) \geq k_{\downarrow i} \quad \text{and} \quad \sum_{j=1} a_{ij} z_j(l_k + 2q_k + 1) < k_i^{\uparrow} \ ,$$

leading to $\Psi_{ik} < k^{\uparrow}{}_i - k_{\downarrow_i}$.

C_k **is of type** 01**:** this case is essentially the same as the 10 case, but here $\Psi_{ik} < k_{\downarrow_i} - k_i^{\uparrow}$.

Using the above four cases, we now have

$$\sum_{j=0}^{n} L(z_i, z_j) = \sum_{k=0}^{p} \Psi_{ik} < 0 + m_{00} \cdot 0 + m_{11} \cdot 0 + m_{10}(k^{\uparrow}{}_i - k_{\downarrow_i}) + m_{01}(k_{\downarrow_i} - k^{\uparrow}{}_i) = 0 \ ,$$

where the last equality follows by Corollary 4. Clearly, this leads to the same contradiction as in the proof of Theorem 14. □

An immediate consequence of Theorem 2 is the following:

Corollary 5. *A synchronous bithreshold GDS may only have fixed points and 2-cycles as limit sets.*

2.3.2 Asynchronous Bithreshold GDSs

Theorem 6. *Let X be a graph, let $\pi \in S_X$ and let $(f_v)_v$ be bithreshold functions all satisfying $\Delta(v) = k_{\downarrow_v} - k^{\uparrow}{}_v \leq 1$. The sequential dynamical system map $\mathbf{F}_\pi$ only has fixed points as limit sets.*

As before, the graph X is finite. Note also that the per-vertex thresholds $k^{\uparrow}$ and $k_{\downarrow}$ need not be uniform for the graph.

Proof. The proof uses a potential function based on a construction in [6], but see also [29]. For a given state $x \in K^n$ we assign to each vertex the potential

$$P(v, x) = \begin{cases} k_{\downarrow_v}, & x_v = 1 \\ d(v) + 2 - k_v^{\uparrow}, & x_v = 0 \ . \end{cases}$$

Note that the quantity $d(v) + 2 - k_v^{\uparrow}$ is the smallest number of vertex states in the local state $x[v]$ that must be zero to ensure that x_v remains in state zero. Similarly, an edge $e = \{v, v'\}$ is assigned the potential

$$P(e = \{v, v'\}, x) = \begin{cases} 1, & x_v \neq x_{v'} \\ 0, & x_v = x_{v'} \ . \end{cases}$$

For bookkeeping, we let $n_i = n_i(v; x)$ denote the number of vertices adjacent to v in state i for $i = 0, 1$ and note that $n_0 + n_1 = d$. The *system potential* $P(x)$ at the state x is the sum of all the vertex and all the edge potentials. For the theorem statement it is clearly sufficient to show that each application of a vertex function that leads to a change in a vertex state causes the system potential to drop.

Consider first the case where x_v is mapped from 0 to 1 which implies that $n_1 \geq k_v^{\uparrow}$. Since a change in system potential only occurs for vertex v and edges incident with v, we may disregard the other potentials when determining this change. Denoting the system potential before and after the update by P and P', we have $P = d+2-{k^{\uparrow}}_v+n_1$ and $P' = {k_{\downarrow}}_v + n_0$ which implies that

$$\begin{aligned} P' - P &= {k_{\downarrow}}_v + n_0 - d - 2 + {k^{\uparrow}}_v - n_1 = {k_{\downarrow}}_v + {k^{\uparrow}}_v - 2n_1 - 2 \\ &\leq -({k^{\uparrow}}_v - {k_{\downarrow}}_v) - 2 = \Delta(v) - 2 \ , \end{aligned}$$

and this is strictly negative whenever $\Delta = k_{\downarrow} - k^{\uparrow} \leq 1$. Similarly, for the transition where x_v maps from 1 to 0 one must have $n_1 + 1 \leq {k_{\downarrow}}_v - 1$ or $n_1 \leq {k_{\downarrow}}_v - 2$. In this case we have

$$\begin{aligned} P' - P &= [d + 2 - {k^{\uparrow}}_v + n_1] - [{k_{\downarrow}}_v + n_0] = 2n_1 + 2 - {k_{\downarrow}}_v - {k^{\uparrow}}_v \\ &\leq 2{k_{\downarrow}}_v - 4 + 2 - {k^{\uparrow}}_v - {k_{\downarrow}}_v = \Delta(v) - 2 \end{aligned}$$

as before, concluding the proof. □

2.3.3 Bifurcations in Asynchronous GDS

A natural question now is what happens in the case where $\Delta = k_{\downarrow} - k^{\uparrow} = 2$ since periodic orbits are no longer excluded by the arguments in the proof above. The following proposition shows that there are graphs and choices of $k^{\uparrow}$ and $k_{\downarrow}$, such that $\Delta = 2$, for which there are periodic orbits of arbitrary length.

Proposition 7. *The bithreshold GDS map over $X = \mathrm{Circ}_n$, with update sequence $\pi = (1, 2, 3, \ldots, n)$ and thresholds $k^{\uparrow} = 1$ and $k_{\downarrow} = 3$, has cycles of length $n - 1$.*

Proof. We claim that the state $x = (0, 0, \ldots, 0, 1, 0)$ is on an $(n-1)$-cycle. Straightforward computations give that the single 1-state is shifted one position to the left upon each application of $\mathbf{F}_{\pi}$ until the state $y = (0, 1, 0, \ldots, 0)$ is reached. The image of this state is $z = (1, 0, 0, \ldots, 0, 0, 1)$ which is easily seen to map to x. The smallest number of iterations required to return to the original state x is $n - 1$, producing a cycle as claimed. □

In other words, by taking Δ as a parameter, we see that the bithreshold sequential dynamical system undergoes a bifurcation at $\Delta = 2$.

2.4 Dynamics of Bithreshold GDSs

2.4.1 Graph Unions

From Proposition 7, we see that for $X = \mathrm{Circ}_n$ with threshold $k^{\uparrow} = 1$ and $k_{\downarrow} = 3$ at each vertex, we obtain an $(n-1)$-cycle for the update sequence $\pi = (1, 2, \ldots, n)$. The following proposition demonstrates how we can combine graphs to obtain larger cycle sizes for bithreshold SDSs with arbitrarily nonuniform $k^{\uparrow}, k_{\downarrow}$. In particular, the result applies to the case where we combine Circ_n graphs where $p = n - 1$ is prime.

Proposition 8. *For $i = 1, 2$ let X_i be a graph for which the bithreshold GDS with update sequence π_i has a cycle in phase space of length c_i. Let $u_i \in \mathrm{v}[X_i]$, and let X be the graph obtained as the disjoint union of X_1 and X_2 plus additionally the vertex $w \notin \mathrm{v}[X_1], \mathrm{v}[X_2]$ with the edges $\{u_1, w\}$ and $\{u_2, w\}$. Moreover, let all thresholds of vertices in X_1 and X_2 be as before, and assign threshold $k^{\uparrow} = 3$ to w. The bithreshold SDS map over X with update sequence $\pi = (\pi_1|\pi_2|w)$ [juxtaposition] has a cycle of length $\mathrm{lcm}(c_1, c_2)$.*

Proof. Let vertex w have $k^{\uparrow} = 3$, so that w will never transition to state 1 from state 0. Let $x = (x_1|x_2|x_w)$ be the state over X constructed from states x_1 and x_2 on the respective c_i-cycle over X_1 and X_2 with $x_w = 0$. The only vertices whose connectivity, and therefore induced vertex function, are affected by the addition of w are u_1 and u_2. But the state transitions for u_1 and u_2 are unaffected because each is predicated on $\sigma(x[u_1])$ and $\sigma(x[u_2])$, respectively, and these latter two quantities are not altered by the state of w because that state is fixed at 0 by construction. Hence, the phase space of X contains a cycle of length $\mathrm{lcm}(c_1, c_2)$ as claimed. □

Thus, for $k^{\uparrow} = 1$ and $k_{\downarrow} = 3$, there exists a circle graph and permutation π that will produce a cycle in phase space of length three or greater, and multiple circle graphs can be combined to produce graphs with large orbit cycles without modifying the thresholds of vertices in X_1 and X_2.

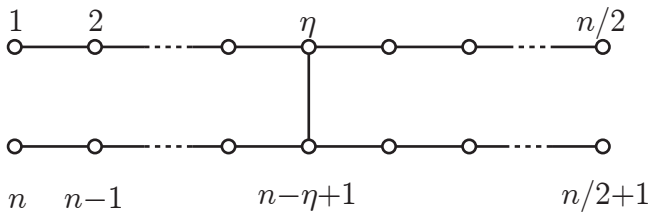

Figure 2.2: The tree H_n used in the proof of Proposition 9.

2.4.2 Trees

Propositions 7 and 8 show how periodic orbits of length > 2 arise over graphs that contain cycles. This section investigates bithreshold SDS maps where X is a tree.

To start, we first recall the notion of κ-equivalence of permutations from [50, 51]. Two permutations $\pi, \pi' \in S_X$ are *κ-equivalent* if the corresponding *induced acyclic orientations* O_π and $O_{\pi'}$ of X are related by a sequence of source-to-sink conversions. Here, the orientation O_π is obtained from π by orienting each edge $\{v, v'\} \in \mathrm{e}[X]$ as (v, v') if v precedes v' in π and as (v', v) otherwise. This is an equivalence relation, and it is shown in [51] that (i) for a tree the number of κ-equivalence classes is $\kappa(X) = 1$, and (ii) that $\mathbf{F}_\pi$ and $\mathbf{F}_{\pi'}$ have the same periodic orbit structure (up to digraph isomorphism/topological conjugation) whenever π and π' are κ-equivalent. As a result, *we only need to consider a single permutation update sequence* to study the possible periodic orbit structures of permutation SDS maps over a tree X.

The following result shows that there can be cycles of length 3 or greater for permutation SDS over a tree.

Proposition 9. *For any integer $c \geq 3$ there is a tree X on $n = 4c - 6$ vertices such that bithreshold permutation SDS maps over X with thresholds $k^{\uparrow} = 1$ and $k_{\downarrow} = 3$ have periodic orbits of length c.*

Proof. An H-tree on $n = 4\beta + 2$ vertices, denoted by H_n, has vertex set $\{1, 2, \ldots, n\}$ and edge set

$$\{\eta, n - \eta + 1\} \cup \left\{ \{i, i+1\}, n/2 + \{i, i+1\} \mid 1 \leq i \leq n/2 - 1 \right\},$$

where $\eta = \beta + 1$ and $\beta \geq 1$. The graph H_n is illustrated in Figure 2.2.

Set $\beta = c - 2$ so that $n = 4\beta + 2$ and $\eta = \beta + 1$. We take $X = H_n$ as the graph and assign thresholds $(k^{\uparrow}, k_{\downarrow}) = (1, 3)$ to all vertices. By the comment preceding Proposition 8, we may simply use $\pi = (1, 2, 3, \ldots, n)$ as the update sequence since all permutations give cycle equivalent maps $\mathbf{F}_{\pi}$.

For the initial configuration, set the state of each vertex v in the range $(n/2) + 1 \leq v \leq n - \eta + 1$ (bottom right branch) to 1 and set all other vertex states to 0 so that

$$x(0) = (0, 0, \ldots, 0, \underbrace{1, 1, \ldots, 1,}_{\text{start at vertex } (n/2)+1} 0, 0, \ldots 0) \, .$$

The number of vertices in a contiguous vertex range with state 1 will always be η; there may be one or two such groups in a system state. The image of $x(0)$ is

$$x(1) = (0, 0, \ldots, 0, \underbrace{1, 1, \ldots, 1,}_{\text{start at vertex } \eta} 0, 0, \ldots 0) \, ,$$

where now the first $\eta - 1$ vertices are in state 0, the next η vertices are in state 1, and the remaining vertices—all those along the bottom arm—are in state 0, as follows. Along the top arm, vertices 1 through $\eta - 1$ will remain in state 0 because all nodes and their neighbors are in state 0. Vertex η, the state of the vertex incident to the crossbar on the top arm, will change to 1 because its neighbor along the crossbar is in state 1. For the given permutation, then, each subsequent vertex v_i in the range $\eta + 1$ through $n/2$ will change to state 1 because $x_{v_{i-1}} = 1$ and $k^{\uparrow} = 1$. For the bottom arm, vertex $(n/2) + 1$ will change from state 1 to state 0 because $\sigma(x[v_{(n/2)+1}]) = 2 < k_{\downarrow}$. For the same reason, each vertex v_i in the range $(n/2) + 2$ to $n - \eta + 1$ will transition to state 0. Vertices from $n - \eta + 2$ through n will remain in state 0.

The next state is

$$x(2) = (0, 0, \ldots, 0, \underbrace{1, 1, \ldots, 1}_{\text{start at vertex } \eta-1} , 0, 0, \ldots 0, \underbrace{1, 1, \ldots, 1}_{\text{start at vertex } n-\eta+1}) \, ,$$

where, for the top arm, the first $\eta - 2$ vertices are in state 0, the next η vertices are in state 1, and the last vertex on the top arm is in state 0. That is, the set of 1's along the top arm has shifted one vertex left, as follows. Let the set of vertices in the top arm in state 1 (in $x(1)$) be denoted v_i through $v_{i+\eta}$. Vertex v_{i-1} will transition $0 \to 1$ because $x_{v_i} = 1$. Vertex v_i will remain in state 1 because $\sigma(x[v_i]) = 3 = k_{\downarrow}$. Likewise v_{i+1} through $v_{i+\eta-1}$ will remain in state 1. However, $v_{i+\eta}$ will transition to state 0 because $\sigma(x[v_{i+\eta}]) = 2 < k_{\downarrow}$. We refer to this behavior as a *left-shift* (the analogous

shift to the right is a *right-shift*). For the bottom arm, the η vertices (labels $(n/2)+1$ through $n-\eta$) remain in state 0. Vertex $n-\eta+1$ transitions to state 1 because the neighbor along the crossbar is in state 1. Subsequently, vertices $n-\eta+2$ through n transition to state 1, in turn, according to π.

The next state is

$$x(3) = (0,0,\ldots,0,\quad \underbrace{1,1,\ldots,1}_{\text{start at vertex } \eta-2}\quad ,0,0,\ldots 0,\quad \underbrace{1,1,\ldots,1}_{\text{start at vertex } n-\eta}\quad) \ ,$$

where the set of η vertices in state 1 in the top arm has shifted left, and the set of η vertices in state 1 in the bottom arm has shifted left. The shifting process embodied in the transition from state $x(2)$ to $x(3)$—where there is a group of vertices in state 1 in each of the top and bottom arms—can happen a total of $(\eta-2)$ times. The state after these $(\eta-2)$ transitions is

$$x(\eta) = (\ \underbrace{1,1,\ldots,1}_{\text{start at vertex } 1}\ ,0,0,\ldots 0,\quad \underbrace{1,1,\ldots,1,}_{\text{start at vertex } n-2\eta+3}\quad 0,0,\ldots,0) \ .$$

The image of $x(\eta)$ is $x(0)$, the initial state. There are $2+(\eta-2)+1$ state transitions, and we have a limit cycle of length $c=\eta+1$. □

Of course, the proof does not guarantee that c is the minimal periodic orbit size, nor that H_n is the minimal order tree with a periodic orbit of this length. Additionally, there may be multiple periodic orbits of length c. The following proposition expands on this in the case where $c \geq 5$: there exists a tree of smaller order than H_n that also admits a c-cycle, namely the Y-tree.

Proposition 10. *For any integer $c \geq 3$ there is a tree on $n = 3c-2$ vertices such that bithreshold permutation SDS maps over this tree with thresholds $k^{\uparrow} = 1$ and $k_{\downarrow} = 3$ have periodic orbits of length c.*

Proof. The proof is analogous to the case of the H-tree. We take as the graph the Y-tree on $n = 3\beta+1$ vertices (see Figure 2.3) with $\beta \geq 1$, which has vertex set $\{1,2,\ldots,n\}$ and, setting $\eta = \beta+1$, edge set

$$\big\{\{i,i+1\} \mid 1 \leq i \leq 2\eta-2\big\} \cup \big\{\{i,i+1\} \mid 2\eta \leq i \leq (n-1)\big\} \cup \{\eta,n\} \ .$$

Let $c \geq 3$ with $n = 3c-2$ so that $X = Y_n$ (and $c = \beta+1$). We assign thresholds $(k^{\uparrow}, k_{\downarrow}) = (1,3)$ to all vertices and use update sequence $\pi = (1,2,3,\ldots,n)$ as before.

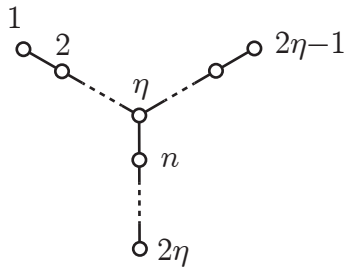

Figure 2.3: The tree Y_n used in the proof of Proposition 10.

As the initial configuration, set the states of the β vertices v in the range $\eta \leq v \leq 2\eta - 2$ (all vertices in the upper right branch except $2\eta - 1$) to 1, and set all other vertex states to 0 to form

$$x(0) = (0, 0, \ldots, 0, \underbrace{1, 1, \ldots, 1,}_{\text{start at vertex } \eta} 0, 0, \ldots 0) \, .$$

The image of $x(0)$ is

$$x(1) = (0, 0, \ldots, 0, \quad \underbrace{1, 1, \ldots, 1,}_{\text{start at vertex } (\eta - 1)} \quad 0, 0, \ldots 0, 1) \, ,$$

where now the first $\eta - 2$ vertices are in state 0, the next β vertices are in state 1, and the remaining vertices—except for vertex n—are in state 0. In the upper two branches, the initial set of β nodes in state 1 *shifts left* for the same reasons described in the proof of Proposition 9. The last vertex, n, will change to 1 because it is adjacent to vertex η, which has state 1.

The image of $x(1)$ is

$$x(2) = (0, 0, \ldots, 0, \quad \underbrace{1, 1, \ldots, 1,}_{\text{start at vertex } (\eta - 2)} \quad 0, 0, \ldots 0, 1, 1) \, ,$$

where the β nodes in state 1 beginning at vertex $\eta - 2$ have shifted left and vertex $n - 1$ transitions to 1 because vertex n is in state 1. Vertex n remains in state 1 because $\sigma(x[v_n]) = 3$.

The mechanics of the last state transition (the left shift of β vertices and nodes transitioning to state 1 in the lower branch) repeats itself a total of $\beta - 2$ times, at

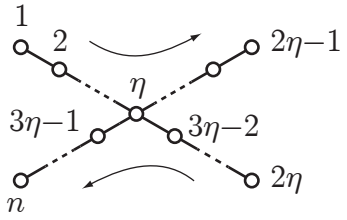

Figure 2.4: The tree X_n used in the proof of Proposition 11 (arrows indicate vertex labeling order).

which point the state is

$$x(\beta-1) = (0,1,\ldots,1, \quad \underbrace{0,0,\ldots,0,}_{\text{start at vertex } (\eta+1)} \quad \underbrace{1,1,\ldots,1}_{\text{start at vertex } (n-\beta+2)} \quad),$$

where the only vertex in the lower vertical branch in state 0 is 2η, the leaf node.

Noting that vertex η remains in state 1 on the next transition because $\sigma(x[v_\eta]) = 3$, all vertices in the upper right branch transition to 1. Vertex 2η also transitions to 1, giving

$$x(\beta) = (1,1,\ldots,1)\ .$$

The next state can be verified to be $x(0)$, thus completing the cycle. The cycle length is therefore $c = \beta + 1$ as stated. □

Interestingly, there is no H-tree nor Y-tree that generates a maximum orbit of size 2 for thresholds $(k^\uparrow, k_\downarrow) = (1,3)$. However, so-called X-trees (defined below) admit cycles of any size $c \geq 1$.

Proposition 11. *For any integer $c \geq 2$ there is a tree X on $n = 4c-3$ vertices such that bithreshold permutation GDS maps over X with thresholds $k^\uparrow = 1$ and $k_\downarrow = 3$ have periodic orbits of length c. For $c = 1$, there is a tree X on $n = 5$ vertices that has periodic orbits of length 1 (fixed points).*

Proof. An X-tree on $n = 4\beta + 1$ vertices with $\beta \geq 1$ has vertex set $\{1,2,\ldots,n\}$ and edge set as illustrated in Figure 2.4. Here $\eta = \beta + 1$ is the unique vertex of degree 4. Note first that for any n the all-zero state over X_n is a fixed point.

We treat the case $c = 2$ separately; use $X = X_5$, $\pi = (1,2,3,4,5)$, and $(k^\uparrow, k_\downarrow) = (1,3)$. It can easily be verified that $x(0) = (0,1,1,0,0)$ is mapped to $x(1) = (1,1,0,1,1)$ which in turn is mapped to $x(0)$, constituting a 2-cycle.

Fix $c \geq 3$, set $n = 4c - 3$ and then $c = \beta + 1$, take as the graph $X = X_n$ with thresholds $(k^{\uparrow}, k_{\downarrow}) = (1, 3)$ for all vertices, and let $\pi = (1, 2, 3, \ldots, n)$.

Define the initial configuration $x(0)$ by assigning the β vertices v with $\eta \leq v \leq 2\eta - 2$ (all vertices in the upper right branch except $2\eta - 1$) to 1 and set all other vertex states to 0, that is,

$$x(0) = (0, 0, \ldots, 0, \underbrace{1, 1, \ldots, 1,}_{\text{start at vertex } \eta} 0, 0, \ldots 0) \, .$$

The image of $x(0)$ is

$$x(1) = (0, 0, \ldots, 0, \quad \underbrace{1, 1, \ldots, 1,}_{\text{start at vertex } (\eta - 1)} \quad 0, 0, \ldots 0, \quad \underbrace{1, 1, \ldots, 1}_{\text{start at vertex } 3\eta - 2} \quad) \, ,$$

where now the first $\eta - 2$ vertices are in state 0, the next β vertices are in state 1, and the remaining vertices in branch 2 are in state 0. In branch 3, only the vertex neighboring vertex η transitions to state 1, while all vertices in branch 4 transition to state 1 because η is in state 1.

State $x(2)$ is generated by a left-shift of the β contiguous states that are 1 in branches 1 and 2, and by a left-shift of the $\beta + 1$ contiguous state-1 vertices in branches 3 and 4; that is,

$$x(2) = (0, 0, \ldots, 0, \quad \underbrace{1, 1, \ldots, 1,}_{\text{start at vertex } (\eta - 2)} \quad 0, 0, \ldots 0, \quad \underbrace{1, 1, \ldots, 1,}_{\text{start at vertex } 3\eta - 3} \quad 0) \, .$$

From $x(1)$ there are $\beta - 2$ such transitions that result in the state

$$x(\beta - 1) = (0, \underbrace{1, 1, \ldots, 1,}_{\text{start at vertex } 2} 0, 0, \ldots 0, \quad \underbrace{1, 1, \ldots, 1,}_{\text{start at vertex } 3\eta - \beta} \quad 0, 0, \ldots, 0) \, .$$

The next transition results in all vertices in branches 1 and 2 in state 1 since η remains in state 1. The contiguous set of $\beta + 1$ vertices in branches 3 and 4 shift left, giving

$$x(\beta) = (1, 1, \ldots, 1, \quad \underbrace{0, 0, \ldots, 0}_{\text{start at vertex } 3\eta} \quad) \, .$$

The image of $x(\beta)$ is $x(0)$, and, since β is the smallest positive time step with this property, we have established the presence of a periodic orbit of length $c = \beta + 1$. $\square$

Finally, we consider a special class of bithreshold SDSs on trees with $k^{\uparrow} = 1$ and $k_{\downarrow} = k_{\downarrow}(v) = d(v) + 1$ for each vertex v. Note that the down-threshold for each vertex depends on its degree as indicated by the index v in $k_{\downarrow}(v)$. We show that such bithreshold SDS maps always have fixed points. In such systems, the state of a vertex v switches from 0 to 1 if it has at least one neighbor in state 1, and from 1 to 0 if it has at least one neighbor in state 0. This is an interesting contrast to the classes of bithreshold SDSs on trees discussed above which have large limit cycles.

Let X be a tree. We choose some arbitrary vertex $r \in v[X]$ as its root, and partition X into levels $X_0, X_1, \ldots, X_D$ with respect to r such that $X_0 = \{r\}$, and for any $i \geq 0$, we let X_{i+1} be the set of vertices adjacent to vertices in set X_i, but not in the set $\cup_{j<i} X_j$. We sometimes refer to X_i as level-i set. Let D be the number of levels. We can also define a parent-child relationship relative to this rooted tree, and denote $p(v)$ as the parent of vertex $v \neq r$. In our arguments below, we use any permutation π of $v[X]$, which consists of all the vertices in X_i before those in X_{i-1} for each i. Our result is based on the following property.

Lemma 12. *Consider a bithreshold SDS $\mathbf{F}_\pi$ on a tree X with an arbitrary root r and permutation π as defined above where $k^{\uparrow} = 1$ and $k_{\downarrow}(v) = d(v) + 1$ for each vertex v. Let x be any state vector and $x' = \mathbf{F}_\pi(x)$. For each vertex v other than the root, we have $x'_v = x_{p(v)}$.*

Proof. Our proof is by induction on the levels, starting from the highest, i.e., X_D. For the base case, consider a leaf $v \in X_D$. We have four cases: $x_v = x_{p(v)} = 1$, $x_v = 0, x_{p(v)} = 1$, $x_v = 1, x_{p(v)} = 0$ and $x_v = x_{p(v)} = 0$. It is easy to verify that in the first two cases, we have $x'_v = 1$ and in the latter two cases, we have $x'_v = 0$, since vertex v is updated before $p(v)$ in π. Therefore, the statement of the lemma holds in the base case for all vertices $v \in X_D$.

Next, consider a vertex v in some level X_j, $j < D$. If v is a leaf in X_j, the lemma follows by exactly the same argument as in the base case. Therefore, consider the case v is not a leaf. Let $w_1, \ldots, w_c$ denote its children. Since level $j + 1$ vertices are updated before those in level j in π, by induction, we have $x'_{w_i} = x_v$ for each w_i. Again, we have a case similar to the base case: when vertex v is updated, it has the same values as its children, and therefore, takes on the state of $p(v)$. Thus, the lemma follows. □

This property immediately gives us the following:

Corollary 13. *Let X be a tree. Let $\pi \in S_X$ and let $(f_v)_v$ be bithreshold functions satisfying $k^{\uparrow} = 1$ and $k_{\downarrow}(v) = d(v) + 1$ for each vertex v. Any SDS map $\mathbf{F}_\pi$ only has fixed points as limit sets.*

Proof. Without loss of generality, we take π to be the permutation in Lemma 12. By applying Lemma 12, it is easy to verify that for any state vector x, all the vertices in levels 0 and 1 have the same state value in $F(x)$, namely x_r. By induction on i, it is easy to verify that for any $i \geq 1$, all vertices in levels $0, \ldots, i$ have the same state value (of x_r) in $F^i(x)$. The statement follows since all permutations for a tree give cycle equivalent SDS maps. □

2.5 Summary and Conclusion

We have analyzed the structure of ω-limit sets of bithreshold GDS. Unlike the synchronous case, bithreshold SDS maps can have long periodic orbits, and this is characterized in terms of the difference of the up- and down-thresholds. We also analyzed certain classes of trees. The following is a list of questions and conjectures for possible further research.

2.5.1 Embedding and Inheritance of Dynamics

A fundamental question in the study of GDSs is the following: if a graph X has a graph X' as an induced subgraph, what are the relations between the dynamics over the two graphs? Here one has to assume that the vertex function, and update sequences if applicable, are appropriately related. For example, is there a projection from the phase space of the GDS over X to the one over X'?

In initial computational experiments we studied the dynamics for bithreshold GDS over trees obtained from, e.g. H-trees by adding a collection of edges – results indicate that there are several classes of outcomes. While this is hardly a surprise, there are clear patterns in how edges are added and the dynamics that result. For example, some classes of edge additions give trees that have long periodic orbits just as in the case of H-trees. For other classes of edge additions, however, the addition of even a single edge causes all periodic orbits of size ≥ 2 to disappear. Further insight into the mechanisms involved could shed light on the fundamental question above.

2.5.2 Minimality of Trees with Given Periodic Orbit Sizes

Our results above on the existence of trees admitting bithreshold SDS with given periodic orbit sizes are not necessarily minimal. For a given $c \geq 1$ there is an X-tree with a periodic orbit of length c, but there may be a smaller tree (or graph in general) which admits periodic orbits of size c as well. While we have obtained some insight on this via sampling, no firm results have been established.

2.6 Appendix: Limit Cycle Structure for Standard Threshold Cellular Automata

This appendix section contains a condensed version of the proof from [26] for standard threshold functions. We have incorporated their proof for two reasons. First, only a portion of the original proof needs to be adapted to cover bithreshold systems, and in this way the paper becomes self-contained. Second, the original proof only appears in French, and we here provide an English version.

Let $K = \{0, 1\}$, let $A = (a_{ij})_{i,j=1}^{n}$ be a real symmetric matrix, let $\theta = (\theta_1, \ldots, \theta_n) \in \mathbb{R}^n$, and let $\mathbf{F} = (f_1, \ldots, f_n)\colon K^n \longrightarrow K^n$ be the function defined coordinate-wise by

$$f_i(x_1, \ldots, x_n) = \begin{cases} 0, & \text{if } \sum_{j=1}^{n} a_{ij} x_j < \theta_i \\ 1, & \text{otherwise .} \end{cases} \tag{2.5}$$

Theorem 14. *For all $x \in K^n$, there exists $s \in \mathbb{N}$ such that $\mathbf{F}^{s+2}(x) = \mathbf{F}^s(x)$.*

The proof of this theorem is based on two lemmas which are given below. Note first that since K^n is finite, for each $x \in K^n$ there exist $s, T \in \mathbb{N}$ (they will generally depend on x) with $T > 0$ such that

$$\mathbf{F}^{s+T}(x) = \mathbf{F}^s(x) \quad \text{and} \quad \mathbf{F}^{s+r}(x) \neq \mathbf{F}^s(x)$$

for all $0 < r < T$. Here s is the transient length of the state x. Next define the $n \times T$ matrix $X(x, T) = (\mathbf{F}^s(x), \ldots, \mathbf{F}^{s+T-1}(x))$ by

$$X(x, T) = \begin{pmatrix} z_1(0) & \ldots & z_1(T-1) \\ \vdots & \ldots & \vdots \\ z_n(0) & \ldots & z_n(T-1) \end{pmatrix} ,$$

where $\mathbf{F}^s(x) = z = (z_1(0), \ldots, z_n(0))$ and $\mathbf{F}^{s+T-1}(x) = (z_1(T-1), \ldots, z_n(T-1))$. In other words, z denotes the first periodic point reached from x (after s steps) and its period is T. The columns of $X(x,T)$ are the T successive periodic points of the cycle containing z.

In general we have

$$\mathbf{F}^{s+l}(x) = (z_1(l), \ldots, z_n(l)) \text{ for } 0 \leq l \leq T-1 \ .$$

Since

$$\mathbf{F}^s(x) = \mathbf{F}^{s+T}(x) = \mathbf{F}(z_1(T-1), \ldots, z_n(T-1))$$

we have $z_i(0) = f_i(z_1(T-1), \ldots, z_n(T-1))$, and from $\mathbf{F}^{s+l+1}(x) = \mathbf{F}(\mathbf{F}^{s+l}(x))$ we have

$$z_i(l+1) = f_i(z_1(l), \ldots, z_n(l)) \text{ for } l = 0, \ldots, T-2.$$

We will call z_i the i^{th} row of the matrix $X(x,T)$ and let γ_i denote the smallest divisor of T such that $z_i(l+\gamma_i) = z_i(l)$ for $l \in \{0, \ldots, T-1\}$, and will say that γ_i is the period of the component z_i. Clearly, we have $z_i(l+T) = z_i(l)$ for $i \in \{1, 2, \ldots, n\}$ and all $l \in \{0, \ldots, T-1\}$. Let $S = \{z_1, \ldots, z_n\}$ be the set of rows of $X(x,T)$. We define the operator $L \colon S \times S \to \mathbb{R}$ by

$$L(z_i, z_j) = a_{ij} \sum_{l=0}^{T-1} (z_j(l+1) - z_j(l-1)) z_i(l) \ ,$$

with indices taken modulo T.

Lemma 15. *The operator L has the following properties:*

(i) $L(z_i, z_j) + L(z_j, z_i) = 0$ *for* $i, j \in \{1, \ldots, n\}$ *(anti-symmetry).*

(ii) If $\gamma_i \leq 2$ *then* $L(z_i, z_j) = 0$ *for* $j \in \{1, \ldots, n\}$.

Proof. For (i), since $a_{ij} = a_{ji}$, we have

$$\begin{aligned} L(z_i, z_j) + L(z_j, z_i) = a_{ij} \sum_{l=0}^{T-1} \big(& [z_i(l) z_j(l+1) - z_i(l-1) z_j(l)] \\ & + [z_i(l+1) z_j(l) - z_i(l) z_j(l-1)] \big) \ , \end{aligned}$$

which clearly evaluates to zero due to periodicity. For part (ii), if $\gamma_i = 1$ then the row z_i is constant and $L(z_i, z_j) = 0$. If $\gamma_i = 2$ then the value of z_i alternates as

$$z_i(0), z_i(1), z_i(0), z_i(1), \ldots, z_i(0), z_i(1)$$

across the i^{th} row, and the terms in $L(z_i, z_j)$ cancel in pairs. □

Let $z_i \in S$ and suppose in the following that $\gamma_i \geq 3$. We set

$$\operatorname{supp}(z_i) = \{l \in \{0, \ldots, T-1\} : z_i(l) = 1\} \ ,$$

and write $\mathcal{I}(l) = \{l, l+2, l+4, \ldots, l-4, l-2\}$. Next, set

$$C_0 = \begin{cases} \varnothing, & \text{if there is no } l_0 \in \{0, \ldots, T-1\} \text{ such that } \mathcal{I}(l_0) \subset \operatorname{supp}(z_i) \\ \mathcal{I}(l_0), & \text{otherwise.} \end{cases}$$

We define C_1 as the set

$$C_1 = \{l_1 + 2s \in \operatorname{supp}(z_i) : s = 0, 1, \ldots, q_1\} \ ,$$

where l_1 is the smallest index not in C_0 satisfying $z_i(l_1 - 2) = 0$ and q_1 satisfies $z_i(l_1 + 2q_1 + 2) = 0$. For $k \geq 2$ we define the sets C_k by

$$C_k = \{l_k + 2s \in \operatorname{supp}(z_i) : s = 0, 1, \ldots, q_k\} \ ,$$

where $l_k = l_{k-1} + r_k \pmod{T} \notin \{l_1, \ldots, l_{k-1}\}$ is the smallest index for which $z_i(l_k - 2) = 0$ and q_k satisfies $z_i(l_k + 2q_k + 2) = 0$.

Since $\gamma_i \geq 3$ (assumption), there always exists $l_1 \in \operatorname{supp}(z_i)$ for which $z_i(l_1 - 2) = 0$. This allows us to build the collection of sets $\mathcal{C} = \{C_0, \ldots, C_p\}$. By construction, $\mathcal{C}$ is a partition of $\operatorname{supp}(z_i)$. The following lemma provides the final piece needed in the proof of the main result.

Lemma 16. *For $z_i \in S$ and with $\gamma_i \geq 3$ we have*

$$\sum_{j=1}^{n} L(z_i, z_j) < 0 \ .$$

Proof. Using the partition $\mathcal{C}$ of $\operatorname{supp}(z_i)$, we have

$$\begin{aligned} \sum_{j=1}^{n} L(z_i, z_j) &= \sum_{j=1}^{n} a_{ij} \sum_{l \in \operatorname{supp}(z_i)} (z_j(l+1) - z_j(l-1)) \cdot 1 \\ &= \sum_{j=1}^{n} a_{ij} \sum_{k=0}^{p} \sum_{l \in C_k} (z_j(l+1) - z_j(l-1)) = \sum_{k=0}^{p} \sum_{j=1}^{n} a_{ij} \sum_{l \in C_k} (z_j(l+1) - z_j(l-1)) \\ &= \sum_{k=0}^{p} \Psi_{ik} \ , \end{aligned}$$

where we have introduced

$$\Psi_{ik} = \sum_{j=1}^{n} a_{ij} \sum_{l \in C_k} (z_j(l+1) - z_j(l-1)) \ . \tag{2.6}$$

If $C_0 = \varnothing$ then $\Psi_{i0} = 0$, and if $C_0 = \{l_0, l_0 + 2, \ldots, l_0 - 2\}$ we have

$$\sum_{l \in C_0} (z_j(l+1) - z_j(l-1)) = 0 \ .$$

In other words, we always have $\Psi_{i0} = 0$, so we assume $k > 0$ in the following. From the assumption that $\gamma_i \geq 3$, there exists $C_k \neq \varnothing$ such that $C_k = \{l_k, l_k + 2, \ldots, l_k + 2q_k\}$, so we can re-write Ψ_{ik} as

$$\begin{aligned} \Psi_{ik} &= \sum_{j=1}^{n} a_{ij} \sum_{s=0}^{q_k} (z_j(l_k + 2s + 1) - z_j(l_k + 2s - 1)) \\ &= \sum_{j=1}^{n} a_{ij} z_j(l_k + 2q_k + 1) - \sum_{j=1}^{n} a_{ij} z_j(l_k - 1) \ . \end{aligned}$$

[**Cross-reference for bithreshold systems**] By the construction of C_k, we have $z_i(l_k + 2q_k + 2) = 0$ and $z_i(l_k) = 1$ which, by the definition of f in Equation (2.5), is only possible if

$$\sum_{j=1}^{n} a_{ij} z_j(l_k + 2q_k + 1) < \theta_i, \quad \text{and} \quad \sum_{j=1}^{n} a_{ij} z_j(l_k - 1) \geq \theta_i \ . \tag{2.7}$$

This implies that $\Psi_{ik} < 0$ and we conclude that

$$\sum_{j=1}^{n} L(z_i, z_j) = \sum_{k=1}^{p} \Psi_{ik} < 0$$

as required. □

Proof of Theorem 14. From Lemma 15 we have that L is anti-symmetric so

$$\sum_{i=1}^{n} \sum_{j=1}^{n} L(z_i, z_j) = 0 \ .$$

However, if we assume that $T \geq 3$, then there is z_i with $\gamma_i \geq 3$ and Lemma 16 produces the desired contradiction. We conclude that $T \leq 2$. □

Chapter 3

Multistate Systems

3.1 Introduction

Threshold-based mechanisms are present in a broad range of phenomena, and many models have been used to capture them. Boolean networks [39] were introduced in the context of gene expression. Although their definition was at first somewhat restrictive, a Boolean network is now generally understood to be an n-dimensional dynamical system map $F = (f_1, \ldots, f_n)$ over $\{0, 1\}$ where the network is the dependency graph of the variables of F. Such a system is a Boolean threshold network if each function f_k is given by a threshold function

$$\tau_k \colon \{0,1\}^m \longrightarrow \{0,1\}, \qquad \tau_k(x_1, \ldots, x_m) = \begin{cases} 1, & \sigma(x_1, \ldots, x_m) \geq k \\ 0, & \text{otherwise,} \end{cases} \tag{3.1}$$

where $\sigma(x_1, \ldots, x_m) = \big|\{i \mid x_i = 1\}\big|$. Other notions of threshold functions have been studied, and Goles et al consider a weighted version with symmetric interaction in for example [27]. In this work, we analyze the long-term dynamics of generalized threshold systems where the state set is finite (not just $\{0, 1\}$) and where the transitions $a \to b$ and $b \to a$ may have different thresholds. The results presented here build on our earlier work [46]. We next describe related work and then motivate our model.

3.1.1 Related Work

There are several works where models possess a subset of our model's features. A progressive 3-state complex contagion model, where vertices transition from state 0 to 1 when a threshold k_{01} of neighbor contributions is received, and transition from state 1 to 2 when a threshold k_{12} of neighbor contributions is received, is presented in [56]. However, in that work, vertices may not transition "down" from state 2 to state 1, nor from state 1 to state 0. Hence, the characterization "progressive." A progressive $0 \to 1$ transition majority model, also a specialization of our work, is described in [19]. In a progressive model of adoption of fads and innovations [43], a vertex moves progressively among $M+1$ states, from 0 to M, with increasing levels of awareness/conviction. Hence, transitions are of the form $i \to i+1$ with $i \in \{0, \ldots, M-1\}$. In their symbology, a vertex only adopts when it reaches state M. Further, a two-threshold back-and-forth voter model, where a vertex may change state repeatedly between states $\{0, 1\}$, but only transitions to state 0 or 1 when a threshold (k_0 or k_1, respectively) number of interactions has taken place over time, is described in [2]. In another work [73], a voter model is adapted where each vertex is in one state from the set $\{0, 1\}$ (e.g., a vertex has opinion 0 or opinion 1, respectively) and is in one state from the set $\{u, c\}$ where u means unsure and c means confident. For example, a vertex in state $(1, u)$ subscribes to opinion 1, but is not wholly committed. This state space and set of transitions are similar to the types of transitions we model here. The models of fanaticism [13, 68, 69] allow some cycles of behavior, but is not as general as our model.

Goles and Martinez [27, p. 28] examine multiple state, multiple threshold transition systems as we do here. However, their work differs from ours in a fundamental way: in their work, the threshold to transition from a vertex state x_v to x' is independent of the current vertex state x_v. Our transitions, in contrast, account for the current vertex state. A simple example illustrates one aspect of this difference. Suppose a manufacturer has outdated equipment and looks to replace it. The equipment it currently possesses corresponds to state 1 (state 0 is having no equipment). There are two options: option a is to purchase machine A at a cost of c_a; option b is to purchase machine B at a cost of $c_b = 2c_a$. We denote option a as state 2 and option b as state 3. Assuming thresholds k_{12} and k_{13} for, respectively, transitions from state 1 to state 2, and from state 1 to state 3, are proportional to cost, we have that $k_{13} = 2k_{12}$. Suppose the company chooses option a and consequently moves to state 2. What happens if the company subsequently chooses option b? In the formulation of [27], $k_{23} = k_{13}$; i.e., the move to state 3 has the same cost (threshold), irrespective of current state. We argue that $k_{23} \neq k_{13}$ and will most

likely be $k_{23} > k_{13}$ because the company would most probably have a net loss from reselling machine A so quickly, and from wasted time in getting up to speed with machine A. Hence, in this sense, our model is more flexible. However, we note that the threshold functions in [27] are more general than those studied here in the sense that states are weighted, $\mathbb{1}(\sum_j a_{ij}x_j - \theta_i)$, where $\mathbb{1}$ is the indicator function, $a_{ij} \in \mathbb{R}$ is a per-edge weight with $a_{ij} = a_{ji}$, and $\theta_i \in \mathbb{R}$ is a per-vertex threshold. We, on the other hand, restrict a_{ij} to $\{0, 1\}$. Our state transition formulation will be described below.

Our results are applicable to two kinds of behavior. The first kind describes situations where there are varying degrees of a single behavior. An example is social protest. A person may not participate (e.g., state 0), or may participate with great frequency and intensity (call this state $r-1$). Thus, there are r states denoting various levels of participation. The second kind is two competing mechanisms. Building on the previous example, it is also possible that a person is pro-government (i.e., opposed to the protest). We model this case as having $2r + 1$ states where state 0 indicates neutrality, with r states describing varying levels of pro-government sentiment and r states describing those for protest. Note in these models that there are no requirements for a neutral state, nor is it required that a set of states be described by a consecutive set of integers. Finally, state transitions need not be symmetric; e.g., there may be a transition from state i to state j, but not from j to i.

3.1.2 Motivation

A *contagion* is any entity or phenomenon such as information or influence that propagates through a networked population. Contagion processes have been empirically verified or indirectly observed in a host of social applications, including spread of healthy practices in drug using communities [48], sharing of financial information among individual investors [66], propagation of online purchase recommendations [47], growth of mass movements [36], and increases in social media membership [71]. A *simple contagion* is one for which infection requires only a single interaction with a person that has already contracted it. This situation is captured as the case where the threshold is $k = 1$. A *complex contagion* requires two or more infected contacts for a person to acquire the contagion, which corresponds to a threshold value $k \geq 2$, see [14,31]. Threshold mechanisms continue to be successfully employed in explaining contagion dynamics (e.g., [30, 71]). In most studies, people can take on one of two states: state 0 (not possessing a contagion) and state 1 (possessing it). Moreover, most of the work is on progressive systems, where irrevocable

decisions are made; e.g., an individual can transition from state 0 to 1 but cannot transition from 1 to 0. We now cover four motivating extensions to these ideas.

Human emotions (e.g., happiness, fear, disgust, anger, sadness) are well-known to be transferable among interacting people [18, 33]. Scales for emotions and the factors that go into them are provided in [18,24], indicating that there are degrees of feeling. Experiments on fear and anger are discussed in [60], and on anger and sadness in [8]; reference [60] indicates that emotions are not binary, but rather inherently have different degrees. A simulation study [70] demonstrates that making fear a binary variable reduces agreement with measurements of actual events of fear propagation in a crowd, compared to making fear a continuous or multi-state variable.

Economics and sociology furnish examples of varying levels of commitment to a behavior. In Macy's contagion dynamics study [52] of the willingness of individuals to contribute resources to a collective good, he quotes Elster [21], "although the assumption of a dichotomous independent variable—the decision [by humans] to cooperate [to meet some goal]—is convenient for many purposes, it is often unrealistic. Often, the problem facing the actor is not *whether* to contribute, but *how much* to contribute." This can apply to various situations, such as joining a strike or adopting a new technology [14,31]: one makes a partial commitment. The idea of varying levels of commitment is also described in [61]. Add Health longitudinal data [32], generated on 7-12 graders in 1994-1995 and a subset of the initial group most recently in 2008, contain survey results clearly illustrating that drinking and smoking behaviors of young adults entail various levels of participation.

Sociology has for decades treated the adoption of many behaviors as threshold systems, which model peer influence in spreading behavior among people [7,14,31,41,64]. A person is regularly influenced by their neighbors (e.g., friends, high-status individuals, or members of a social group). Macy devises a threshold model to study the dynamics of group participation in activities at various levels [52]. Diffusion of emotions using agent-based models is studied in [70]; see this work for references to others. Models for participating in a revolution, and more generally for spreading fanaticism of any kind, incorporate varying levels of commitment [13, 68, 69]. Other diffusive simulation studies use a continuous $[0, 1]$ variable value to model levels of fear [35]. Through online data mining, evidence is mounting for threshold-based behaviors at large scales for such things as online purchases, joining social sites such as Facebook and LiveJournal, and participating in mass protests [30, 42, 47, 71]. Further, the single biggest factor in youth smoking initiation is peer influence [34], indicating that it can be treated as a propagating contagion governed by threshold behavior [45]. Watts [74] argues that many human decision processes are in practice

reduced to threshold-based decisions.

We also note that changes in behavior are not always progressive; i.e., they do not always move in one direction. A primary example is dieting, where starting and stopping diets is so common that it is given a name: yo-yo dieting [3]. Other sociological examples are provided in [7,64], and Schelling [64] states that "Numerous social phenomena display cyclic behavior ..." Several works [54,59,62] on social movements and violence provide evidence for, and motivate the need for, models where individuals can commit and then either retreat or naturally desist as a movement wanes; only to participate again when a new cycle of events arises. The cyclic nature of rumors, called *rumor recursion*, is explored in [40].

We thus note a number of issues: (*i*) human emotions and behaviors can have various degrees of strength, (*ii*) people can change (e.g., repeatedly move back and forth) among degrees of behavior, (*iii*) emotions and behaviors are contagions and can be propagated through a population, and (*iv*) behavioral contagions can be modeled as threshold systems. These observations motivate our work, wherein we seek to understand the long-term dynamics of systems with these characteristics. The model, defined formally later, is a multi-state model of a specified behavior, where transitions between every pair of vertex states is governed by a transition-specific threshold.

Contributions and organization. We provide in Section 3.2 the graph dynamical system preliminaries. In Section 3.3 we describe the 3-state multithreshold model and the proof of sufficient conditions to guarantee that such asynchronous systems only have fixed points as limit sets. We also identify bifurcation points and show how long cycles can arise at these points. We demonstrate that the conditions for fixed points can be tight. That is, minimally violating each fixed point condition can lead to arbitrarily large limit cycles. We generalize our results for 3-state to r-state multithreshold systems ($r > 3$) in Section 3.4 and give procedures for determining the corresponding fixed point conditions. Both in the 3-state and in the r-state cases we permit arbitrary transitions among vertex states. We finally conclude in Section 3.5.

3.2 Background and Terminology

3.2.1 Graph Dynamical System

Let X denote an undirected graph with vertex set $\mathrm{v}[X] = \{1, 2, \ldots, n\}$ and edge set $\mathrm{e}[X]$. To each vertex v we assign a state $x_v \in K = \{0, 1, \ldots, r-1\}$, for some fixed integer $r \geq 2$, and refer to this as the *vertex state*. The *system state* is $x = (x_1, x_2, \ldots, x_n)$. Next, let $n[v]$ represent the sequence of vertices in the 1-neighborhood of v, sorted in increasing order, let $n[v](i)$ denote the ith vertex, and write

$$x[v] = (x_{n[v](1)}, x_{n[v](2)}, \ldots, x_{n[v](d(v)+1)})$$

for the corresponding sequence of vertex states called the *restricted state*. Here $d(v)$ denotes the degree of v. The dynamics of vertex states is governed by a list of *vertex functions* $(f_v)_v$ where each $f_v \colon K^{d(v)+1} \longrightarrow K$ maps as

$$x_v = f_v\big(x[v]\big) \ .$$

In other words, the state of vertex v at time $t+1$ is given by f_v evaluated at the restricted state $x[v]$ at time t. An *update mechanism* governs how the list of vertex functions assembles to a *graph dynamical system* map (see e.g. [51, 58])

$$\mathbf{F} \colon K^n \longrightarrow K^n$$

sending the system state at time t to the one at time $t+1$.

We largely consider *asynchronous* updates given by permutation *update sequences*. For this we first introduce the notion of *X-local functions*. Here the X-local function $F_v \colon K^n \longrightarrow K^n$ is given by

$$F_v(x_1, \ldots, x_n) = (x_1, x_2, \ldots, f_v(x[v]), \ldots, x_n) \ .$$

Using $\pi = (\pi_1, \ldots, \pi_n) \in S_X$ (the set of all permutations of $\mathrm{v}[X]$) as an update sequence, where both π_i and $\pi(i)$ represent the ith vertex of the permutation, the corresponding asynchronous (or sequential) graph dynamical system map $\mathbf{F}_\pi \colon K^n \longrightarrow K^n$ is given by

$$\mathbf{F}_\pi = F_{\pi(n)} \circ F_{\pi(n-1)} \circ \cdots \circ F_{\pi(1)} \ . \tag{3.2}$$

We also refer to this class of asynchronous systems as (permutation) *sequential dynamical systems* (SDSs) [57].

The phase space of the GDS map $\mathbf{F}\colon K^n \longrightarrow K^n$ is the directed graph with vertex set K^n and edge set $\{\big(x, \mathbf{F}(x)\big) \mid x \in K^n\}$. A state x for which there exists a positive integer p such that $\mathbf{F}^p(x) = x$ is a *periodic point*, and the smallest such integer p is the *period* of x. If $p = 1$ we call x a *fixed point* for $\mathbf{F}$. A state that is not periodic is a *transient state*. Classically, the *omega-limit set* of x, denoted by $\omega(x)$, is the set of accumulation points of the sequence $\{\mathbf{F}^k(x)\}_{k\geq 0}$. In the finite case, the omega-limit set is the unique periodic orbit reached from x under $\mathbf{F}$.

We remark that graph dynamical systems generalize concepts such as cellular automata and Boolean networks, and can describe a wide range of distributed, nonlinear phenomena.

3.2.2 Multithreshold Functions

In this paper we consider graph dynamical systems where each vertex function is a multithreshold function. To define this function class, let X be a graph as before and $v \in \mathrm{v}[X]$. We first define the function σ_v by

$$\sigma_v(x) = x_v + \sum_{i=1}^{r-1} i \cdot n_{i,v}(x) \tag{3.3}$$

where sums are taken in $\mathbb{N}$ and $n_{i,v}(x) = \big|\{(v, v') \mid x_{v'} = i\}\big|$. Here $d(v) = \sum_{i=0}^{r-1} n_{i,v}(x)$, a fact that we will use in several proofs. We will omit the vertex reference in $n_{i,v}$ and σ_v when this is clear from context.

We write $\boldsymbol{k}$ for the sequence of thresholds k_{ij} with $i \neq j \in K = \{0, 1, 2, \ldots, r-1\}$ that governs the vertex state transitions. The threshold function $\tau_{v,\boldsymbol{k}}\colon K^m \longrightarrow K$ is defined by

$$\tau_{v,\boldsymbol{k}}(x_1, \ldots, x_m) = \begin{cases} j, & \text{if } x_v = i \text{ and } j > i \text{ is maximal such that } \sigma_v(x) \geq k_{i,j}; \\ j', & \text{if instead } x_v = i \text{ and } j' < i \text{ is minimal with } \sigma_v(x) < k_{i,j'}; \\ x_v, & \text{otherwise.} \end{cases} \tag{3.4}$$

For example, in the 3-state system of Figure 3.1, we have $\boldsymbol{k} = (k_{01}, k_{10}, k_{12}, k_{21}, k_{02}, k_{20})$. Note that for each vertex state, there are multiple thresholds that describe possible state changes, but the definition of $\tau_{v,\boldsymbol{k}}$ in Equation (3.4) makes it unambiguous. For this generalized threshold function, arbitrary hops (i.e., transitions between states) are possible. In some cases, we want to limit vertex state transitions so that the new

vertex state may differ by at most one from the current state. For this we define the function $\tau^1_{v,\boldsymbol{k}} \colon K^m \longrightarrow K$ by

$$\tau^1_{v,\boldsymbol{k}}(x_1,\ldots,x_m) = \begin{cases} x_v + 1, & \text{if } \sigma_v(x) \geq k_{x_v,x_v+1}; \\ x_v - 1, & \text{if instead } \sigma_v(x) < k_{x_v,x_v-1}; \\ x_v, & \text{otherwise,} \end{cases} \tag{3.5}$$

with the obvious adjustments to the cases where $x_v = 0$ and $x_v = r-1$. Here, we call a threshold k_{ij} with $i < j$ ($i > j$) an *up-threshold* (*down-threshold*). We remark that both $\tau_{v,\boldsymbol{k}}$ and $\tau^1_{v,\boldsymbol{k}}$ are *semi-totalistic* (or outer-symmetric) functions [58]. We thus have vertex functions $f_v = f_{v,\boldsymbol{k}} := \tau_{v,\boldsymbol{k}}$ or $f_v = f_{v,\boldsymbol{k}} := \tau^1_{v,\boldsymbol{k}}$.

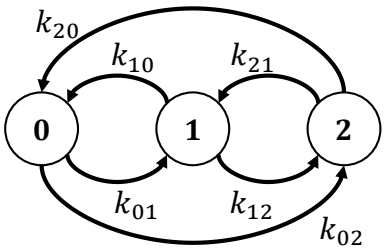

Figure 3.1: The six vertex state transitions and thresholds k_{ij} for 3-state multithreshold systems.

For some applications it may be natural to impose that for example $k_{01} < k_{02}$ and so on. We refer to these conditions as the *elementary threshold conditions* (ETCs). In the case of $r = 3$ they become

$$\begin{aligned} &k_{01} < k_{02} && \text{transition from extreme low state (state 0)} \\ &k_{20} < k_{21} && \text{transition from extreme high state (state 2)} \\ &k_{10} \leq k_{12} && \text{transitions for each internal state (here, state 1) must be unambiguous .} \end{aligned} \tag{3.6}$$

Similarly, applications may sometimes motivate conditions of the form $k_{02} \geq k_{01} + k_{12}$. We refer to this set of conditions as the *transition order preserving threshold constraints*, abbreviated *TOPTCs*, which for $r = 3$ become

$$\begin{aligned} k_{02} &\geq k_{01} + k_{12} \\ k_{20} &\leq k_{21} + k_{10} \ . \end{aligned} \tag{3.7}$$

Mathematically, we may of course consider any combination of thresholds. A graph dynamical system map is a *generalized threshold GDS map* if every vertex function is of the form in Equation (3.4), or of the form in Equation (3.5) if we only permit 1-transitions. In general, the threshold $\boldsymbol{k}$ may vary across the vertex set.

3.3 The 3-State Threshold Model

Before handling the general case, we first consider the case $r = 3$ with $K = \{0, 1, 2\}$ and transitions as illustrated in Figure 3.1. Much of the insight developed in this case carries over to the general case. We call a vertex state transition where x_v is mapped from i to j with $|i - j| = h$ an h-hop or an h-transition. The 3-state model only admits 1- and 2-transitions. For $r = 3$, the threshold is $\boldsymbol{k} = (k_{01}, k_{10}, k_{12}, k_{21}, k_{02}, k_{20})$, $d(v) = n_{0,v} + n_{1,v} + n_{2,v}$, and

$$\sigma_v(x) = x_v + n_{1,v}(x) + 2n_{2,v}(x) \ . \tag{3.8}$$

The vertex functions can in this case be written

$$\tau_{v,\boldsymbol{k}}(x[v]) = \begin{cases} \begin{cases} 2, & \text{if } \sigma_v(x) \geq k_{02} \\ 1, & \text{if instead } \sigma_v(x) \geq k_{01} \ , \\ 0, & \text{otherwise} \end{cases} & \text{if } x_v = 0 \\ \begin{cases} 2, & \text{if } \sigma_v(x) \geq k_{12} \\ 0, & \text{if instead } \sigma_v(x) < k_{10} \ , \\ 1, & \text{otherwise} \end{cases} & \text{if } x_v = 1 \\ \begin{cases} 0, & \text{if } \sigma_v(x) < k_{20} \\ 1, & \text{if instead } \sigma_v(x) < k_{10} \ , \\ 2, & \text{otherwise} \end{cases} & \text{if } x_v = 2, \end{cases} \tag{3.9}$$

and similarly for $\tau^1_{v,\boldsymbol{k}}$. Note again that the multithreshold function returns the largest up-transition that is possible, the largest down-transition if no up-transition is possible, or x_v otherwise. We will be concerned with the following questions:

(I) Under what conditions on the threshold will asynchronous GDS maps only have fixed points as limit cycles?

(*II*) If these conditions do not hold, can we have periodic orbits of length two or greater?

(*III*) Are the bounds sharp?

(*IV*) Can we obtain arbitrarily long periodic orbits?

We will work with the dynamics of $\tau_{v,\boldsymbol{k}}$ systems and specialize to $\tau^1_{v,\boldsymbol{k}}$ systems.

3.3.1 Fixed Point Conditions

In this section we derive sufficient conditions for asynchronous multithreshold GDS maps to only have fixed points as limit sets. It is convenient to write differences in thresholds between two state i and j for vertex v as

$$\Delta_{ij} = k_{ji} - k_{ij}, \quad \text{with} \quad i < j \ ,$$

which for the 3-state case gives

$$\Delta_{01} = k_{10} - k_{01}, \qquad \Delta_{12} = k_{21} - k_{12}, \quad \text{and} \quad \Delta_{02} = k_{20} - k_{02} \ . \tag{3.10}$$

In the proof of Theorem 17 below, we will use the following vertex and edge potential functions, which are motivated by several works [6, 28]. Vertex potentials are

$$\hat{P}(v,x) = \begin{cases} \hat{P}_2(v,x) = k_{21} + k_{10} + C_2 - n_{0,v} - 3n_{1,v} - 4n_{2,v}, & \text{if } x_v = 2, \\ \hat{P}_1(v,x) = -k_{12} + k_{10} + C_1 - n_{0,v} - n_{2,v}, & \text{if } x_v = 1, \text{ and} \\ \hat{P}_0(v,x) = -k_{12} - k_{01} + 1n_{1,v} + 3n_{2,v}, & \text{if } x_v = 0. \end{cases} \tag{3.11}$$

where $\hat{P}_i(v,x)$ is the vertex potential of vertex v in state i for system state x, and $C_1, C_2 \in \mathbb{Z}$ are constants. Similarly, each edge $e = \{v, v'\}$ is assigned the potential

$$\hat{P}(e = \{v, v'\}, x) = \begin{cases} 1, & x_v \neq x_{v'} \\ 0, & x_v = x_{v'} \ . \end{cases} \tag{3.12}$$

The total system potential for a state x is $P(x) = \sum_{v \in v[X]} \hat{P}(v,x) + \sum_{e \in e[X]} \hat{P}(e,x)$. Below we are interested in the change in the system potential that results when a single vertex v changes state, and in this case, only the vertex potential of v and edge

potentials of edges incident to v are relevant. We therefore introduce the potential associated with v as

$$P(v,x) = \hat{P}(v,x) + \sum_{e=\{v,v'\}\in e[X]} \hat{P}(e,x)\ , \tag{3.13}$$

or

$$P(v,x) = \begin{cases} P_2(v,x) = k_{21} + k_{10} + C_2 - 2n_{1,v} - 4n_{2,v}, & \text{if } x_v = 2, \\ P_1(v,x) = -k_{12} + k_{10} + C_1, & \text{if } x_v = 1, \text{ and} \\ P_0(v,x) = -k_{12} - k_{01} + 2n_{1,v} + 4n_{2,v}, & \text{if } x_v = 0. \end{cases} \tag{3.14}$$

The arguments of P_i will be omitted when they are clear from the context. We can now state our result for Question (I) above for the case $r = 3$.

Theorem 17. *Let X be a graph, w a word over $\mathrm{v}[X]$, $K = \{0,1,2\}$ and $\mathbf{F}_w$ a multithreshold GDS map over K^n where each vertex function is of the form $\tau_{v,\boldsymbol{k}}$. Then the map $\mathbf{F}_w$ has only fixed points as limit sets if*

(i) $\Delta_{01} \le \min\{-C_1 - 1, C_1 + 3\}$,

(ii) $\Delta_{12} \le \min\{C_1 - C_2 - 3, -C_1 + C_2 + 5\}$,

(iii) $(k_{21} + k_{12}) + (k_{10} + k_{01}) - 4k_{02} \le -C_2 - 1$ *and*

(iv) $-(k_{21} + k_{12}) - (k_{10} + k_{01}) + 4k_{20} \le C_2 + 11$,

where C_1 and C_2 are constants.

Proof. It is sufficient to show that the potential drops whenever the application of an X-local function F_v changes the state of vertex v. By composition, it then follows that the application of $\mathbf{F}_w$ will lead to a potential drop and hence that periodic orbits of length two or greater are not possible. We consider each transition shown in Figure 3.1 in turn. For the vertex state transition $i \to j$ we write the potential drop ΔP_{ij} as $\Delta P_{ij} = P_j - P_i$, and derive conditions ensuring that $\Delta P_{ij} \le -1$.

Transition $0 \to 1$: Here $\sigma_v = n_{1,v} + 2n_{2,v} \ge k_{01}$, and thus $-2(n_{1,v} + 2n_{2,v}) \le -2k_{01}$ which, using Equation (3.14), gives

$$\begin{aligned} \Delta P_{01} = P_1 - P_0 &= k_{10} + k_{01} + C_1 - 2n_{1,v} - 4n_{2,v} \\ &\le k_{10} + k_{01} + C_1 - 2k_{01} = \Delta_{01} + C_1\ . \end{aligned}$$

To ensure that $\Delta P_{01} \leq -1$, we need $\Delta_{01} + C_1 \leq -1$, or $\Delta_{01} \leq -C_1 - 1$.

Transition $1 \to 0$: Here $\sigma_v = 1+n_{1,v}+2n_{2,v} \leq k_{10}-1$, so that $2(n_{1,v}+2n_{2,v}) \leq 2k_{10}-4$, and

$$\begin{aligned}\Delta P_{10} = P_0 - P_1 &= -k_{10} - k_{01} - C_1 + 2n_{1,v} + 4n_{2,v} \\ &\leq -k_{10} - k_{01} - C_1 - 4 + 2k_{10} = \Delta_{01} - C_1 - 4 \ .\end{aligned}$$

For $\Delta P_{10} \leq -1$, we need $\Delta_{01} - C_1 - 4 \leq -1$. From this last inequality and the one from the $0 \to 1$ transition, we have condition (i).

Transition $1 \to 2$: Here the potential change is

$$\begin{aligned}\Delta P_{12} = P_2 - P_1 &= k_{21} + k_{12} + C_2 - C_1 - 2n_{1,v} - 4n_{2,v} \\ &\leq k_{21} + k_{12} + C_2 - C_1 + 2 - 2k_{12} = \Delta_{12} + C_2 - C_1 + 2 \ ,\end{aligned}$$

where we have used the fact that $\sigma_v = 1 + n_{1,v} + 2n_{2,v} \geq k_{12}$, and hence that $-2(1 + n_{1,v} + 2n_{2,v}) \leq -2k_{12}$. For $\Delta P_{12} \leq -1$, we need $\Delta_{12} + C_2 - C_1 + 2 \leq -1$.

Transition $2 \to 1$: In this case, we have $\sigma_v = 2 + n_{1,v} + 2n_{2,v} \leq k_{21} - 1$ which leads to

$$\begin{aligned}\Delta P_{21} = P_1 - P_2 &= -k_{21} - k_{12} + C_1 - C_2 + 2n_{1,v} + 4n_{2,v} \\ &\leq -k_{21} - k_{12} + C_1 - C_2 - 6 + 2k_{21} = \Delta_{12} + C_1 - C_2 - 6\end{aligned}$$

For $\Delta P_{21} \leq -1$ it is sufficient that $\Delta_{12} \leq -C_1 + C_2 + 5$. By combining the conditions on Δ_{12} from the $1 \to 2$ and the $2 \to 1$ transitions, we see that $\Delta_{12} \leq \min\{C_1 - C_2 - 3, -C_1 + C_2 + 5\}$, which is our condition (ii).

Transition $0 \to 2$: Here we have $\sigma_v = n_{1,v} + 2n_{2,v} \geq k_{02}$, or $-4(n_{1,v} + 2n_{2,v}) \leq -4k_{02}$ giving

$$\begin{aligned}\Delta P_{02} = P_2 - P_0 &= (k_{21} + k_{12}) + (k_{10} + k_{01}) + C_2 - 4n_{1,v} - 8n_{2,v} \\ &\leq (k_{21} + k_{12}) + (k_{10} + k_{01}) + C_2 - 4k_{02} \ .\end{aligned} \tag{3.15}$$

Requiring this to be ≤ -1 leads to our condition (iii).

Transition $2 \to 0$: For this transition we have $\sigma_v = 2 + n_{1,v} + 2n_{2,v} \leq k_{20} - 1$ and $4(n_{1,v} + 2n_{2,v}) \leq 4k_{20} - 12$. The associated potential change is

$$\begin{aligned}\Delta P_{20} = P_0 - P_2 &= -(k_{21} + k_{12}) - (k_{10} + k_{01}) - C_2 + 4n_{1,v} + 8n_{2,v} \\ &\leq -(k_{21} + k_{12}) - (k_{10} + k_{01}) - C_2 - 12 + 4k_{20},\end{aligned} \tag{3.16}$$

and requiring this to be negative gives condition (iv). □

Remark 18. *The four conditions in Theorem 17 are called the* fixed point conditions *(FPCs). While the parameters C_1 and C_2 are arbitrary, there are considerations to guide their selections. Condition (ii) of the FPCs motivates the selection of $C_1 - C_2 = 4$, since this maximizes its right hand side (RHS). This, however, reduces the RHS of (i) through the first argument in the min function. Examining FPCs (iii) and (iv), as $|C_2|$ increases, the permissible range of (iv) increases, but that for (iii) decreases. Nonetheless, C_1, C_2 may be advantageously tuned for specific problems.*

The fixed point conditions for the GDS map $\mathbf{F}_w$, where the vertex functions are $\tau^1_{v,\boldsymbol{k}}$, which only permit 1-transitions (see Figure 3.2), are easily derived from the proof of Theorem 17.

Corollary 19. *With the same conditions as in Theorem 17, the map $\mathbf{F}_w$ where each vertex function is given by $\tau^1_{v,\mathbf{k}}$, has only fixed points as limit sets if*

(i) $\Delta_{01} \leq \min\{-C_1 - 1, C_1 + 3\}$,

(ii) $\Delta_{12} \leq \min\{C_1 - C_2 - 3, -C_1 + C_2 + 5\}$,

where C_1 and C_2 are constants.

Proof. The proof follows immediately from the proof of Theorem 17 since in this case we can omit the conditions (iii) and (iv) arising for the transitions $0 \to 2$ and $2 \to 0$. □

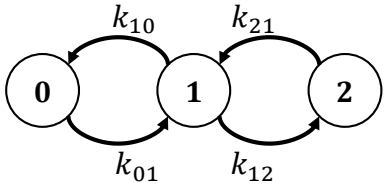

Figure 3.2: The four 1-transitions and thresholds k_{ij} for the 3-state ($K = \{0, 1, 2\}$) multithreshold functions.

Consider the two sequences of transitions: (i) $0 \to 1 \to 2$ and (ii) $0 \to 2$. Both sets of transitions ultimately cause a change in state from 0 to 2. Recalling that

$k_{01} < k_{02}$ under the threshold constraints of Equation (3.6), we see that it is easier to transition from 0 to 1 than from 0 to 2. However, there is no condition on the relation between k_{12} and k_{02}. In fact, we can have k_{12} much larger than k_{02}, meaning that once a vertex transitions from state 0 to 1, it is very difficult to then transition to state 2. For this reason, we consider the additional inequality $k_{02} \geq k_{01} + k_{12}$. This means that if v is the only vertex to change state in two consecutive time steps, all else being the same, it is easier for v to transition $0 \to 1 \to 2$ than it is for it to transition directly from state 0 to state 2. (Even for a strict equality $[k_{02} = k_{01}+k_{12}]$, the two transitions will be easier than one because when v is in state 0 (1), $x_v = 0$ ($x_v = 1$), producing different contributions to σ_v for a transition to state 2.) A similar argument holds for down transitions starting from state 2. These are the conditions (TOPTCs) from Equation (3.7) which are used in the next lemma.

Lemma 20. *With the same conditions as in Theorem 17 where we additionally impose the TOPTCs of Equation* (3.7)*, the map* $\mathbf{F}_w$ *has only fixed points as limit sets when the following conditions are met:*

(*i*) $\Delta_{01} \leq \min\{-C_1 - 1, C_1 + 3\}$,

(*ii*) $\Delta_{12} \leq \min\{C_1 - C_2 - 3, -C_1 + C_2 + 5\}$,

(*iii*) $\Delta_{12}+\Delta_{01}-2k_{01}-2k_{12} \leq -C_2-1$ *[equivalently,* $k_{21}-3k_{12}+k_{10}-3k_{01} \leq -C_2-1$*], and*

(*iv*) $\Delta_{12}+\Delta_{01}+2k_{10}+2k_{21} \leq C_2+11$ *[equivalently,* $3k_{21}-k_{12}+3k_{10}-k_{01} \leq C_2+11$*].*

where C_1 *and* C_2 *are constants.*

Proof. The additional restrictions on thresholds do not affect transitions $0 \leftrightarrow 1$ and $1 \leftrightarrow 2$, so conditions (*i*) and (*ii*) are as in Theorem 17. For the transition $0 \to 2$, we substitute $k_{02} \geq k_{01} + k_{12}$, in the form $-4k_{02} \leq -4k_{01} - 4k_{12}$, into the last line of Equation (3.15) to obtain $\Delta P_{02} = P_2 - P_0 \leq (k_{21}-k_{12})+(k_{10}-k_{01})+C_2-2k_{01}-2k_{12}$, which must be -1 or less, leading to condition (*iii*). Similarly, we substitute $k_{20} \leq k_{21} + k_{10}$ into the last line of Equation (3.16) to obtain condition (*iv*). □

3.3.2 Bifurcations in Multithreshold GDS maps

It is natural to ask whether periodic orbits of length two or greater can arise when the conditions of Theorem 17 fail to hold. The following example shows that this

is indeed the case, and hence that the class of multithreshold systems undergoes bifurcations. These results answer Questions (II) and (IV).

Example 21. *Let* $X = \mathrm{Circ}_4$ *be the graph on four vertices as shown in the top left corner of Figure 3.3. Here we use threshold* $\boldsymbol{k} = (k_{01}, k_{10}, k_{12}, k_{21}, k_{02}, k_{20}) = (1, 4, 4, 6, 2, 5)$ *and sequential update. For this graph, there are at most* $\kappa(X) = 3$ *limit cycle structures, as we have shown in [51].*

For this particular class of maps, and for the given graph X*, it turns out that there are two cycle equivalence classes. That is, each permutation* $\pi \in S_X$ *induces a map* $\mathbf{F}_\pi$ *that has one of two periodic orbit structures. Representative update sequences for these two cycle structures are* $\pi_1 = (0, 1, 2, 3)$*, which induces a map* $\mathbf{F}_{\pi_1}$ *with cycle structure* $[1(2), 3(6)]$*, and* $\pi_2 = (0, 2, 1, 3)$ *which induces a map* $\mathbf{F}_{\pi_2}$ *with cycle structure* $[1(2), 2(6)]$*. Here the notation* $a(b)$ *means* b *cycles, all of length* a*. The periodic orbits of the two maps are shown in Figure 3.3. Note that the long-term dynamics does not decompose in the following sense: there are periodic orbits where all three states of* $K = \{0, 1, 2\}$ *occur. In principle, one could obtain periodic orbits of length larger than one that would only involve vertex states 0 and 1, see [46].*

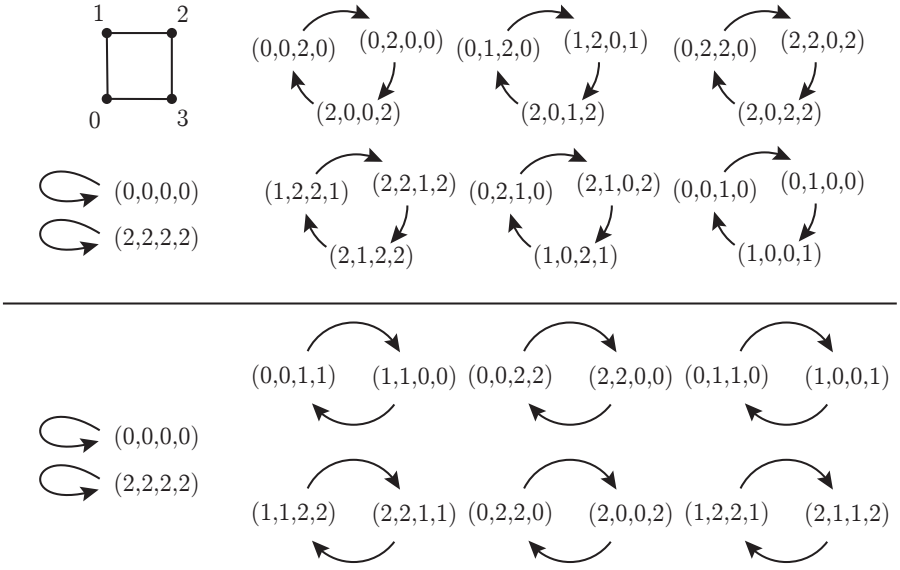

Figure 3.3: The two cycle structures for the multithreshold systems of Example 21. The update sequences in the top and bottom part of the diagram are $\pi_1 = (0, 1, 2, 3)$ and $\pi_2 = (0, 2, 1, 3)$, respectively.

The following proposition generalizes the results from Example 21.

Proposition 22. *There are asynchronous, multithreshold GDS maps* $\mathbf{F}\colon K^n \longrightarrow K^n$ *with periodic orbits of length at least* $n-1$.

Proof. We will show that the GDS map given by Equations (3.9) with thresholds

$$\boldsymbol{k} = (k_{01}, k_{10}, k_{12}, k_{21}, k_{02}, k_{20}) = (1, 4, 4, 6, 2, 5)$$

over the graph $X = \mathrm{Circ}_n$ and update sequence $\pi = (n, n-1, n-2, \ldots, 2, 1)$ has periodic orbits of length $n-1$ for all $n \geq 4$. Note that the ETCs are satisfied.

We set $x'_v = f_v(x[v])$ and handle the case $n \geq 5$ first. The case $n = 4$ will be treated separately. Also, let $x(t)$ denote the system state at time t, and consider the initial state $x(0) = (1, 2, 0, 0, \ldots, 0, 1)$ with $n-3$ consecutive states 0. The first vertex, n, of the permutation has a restricted state $x[n] = (x_1, x_{n-1}, x_n) = (1, 0, 1)$. Thus, $\sigma_n = 2 < k_{10} = 4$, and hence $x'_n = 0$. Vertex $n-1$ has restricted state $x[n-1] = (x_{n-2}, x_{n-1}, x'_n) = (0, 0, 0)$. We have $\sigma_{n-1} = 0$ and hence $x'_{n-1} = 0$. This last result is repeated for vertices $n-2$ down through vertex 4, and therefore $x'_i = 0$ for $i \in \{4, 5, \ldots, n-1\}$. For vertex 3, the restricted state is $v[3] = (x_2, x_3, x'_4) = (2, 0, 0)$ and because $\sigma_3 = 2 \geq k_{02} = 2$ one has $x'_3 = 2$. For vertex 2, the restricted state is $x[2] = (x_1, x_2, x'_3) = (1, 2, 2)$ and thus $\sigma_2 = 5 < k_{21} = 6$; note that $\sigma_2 \not< k_{20} = 5$. Therefore, $x'_2 = 1$. For vertex 1, $x[1] = (x_1, x'_2, x'_n) = (1, 1, 0)$; then $\sigma_1 = 2 < k_{10} = 4$, and so $x'_1 = 0$. This completes the first update of all vertices in the order given by π and we have $x(1) = (0, 1, 2, 0, \ldots, 0)$ where there are $n-3$ consecutive vertices in state 0.

We now compute $x(2)$ from $x(1)$. The first vertex, n, has a restricted state $x[n] = (x_1, x_{n-1}, x_n) = (0, 0, 0)$ and consequently $\sigma_n = 0$ so $x'_n = 0$. This same outcome is repeated for vertices $n-1$ through 5 so that $x'_i = 0$ for $i \in \{5, \ldots, n\}$. For vertex 4, $x[4] = (x_3, x_4, x'_5) = (2, 0, 0)$. Thus, $\sigma_4 = 2 \geq k_{02} = 2$, and $x'_4 = 2$. For vertex 3, $x[3] = (x_2, x_3, x'_4) = (1, 2, 2)$. So $\sigma_3 = 5 < k_{21} = 6$ and $x'_3 = 1$ (note $\sigma_3 \not< k_{20} = 5$). For vertex 2, $x[2] = (x_1, x_2, x'_3) = (0, 1, 1)$; then $\sigma_2 = 2 < k_{10} = 4$ and $x'_2 = 0$. Finally, for vertex 1, $x[1] = (x_1, x'_2, x'_n) = (0, 0, 0)$; so $\sigma_0 = 0 < k_{01}$, k_{02}; so $x'_1 = 0$. The final state is therefore $x(2) = (0, 0, 1, 2, 0, \ldots, 0)$ where the last $n-4$ vertex states are 0.

Comparing the last two system states, we see that the vertices with states 1 and 2 shift to the right by one entry, and it can be verified that this process will continue until the system state is $(0, 0, \ldots, 0, 1, 2, 0)$. From state $x(1)$, there is a total of $n-3$

such system states, generated by $n-4$ system state transitions. To this point, there are $1+(n-3)=n-2$ system states. There is one more state in the cycle.

For the last state, vertex n has restricted state $x[n]=(x_1,x_{n-1},x_n)=(0,2,0)$. Therefore $\sigma_n=2\geq k_{02}=2$ and $x'_n=2$. For vertex $n-1$, $x[n-1]=(x_{n-2},x_{n-1},x'_n)=(1,2,2)$ and $\sigma_{n-1}=5$ and therefore $x'_{n-1}=1$. For vertex $n-2$, $x[n-2]=(x_{n-3},x_{n-2},x'_{n-1})=(0,1,1)$, so $\sigma_{n-2}=2$, and because $\sigma_{n-2}<k_{10}=4$, we have $x'_{n-2}=0$. For vertex $n-3$ one has $x[n-3]=(x_{n-4},x_{n-3},x'_{n-2})=(0,0,0)$ and therefore $\sigma_{n-3}=0$, producing $x'_{n-3}=0$. This last result holds for vertices down through and including vertex 2, that is, $x'_i=0$ for $i\in\{2,\ldots,n-2\}$. For vertex 1, $x[1]=(x_1,x'_2,x'_n)=(0,0,2)$, so $\sigma_1=2\geq k_{02}=2$ and $x'_1=2$. From the resulting state $x(n-1)=(2,0,0,\ldots,0,1,2)$, it can be verified that the next state is $x(0)$, the initial state. Thus, a cycle of length $n-1$ is generated for the case $n\geq 5$.

For the case $n=4$, the same structure in states and state transitions holds, but in each system state, there is only one zero. For the initial state $x(0)=(1,2,0,1)$, we have successive states $(0,1,2,0)$, and $(2,0,1,2)$, with the last state transitioning back to $x(0)$, thus producing an $(n-1)$-cycle. □

Remark 23. *All vertices in* Circ_n *in the proof of Proposition 22 transition among states as follows: 0, 2, 1, and back to zero. Further, there is another cycle of length* $n-1$*, containing state* $x=(2,1,0,0,\ldots,0,2)$*, and for the same permutation, where vertices visit states in the order 0, 1, 2, and back to 0. Thus, all states are visited by all vertices in some cycles, and consequently, there is no decomposition in a trivial way to the Boolean case.*

We also note that the multiplicity of cycles of length $n-1$ increases as n increases. For example, for Circ_4 through Circ_{10} inclusive, the multiplicities of the numbers of cycles of length $n-1$ are, respectively, 6, 12, 30, 65, 162, 381, and 940. Thus, a factor of 2.5 increase from $n=4$ to 10 results in a factor of 156.7 ($=940/6$) increase in multiplicity. Finally, we note that Proposition 22 holds for $n=3$, but each of the three 2-cycles involves exactly 2 of 3 possible vertex states. For example, a 2-cycle arises between states $(0,2,0)$ and $(2,0,2)$.

As the following example shows, long cycles also arise for the 1-transition multithreshold systems with functions $\tau^1_{v,\boldsymbol{k}}$. The following result demonstrates that arbitrarily long cycles can be generated in multithreshold dynamical systems when only 1-hop transitions are permitted.

Proposition 24. *There exist asynchronous, 1-hop multithreshold GDS maps where* $\mathbf{F}\colon K^n\longrightarrow K^n$ *have periodic orbits of length at least* $n-1$*.*

Proof. We will show that the GDS map given by the 1-hop vertex functions of Equations (3.5) with thresholds $\boldsymbol{k} = (k_{01}, k_{10}, k_{12}, k_{21}) = (1, 3, 4, 6)$, over the graph $X = \mathrm{Circ}_n$ with update sequence $\pi = (1, 2, \ldots, n-1, n)$ has periodic orbits of length $n-1$ for all $n \geq 5$. Note that the ETCs are again satisfied. Also, the two FPCs of Corollary 19 are not satisfied. The RHSs of the two inequalities are maximum when $C_1 = -2$ and $C_2 = -6$, giving $\Delta_{01} \leq 1$ and $\Delta_{12} \leq 1$ for the FPCs. Here, we have $\Delta_{01} = \Delta_{12} = 2$, so that the two FPCs are at the boundary of producing fixed points.

We set $x'_v = f_v(x[v])$ and handle the case $n \geq 6$ first. Then $n = 5$ is treated as a special case. Consider the initial state $x(0) = (0, \ldots, 0, 1, 2, 1, 0)$ with $n-4$ consecutive states 0. For the given permutation, we have $x'_i = 0$ for $i \in \{1, 2, \ldots, n-5\}$ because the restricted state for each x_i is $x[i] = (0, 0, 0)$, so $\sigma_i = 0 < k_{01} = 1$. To compute x'_{n-4}, we have $x[n-4] = (x'_{n-5}, x_{n-4}, x_{n-3}) = (0, 0, 1)$ and hence $x'_{n-4} = 1$ because $\sigma_{n-4} = 1 \geq k_{01}$. Since $x[n-3] = (1, 1, 2)$, $\sigma_{n-3} = 4 \geq k_{12} = 4$, and so $x'_{n-3} = 2$. Similarly, $x[n-2] = (2, 2, 1)$, and therefore $\sigma_{n-2} = 5 < k_{21} = 6$ and consequently $x'_{n-2} = 1$. With $x[n-1] = (1, 1, 0)$, we have $\sigma_{n-1} = 2 < k_{10} = 3$; thus, $x'_{n-1} = 0$. For vertex n, $x[n] = (0, 0, 0)$, and so $x'_n = 0$. We have the state at $t = 1$ of $x(1) = (0, \ldots, 0, 1, 2, 1, 0, 0)$.

The state transition just described effectively reduces by one the vertex which starts the unique sequence of three consecutive vertex states (1,2,1). This pattern repeats for $t = 2$ through $t = n-5$, giving $x(n-5) = (0, 1, 2, 1, 0, \ldots, 0)$; the latter state has the feature that the three states (1,2,1) start at vertex 2. Including the initial state, this pattern consists of $n-4$ states. It can be verified that the next three states are $x(n-4) = (1, 2, 1, 0, \ldots, 0, 1)$, $x(n-3) = (2, 1, 0, \ldots, 0, 1, 2)$, and $x(n-2) = (1, 0, \ldots, 0, 1, 2, 1)$. From $x(n-2)$, the next state is $x(0)$, thus producing a cycle of length $n-1$. This finishes the proof for the case $n \geq 6$.

The case $n = 5$ requires only a slight modification in the above argument. Specifically, the initial state is $x(0) = (0, 1, 2, 1, 0)$ and hence this state is also the state at $x(n-5)$ given above. Here, then, the states $x(1)$, $x(2)$, and $x(3)$ are, respectively, the states given above as $x(n-4)$, $x(n-3)$, and $x(n-2)$, except that the sequence of $n-4$ consecutive vertex state values of 0 is reduced to a single vertex. Here, the transition from $x(3)$ results in $x(0)$ and hence we have a 4-cycle for $n = 5$. □

We note that in the foregoing construction, all vertices visit all states.

3.3.3 Quality of FPC Bounds

A natural question arises for the quality of the fixed point conditions of Theorem 17. For example, to obtain cycles of length two or greater, is it sufficient to have just one condition fail for one vertex? For a regular graph and a GDS map with uniform thresholds, is it sufficient that just one of the conditions fails to hold? The following result illustrates that it is enough that one condition can fail to hold, and thereby answers Question (III). Further, when only one FPC does not hold, limit cycles can be arbitrarily large, addressing Question (IV). Hence, a necessary condition for the length of limit cycles > 1 is that at least one FPC not hold.

Proposition 25. *There exist asynchronous multithreshold GDS maps* $\mathbf{F}\colon K^n \longrightarrow K^n$ *for which the FPCs of Theorem 17 are tight bounds. Moreover, the cycles in the orbits arising in the bifurcations can be arbitrarily large.*

Proof. Each of four cases are addressed in turn. For each case, one FPC is minimally violated while the other three FPCs are satisfied. The $\boldsymbol{k}$s and the FPC violated are

1. Threshold: $\boldsymbol{k} = (1, 3, 6, 6, 4, 5)$ — Failed FPC: (i)
2. Threshold: $\boldsymbol{k} = (1, 1, 4, 6, 4, 4)$ — Failed FPC: (ii)
3. Threshold: $\boldsymbol{k} = (2, 2, 6, 6, 2, 5)$ — Failed FPC: (iii)
4. Threshold: $\boldsymbol{k} = (1, 2, 4, 5, 2, 5)$ — Failed FPC: (iv) .

We show in each case that cycles of length $n-1$ can be produced in the graph $X = \mathrm{Circ}_n$ for $n \geq 4$. Thus, cycles of arbitrary length can be generated by suitable choice of n. Each case involves a different $\boldsymbol{k} = (k_{01}, k_{10}, k_{12}, k_{21}, k_{02}, k_{20})$. In all cases, we set $C_1 = -2$ and $C_2 = -6$ in order to maximize the RHSs of FPCs (i) and (ii), giving the FPCs as: (i) $\Delta_{01} \leq 1$; (ii) $\Delta_{12} \leq 1$; (iii) $(k_{21} + k_{12}) + (k_{10} + k_{01}) - 4k_{02} \leq 5$; and (iv) $-(k_{21} + k_{12}) - (k_{10} + k_{01}) + 4k_{20} \leq 5$. We use permutation $\pi = (1, 2, \ldots, n-1, n)$ in all cases.

FPC (i) is not satisfied; FPCs (ii)–(iv) are satisfied.

Let $\boldsymbol{k} = (1, 3, 6, 6, 4, 5)$. It can be verified that all four FPCs are satisfied except (i), and that FPC (i) is on the boundary; i.e., $\Delta_{01} = 2$.

Let the initial state be $x(0) = (0, 0, \ldots, 0, 1, 0)$. Vertex 1 is the first of the permutation, and its restricted state at $t = 1$ is $x[1] = (x_1, x_2, x_n) = (0, 0, 0)$. Thus, $\sigma_1 = 0 < k_{01} = 1$ and so $x'_1 = 0$. This result holds for the first $n - 3$ vertices and so $x'_i = 0$ for $i \in \{1, \ldots, n - 3\}$. For vertex $n - 2$, we have $x[n - 2] = (0, 0, 1)$ and thus $\sigma_{n-2} = 1 \geq k_{01}$, and hence $x'_{n-2} = 1$. For vertex $n - 1$, we have $x[n - 1] = (1, 1, 0)$; $\sigma_{n-1} = 2 < k_{10} = 3$ and $x'_{n-1} = 0$. For vertex n, we have $x[n] = (x'_1, x'_{n-1}, x_n) = (0, 0, 0)$; $\sigma_n = 0 \ngeq k_{01} = 1$, so $x'_n = 0$. The system state at $t = 1$ is accordingly $x(1) = (0, 0, \ldots, 1, 0, 0)$.

In effect, the single vertex ID whose state is 1 has decreased by one in going from $x(0)$ to $x(1)$, the other vertex states being 0. This pattern of shifting state 1 to the left by one vertex repeats $n - 3$ times, for a total of $n - 2$ system states, where $x(n - 3) = (0, 1, 0, \ldots, 0)$.

The next state, $x(n-2)$, begins with vertex 1, with restricted state $x[1] = (x_1, x_2, x_n) = (0, 1, 0)$. So $\sigma_1 = 1 \geq k_{01}$ and so $x'_1 = 1$. For x_2, $x[2] = (x'_1, x_2, x_3) = (1, 1, 0)$, and because $\sigma_2 = 2 < k_{10} = 3$, $x'_2 = 0$. For vertex 3, $x[3] = (x'_2, x_3, x_4) = (0, 0, 0)$ and $x'_3 = 0$. The result for vertex 3 repeats a total of $n-3$ times, meaning that this takes us to the update of the last vertex, n. Since $x[n] = (x'_1, x'_{n-1}, x_n) = (1, 0, 0)$, we have $\sigma_n = 1 \geq k_{01}$ and $x'_n = 1$. Thus, the system state is $x(n - 2) = (1, 0, \ldots, 0, 1)$. It can be verified that $x(n - 2)$ transitions to $x(0)$, giving $n - 1$ states in the cycle for Circ_n.

Now, consider an increase of k_{01} by one, to 2, so that $\boldsymbol{k} = (2, 3, 6, 6, 4, 5)$. FPC (i) is now just satisfied; i.e., $\Delta_{01} = k_{10} - k_{01} = 3 - 2 = 1$, and it can be verified that the other three FPCs remain satisfied. Therefore, by Theorem 17, the only limit points are fixed points. Hence, the bifurcation at the boundary for FPC (i) can be made arbitrarily large by suitable choice of n.

FPC (ii) is not satisfied; FPCs (i), (iii), and (iv) are satisfied.

Let $\boldsymbol{k} = (1, 1, 4, 6, 4, 4)$ and hence FPC (ii) gives $\Delta_{12} = 2$, which is at the boundary of the FPCs. Let the initial state be $x(0) = (1, 1, \ldots, 1, 2, 1)$. Vertex 1 is the first of the permutation, and its restricted state at $t = 1$ is $x[1] = (x_1, x_2, x_n) = (1, 1, 1)$. Therefore, $\sigma_1 = 3$, and since $1 = k_{10} < \sigma_1 < k_{12} = 4$, $x'_1 = 1$. That is, vertex 1 does not change state. This result holds for the first $n - 3$ vertices and so $x'_i = 1$ for $i \in \{1, \ldots, n - 3\}$. For vertex $n - 2$, we have $x[n - 2] = (1, 1, 2)$ and thus $\sigma_{n-2} = 4 \geq k_{12} = 4$ and hence $x'_{n-2} = 2$. For vertex $n-1$, we have $x[n-1] = (2, 2, 1)$; $\sigma_{n-1} = 5 < k_{21} = 6$ (but $\sigma_{n-1} \not< k_{20} = 4$) and so $x'_{n-1} = 1$. For vertex n, we have $x[n] = (x'_1, x'_{n-1}, x_n) = (1, 1, 1)$ and $\sigma_n = 3$. So vertex n does not change state; i.e.,

$x'_n = 1$. The system state at $t = 1$ is accordingly $x(1) = (1, 1, \ldots, 2, 1, 1)$.

The change from $x(0)$ to $x(1)$ is that the sole vertex in state 2 is reduced by one; i.e., the state 2 shifts left by one vertex. There is a total of $n-3$ such transitions starting from $x(0)$ and hence $x(n-3) = (1, 2, 1, \ldots, 1)$. It is straight-forward to verify that the next state is $x(n-2) = (2, 1, \ldots, 1, 2)$, and using the same procedures, that $x(n-2)$ transitions to $x(0)$. Thus, there are $n-1$ states forming a cycle.

If we increase k_{12} by one, we obtain the threshold vector $\boldsymbol{k} = (1, 1, 5, 6, 4, 4)$. Now all FPCs are satisfied, where FPC (ii) is just satisfied at the boundary. By Theorem 17, the only limit points are fixed points. Thus, we can establish an arbitrarily large bifurcation at the boundary of FPC (ii) by suitable choice of n.

FPC (iii) is not satisfied; FPCs (i), (ii), and (iv) are satisfied.

Let $\boldsymbol{k} = (2, 2, 6, 6, 2, 5)$ and hence FPC (iii) gives $4 + 12 - 4(2) = 8 \not\leq 5$, which is at the boundary of the FPC. That is, if k_{02} is increased by 1 to 3, then FPC (iii) is satisfied because $4 + 12 - 4(3) = 4 \leq 5$. It can be verified that $\boldsymbol{k}$ satisfies the remaining FPCs.

Let the initial state be $x(0) = (0, 0, \ldots, 0, 2, 0)$. Vertex 1 is the first of the permutation, and its restricted state at $t = 1$ is $x[1] = (x_1, x_2, x_n) = (0, 0, 0)$. Therefore, $\sigma_1 = 0 < k_{01} = 2$, and thus $x'_1 = 0$. This result holds for the first $n-3$ vertices and so $x'_i = 1$ for $i \in \{1, \ldots, n-3\}$. For vertex $n-2$, we have $x[n-2] = (0, 0, 2)$ and thus $\sigma_{n-2} = 2$. Since $\sigma_1 \geq k_{01} = 2$ and $\sigma_1 \geq k_{02} = 2$, $x'_{n-2} = 2$ because we make the maximal transition per Equation (3.4). For vertex $n-1$, we have $x[n-1] = (2, 2, 0)$; $\sigma_{n-1} = 4$. Since $\sigma_{n-1} < k_{21} = 6$ and $\sigma_{n-1} < k_{20} = 5$, we have $x'_{n-1} = 0$ because the maximal transition is made. For vertex n, we have $x[n] = (x'_1, x'_{n-1}, x_n) = (0, 0, 0)$; $\sigma_n = 0$, so vertex n remains in state 0. The system state at $t = 1$ is $x(1) = (0, 0, \ldots, 0, 2, 0, 0)$.

Again we see that in going from $x(0)$ to $x(1)$, the vertex whose state is 2 decreases by one, effectively shifting state 2 left by one. This process repeats a total of $n-3$ times, producing $x(n-3) = (0, 2, 0, \ldots, 0)$. It can be verified that the next state is $x(n-2) = (2, 0, \ldots, 0, 2)$ and that the subsequent state is $x(0)$, resulting in a cycle of length $n-1$.

Now, as shown at the beginning of this portion of the proof, increasing k_{02} by 1, so that $\boldsymbol{k} = (2, 2, 6, 6, 3, 5)$, just satisfies FPC (iii). It can be verified that all FPCs are satisfied and therefore by Theorem 17, $\boldsymbol{k}$ generates only fixed points as limit cycles. Thus, we can establish arbitrarily large bifurcations at the boundary of satisfying

FPC (*iii*).

FPC (*iv*) is not satisfied; FPCs (*i*)–(*iii*) are satisfied.

Let $\boldsymbol{k} = (1, 2, 4, 5, 2, 5)$ and hence FPC (*iv*) gives $-3 - 9 + 4(5) = 8 \not\leq 5$, which is at the boundary of the FPC. That is, if k_{20} is decreased by 1 to 4, then FPC (*iv*) is satisfied because $-3 - 9 + 4(4) = 4 \leq 5$. It can be verified that $\boldsymbol{k}$ satisfies the remaining FPCs.

We first address the case $n \geq 5$; then we will handle $n = 4$. Let the initial state be $x(0) = (0, 0, \ldots, 0, 1, 2, 0)$. The restricted state for vertex 1 at $t = 1$ is $x[1] = (x_1, x_2, x_n) = (0, 0, 0)$. Therefore, $\sigma_1 = 0 < k_{01} = 1$, and thus $x'_1 = 0$. This result holds for the first $n - 4$ vertices and so $x'_i = 0$ for $i \in \{1, \ldots, n - 4\}$. For vertex $n - 3$, we have $x[n - 3] = (0, 0, 1)$ and thus $\sigma_{n-3} = 1$. Since $\sigma_1 \geq k_{01} = 1$, $x'_{n-3} = 1$. For vertex $n - 2$, we have $x[n - 2] = (1, 1, 2)$; $\sigma_{n-2} = 4$. Since $\sigma_{n-2} \geq k_{12} = 4$, we have $x'_{n-2} = 2$. For vertex $n - 1$, we have $x[n - 1] = (2, 2, 0)$; $\sigma_{n-1} = 4$. Since $k_{21} = k_{20} = 5$, the largest transition is to state 0, and hence $x'_{n-1} = 0$. For vertex n, we have $x[n] = (x'_1, x'_{n-1}, x_n) = (0, 0, 0)$; $\sigma_n = 0$, so vertex n remains in state 0. The system state at $t = 1$ is $x(1) = (0, 0, \ldots, 0, 1, 2, 0, 0)$.

The transition $x(0)$ to $x(1)$ is repeated a total of $n - 4$ times, involving $n - 3$ states and finally producing $x(n - 4) = (0, 1, 2, 0, \ldots, 0)$. It can be verified that the next two states are $(1, 2, 0, \ldots, 0, 1)$ and $(2, 0, \ldots, 0, 1, 2)$. The latter state transitions to $x(0)$, generating a cycle of length $n - 1$.

If k_{20} is decreased by 1 to 4, as described above, then FPC (*iv*) is satisfied, as are the other FPCs, and hence by Theorem 17, the system produces only fixed points. Thus, by choice of n, arbitrarily large bifurcations can be generated at the boundary of FPC (*iv*).

The case $n = 4$ is handled by verifying that $x(0) = (0, 1, 2, 0)$, $x(1) = (1, 2, 0, 1)$, and $x(2) = (2, 0, 1, 2)$, with $x(2)$ transitioning to $x(0)$.

These cases, taken in totality, show that the magnitude of bifurcations; i.e., how large a limit cycle can be at the boundary of the FPCs, compared to the limit cycle of 1 for fixed points, can be arbitrarily large by choosing n for the graph Circ_n. □

We demonstrate that the FPCs of Corollary 19 for the 4-transition, 3-vertex state system can be tight by building on the construction and result of Proposition 24.

Proposition 26. *There exist asynchronous, 1-hop multithreshold GDS maps of the*

form $\mathbf{F}\colon K^n \longrightarrow K^n$ *for which the FPCs of Corollary 19 are tight bounds. Moreover, the bifurcations caused by the FPCs can be arbitrarily large.*

Proof. Consider the graph $X = \mathrm{Circ}_n$ with $n \geq 5$ and update sequence $(1, 2, \ldots, n)$. Our approach is to begin with a threshold vector $\boldsymbol{k} = (k_{01}, k_{10}, k_{12}, k_{21})$ that satisfies the FPCs of Corollary 19, thus producing a GDS that generates only fixed points as limit cycles. We then change by one unit a particular threshold value, in turn, so that one of the two FPCs is not satisfied. We show in these cases that arbitrarily long limit cycles are produced when the FPCs are minimally violated; i.e., that bifurcations can be arbitrarily large when even one of the FPCs does not hold. We then show that if both conditions are violated by the minimal amount, long limit cycles are also produced, and in this case, all vertices visit all three states. From the proof of Proposition 24, the conditions that maximize the RHSs of the FPCs of Corollary 19 are $C_1 = -2$ and $C_2 = -6$, giving $\Delta_{01} \leq 1$ and $\Delta_{12} \leq 1$. These threshold conditions represent the boundary or limits of the FPCs.

FPC (i) satisfied; FPC (ii) satisfied.

Let $\boldsymbol{k}_0 = (1, 2, 5, 6)$ so that $\Delta_{01} = \Delta_{12} = 1$, which satisfy the FPCs at the boundary and hence by Corollary 19, the GDS produces only fixed points as limit cycles.

FPC (i) satisfied; FPC (ii) not satisfied

Starting with $\boldsymbol{k}_0$ above, decrease k_{12} by one so that $\boldsymbol{k} = (1, 2, 4, 6)$. Now $\Delta_{01} = 1$ and $\Delta_{12} = 2$; therefore FPC (i) is satisfied while (ii) is not. We now show that these thresholds give rise to arbitrarily large cycles that only involve vertex states 1 and 2.

Let the initial system state be $x(0) = (1, 1, \ldots, 1, 2, 1)$. Since $x[1] = (x_1, x_2, x_n) = (1, 1, 1)$, we have $\sigma_1 = 3$, and because $2 = k_{10} \leq \sigma_1 < k_{12} = 4$, the state of vertex 1 remains unchanged; i.e., $x_1' = 1$. This same result also applies to vertices 2 through $n - 3$ for the same reason, giving in total $x_i' = 1$ for $i \in \{1, 2, \ldots, n - 3\}$. For vertex $n - 2$, $x[n - 2] = (1, 1, 2)$ and so $\sigma_{n-2} = 4 \geq k_{12}$. Therefore, $x_{n-2}' = 2$. Vertex $n - 1$ has $x[n - 1] = (2, 2, 1)$, giving $\sigma_{n-1} = 5 < k_{21} = 6$, and so $x_{n-1}' = 1$. For the last vertex in the update sequence, we have $x[n] = (x_1', x_{n-1}', x_n) = (1, 1, 1)$, yielding $\sigma_n = 3$, and since $k_{10} \leq \sigma_n < k_{12}$, we have $x_n' = 1$. Thus, $x(1) = (1, \ldots, 1, 2, 1, 1)$.

Comparing $x(0)$ to $x(1)$, we see that the unique sequence of three consecutive vertices that has states $(1, 2, 1)$ has "shifted left" (i.e., the vertex whose state begins this 3-vertex state sequence decreases by one). Using the same procedures as above, this pattern continues for system states up through and including $x(n - 3) =$

$(1, 2, 1, \ldots, 1)$. Accordingly, we have thus far $n-2$ unique system states. It can be verified that the next system state is $x(n-2) = (2, 1, \ldots, 1, 2)$, and that the subsequent state transition produces $x(0)$. We have produced a limit cycle of length $n-1$ when only the first of the two FPCs of Corollary 19 is satisfied.

FPC (i) not satisfied; FPC (ii) satisfied

Starting with $\boldsymbol{k}_0$ above, increase k_{10} by one so that $\boldsymbol{k} = (1, 3, 5, 6)$. Now $\Delta_{01} = 2$ and $\Delta_{12} = 1$. Therefore FPC (i) is not satisfied while (ii) is. We now show that these thresholds give rise to arbitrarily large cycles that only involve vertex states 0 and 1.

Let the initial system state be $x(0) = (0, 0, \ldots, 1, 0)$. Then $x[1] = (x_1, x_2, x_n) = (0, 0, 0)$, so $x_1' = 0$. For the same reason, we have in total that $x_i' = 0$ for $i \in \{1, 2, \ldots, n-3\}$. For vertex $n-2$, $x[n-2] = (0, 0, 1)$ and with $1 = \sigma_1 \geq k_{01} = 1$, we get $x_{n-2}' = 1$. For vertex $n-1$, $x[n-1] = (1, 1, 0)$, so that $2 = \sigma_{n-1} < k_{10} = 3$, and hence $x_{n-1}' = 0$. Analogously, $x_n' = 0$. The state at $t = 1$ is $x(1) = (0, \ldots, 0, 1, 0, 0)$.

On comparing $x(0)$ to $x(1)$, we see that the unique sequence of three consecutive vertices that has states $(0, 1, 0)$ has "shifted left." This pattern continues for system states up through and including $x(n-3) = (0, 1, 0, \ldots, 0)$. At this point, there are $n-2$ unique system states. It is straight-forward to verify that $x(n-2) = (1, 0, \ldots, 0, 1)$, and that the next state transition produces $x(0)$, thus generating a length $n-1$ limit cycle when only the second of the two FPCs of Corollary 19 is satisfied.

FPC (i) not satisfied; FPC (ii) not satisfied

Starting with $\boldsymbol{k}_0$ above, increase k_{10} by one and decrease k_{12} by one, giving $\boldsymbol{k} = (1, 3, 4, 6)$. Now $\Delta_{01} = \Delta_{12} = 2$. Therefore, neither FPC (i) nor (ii) is satisfied. This threshold vector generates the GDS of Proposition 24. Thus, limit cycles of length $n-1$ are produced for Circ_n.

These cases again show that the magnitude of bifurcations in limit cycles, compared to the limit cycle of 1 for fixed points, can be arbitrarily large by choosing n for the graph Circ_n. □

Remark 27. *For the 4-transition system, if FPC (i) of Corollary 19 is satisfied and FPC (ii) is not, then limit cycles of length > 1 may only possess vertex states of 1 and 2. Similarly, if FPC (ii) is satisfied and FPC (i) is not, then limit cycles of length > 1 may only be comprised of vertex states of 0 and 1.*

Remark 28. *Even if, say, cycles are only observed between system states where all vertex states are in either state 0 or state 1, the FPC for transitions to state 2 must be satisfied, in general, because satisfying the FPCs for* $0 \leftrightarrow 1$ *may drive the system into cycles that include vertex states of 2.*

3.4 The r-State Multithreshold Model

In this section we generalize results derived in the previous section to the case where the vertex state set is $K = \{0, 1, 2, \ldots, r-1\}$. As before, we will consider the vertex functions $\tau_{v,\boldsymbol{k}}$ and $\tau^1_{v,\boldsymbol{k}}$ from Equations (3.4) and (3.5). We omit writing out these functions as in we did in Equation (3.9).

3.4.1 Potential Functions and Fixed Point Conditions

We give a general approach for constructing potential functions and associated fixed point conditions for the case $K = \{0, 1, 2, \ldots, r-1\}$. For vertex v, the construction involves σ_v, the vertex thresholds, the quantities $n_{l,v}$ for $l \in K$, and the transition criteria. The resulting potential functions, which are constructed so that each potential difference only involves the threshold values, allow us to derive conditions for which fixed points are the only possible limit sets.

Motivated by the case $r = 3$, we seek potential functions of the form

$$P_{m,v} = \sum_{s,t} a^m_{st} k_{st,v} + C_{m,v} + \sum_s c_{ms} n_{s,v} \ , \tag{3.17}$$

where the m-index references the state. In the following we will omit the subscript v since the potential differences considered only involve a single vertex v. Just as in the case $r = 3$, the potential in Equation (3.17) includes the potential of the vertex and its adjacent edges.

The construction, which determines the values of the a^m_{ij}s and the c_{ms}s, is done so that ΔP_{ij} only involves the thresholds k_{ij} and the constants C_m. The edge potentials are defined as before. Consider the case where vertex v transitions from state i to state j under the application of its vertex function. In this case, the potential difference

ΔP_{ij} is given by

$$\Delta P_{ij} = P_j - P_i = \sum_{s,t}(a^j_{st} - a^i_{st})k_{st} + \sum_s [c_{js} - c_{is}]n_s + C_j - C_i \tag{3.18}$$

$$= \sum_{s,t}(a^j_{st} - a^i_{st})k_{st} + \sum_s \gamma_{s,ij} n_s + C_j - C_i \; . \tag{3.19}$$

If the transition is an up-transition, we have $\sigma \geq k_{ij}$ where j is the maximal index for which this inequality holds. Similarly, if the transition is a down-transition, then $\sigma \leq k_{ij} - 1$ and j is minimal such that this holds. Our goal is to have the sum of all the terms involving the quantities n_s in Equation (3.18) be a suitable multiple of σ_v. If we can accomplish this, then we can eliminate all these terms by using the condition that σ_v satisfies for the appropriate transition. The fixed point conditions would then only involve the thresholds and the constants. A priori, it is not clear that we can accomplish this, but as Theorem 30 states, this is indeed possible.

Recall that $\sigma_v(x) = x_v + \sum_{s=1}^{r-1} s \cdot n_{s,v}(x)$. For a transition from $x_v = i$ to $x_v = j$ we have $\sigma = i + \sum_{s=1}^{r-1} s \cdot n_s$.

The $\gamma_{s,ij}$ are computed directly from the potentials. For example, in the 3-state system of Section 3.3, we have from Equation (3.14) for the $0 \to 1$ transition that $\gamma_{1,01} = -2$ and $\gamma_{2,01} = -4$; for the $1 \to 2$ transition that $\gamma_{1,12} = -2$ and $\gamma_{2,12} = -4$; for the $1 \to 0$ transition, $\gamma_{1,10} = -\gamma_{1,01}$ and $\gamma_{2,01} = -\gamma_{2,10}$; and for the $2 \to 1$ transition, $\gamma_{1,21} = -\gamma_{1,12}$ and $\gamma_{2,21} = -\gamma_{2,12}$.

For our construction, it is clear from the structure of σ that the ratios of the coefficients for $n_{l,v}$ and $n_{m,v}$ in ΔP_{ij} must satisfy

$$\beta_{lm,ij} := \frac{\gamma_{l,ij}}{\gamma_{m,ij}} = l/m \; . \tag{3.20}$$

Consider first the case where $j - i = 1$. Without loss of generality, we choose the coefficient on $n_{1,v}$ in ΔP_{ij} to be $\gamma_{1,ij} = \phi_b = -2$, and it follows that $\gamma_{l,ij} = l \cdot \phi_b$ for $1 \leq l \leq r-1$. That is, the contribution of all $n_{l,v}$ terms to ΔP_{ij} is $\phi_b \sigma = \sum_{l=1}^{r-1} l \cdot \phi_b \cdot n_{l,v}$. For an up-transition, the state transition criterion $\sigma_v \geq k_{ij}$ multiplied by ϕ_b gives $-2\sigma_v \leq -2k_{ij}$, and, modulo the constant term x_v in σ_v, this enables $-2\sigma_v$ to be exactly substituted for all $n_{l,v}$ terms in ΔP_{ij}. Since the foregoing involves only linear operations, we can generalize it to the transition $i \to j$ between any two states i and j by using

$$\gamma_{1ij} = \phi_{ij} = (j - i)\phi_b = (j - i)(-2) \tag{3.21}$$

and the substitution into ΔP_{ij} is now $\phi_{ij}\sigma = \sum_{l=1}^{r-1} \phi_{ij} \cdot l \cdot n_{l,v}$, with the remainder of the above description unchanged for $j - i > 0$. When $j - i < 0$, the state transition

criterion is $\sigma_v \leq k_{ij} - 1$ but the substitution of $\phi_{ij}\sigma$ still holds. Our last issue is the thresholds and constant term C_i that appear in the total vertex potentials. The coefficients for the thresholds are chosen from the set $\{-1, 0, 1\}$ in a manner such that adjacent transitions have potential difference ΔP_{ij} only involving Δ_{ij} and the constants C_i and C_j.

This turns out to be possible, and the construction is described algorithmically in Algorithm 1, which produces potentials in the form of Equation (3.17). The idea is to build out the potentials in steps. First, for each potential, terms involving the thresholds and constants are determined. Second, the terms in $n_{l,v}$ are established. The coefficient on $n_{1,v}$ for P_0 is set as 2. Then the remaining coefficients of $n_{l,v}$ in P_0 are computed from $n_{1,v}$. Finally, for each remaining potential P_j ($j \neq 0$), the coefficient on $n_{1,v}$ is computed from $n_{1,v}$ on P_0, and then the remaining $n_{l,v}$ for P_j are computed from its corresponding $n_{1,v}$ value. We write the algorithm in detail so that it may be coded; e.g., in Mathematica. An example result is given below.

Example 29. *Executing the procedure in Algorithm 1 for $r = 5$ gives the following potential functions.*

$$\begin{aligned}
P_4 &= [\ \ k_{10} + k_{21} + k_{32} + k_{43} + C_4\ \ ] - 6(n_{1,v} + 2n_{2,v} + 3n_{3,v} + 4n_{4,v}) \\
P_3 &= [\ \ k_{10} + k_{21} + k_{32} - k_{34} + C_3\ \ ] - 4(n_{1,v} + 2n_{2,v} + 3n_{3,v} + 4n_{4,v}) \\
P_2 &= [\ \ k_{10} + k_{21} - k_{23} - k_{34} + C_2\ \ ] - 2(n_{1,v} + 2n_{2,v} + 3n_{3,v} + 4n_{4,v}) \\
P_1 &= [\ \ k_{10} - k_{12} - k_{23} - k_{34} + C_1\ \ ] \\
P_0 &= [-k_{01} - k_{12} - k_{23} - k_{34}\ \ ] + 2(n_{1,v} + 2n_{2,v} + 3n_{3,v} + 4n_{4,v})
\end{aligned}$$

We are now in a position to state the FPCs for an r-state GDS.

Theorem 30. *If ϕ_{ij} is as in Equation* (3.21)*, and the potentials P_i are constructed using Algorithm 1, then each potential difference ΔP_{ij} has the desired form involving only the thresholds, constant terms and multiples of σ. For an up-transition $i \to j$, the fixed point condition is*

$$\Gamma_{ij}^{\text{up}} := \sum_{l=i}^{j-1}(k_{l,l+1} + k_{l+1,l}) + \phi_{ij}k_{ij} \leq C_i - C_j + i\phi_{ij} - 1\ , \tag{3.22}$$

and for a down-transition $i \to j$, the fixed point condition is

$$\Gamma_{ij}^{\text{down}} := \sum_{l=j}^{i-1} -(k_{l,l+1} + k_{l+1,l}) + \phi_{ij}k_{ij} \leq C_i - C_j + (i+1)\phi_{ij} - 1\ . \tag{3.23}$$

Algorithm 1: Compute the complete potential function for each vertex state.

input : The number r of states in the dynamical system. (States are 0 through $r-1$.)

output: The expressions for the potential functions P_j $(0 \leq j \leq r-1)$.

// Form potential terms in thresholds and constants.

Construct $P_{r-1} \longleftarrow \left[\sum_{p=0}^{r-2} k_{p+1,p}\right] + C_{r-1}$.

for *($j = r-2$* **to** *0)* **do**

  Construct $P_j \longleftarrow P_{j+1}$.

  Remove from P_j the $k_{j+1,j}$ term and replace it with $-k_{j,j+1}$.

  Remove from P_j the constant C_{j+1} and replace it with C_j.

  if *($j == 0$)* **then**

    Set $C_j \longleftarrow 0$.

// To these potentials add the terms in $n_{l,v}$ $(1 \leq l \leq r-1)$.

// c_{jl} is the coefficient of $n_{l,v}$ in P_j.

Set $c_{01} \longleftarrow 2$.

for *($l = 2$* **to** *$r-1$)* **do**

  Set $c_{0l} \longleftarrow l c_{01}$.

  Set $P_0 \longleftarrow P_0 + c_{0l} n_{l,v}$.

for *($j = 1$* **to** *$r-1$)* **do**

  Set $\gamma_{1,0j} \longleftarrow (j-0)(-2)$.

  Set $c_{j1} \longleftarrow \gamma_{1,0j} + c_{01}$.

  Set $P_j \longleftarrow P_j + c_{j1} n_{1,v}$.

  for *($l = 2$* **to** *$r-1$)* **do**

    Set $c_{jl} \longleftarrow l c_{j1}$.

    Set $P_j \longleftarrow P_j + c_{jl} n_{l,v}$.

Return all P_j expressions.

Proof. We first consider an arbitrary up-transition $i \to j$ where $j > i$, by producing the terms of ΔP_{ij} involving (i) thresholds, (ii) constant terms, and (iii) terms of $n_{l,v}$. Let $j - i = m_{ij} \geq 1$. Consider the terms k_{pq} in ΔP_{pq} where $q - p = 1$. From the first **for** loop in Algorithm 1, examining only the threshold terms, we see that the only difference between P_{j+1} and P_j is that P_{j+1} contains $k_{j+1,j}$ whereas P_j contains $-k_{j,j+1}$. Thus, for ΔP_{pq}, we obtain the threshold term $k_{qp} - (-k_{pq}) = k_{qp} + k_{pq}$. Since P_k is linear in thresholds, for $u - q = 1$ we have $\Delta P_{pu} = \Delta P_{pq} + \Delta P_{qu}$. This produces threshold terms $(k_{qp} + k_{pq}) + (k_{uq} + k_{qu})$. Using induction on $u - q$, we have that for $m_{ij} \geq 1$

$$\begin{aligned} \text{threshold terms in } \Delta P_{ij} &= (k_{i,i+1} + k_{i+1,i}) + (k_{i+1,i+2} + k_{i+2,i+1}) + \cdots + (k_{j-1,j} + k_{j,j-1}) \\ &= \sum_{l=i}^{j-1} (k_{l,l+1} + k_{l+1,l}). \end{aligned} \tag{3.24}$$

Analogously, from the same loop in Algorithm 1, each P_k contains C_k, so, using induction on $u - q$, we have

$$\text{constant term in } \Delta P_{ij} = C_j - C_i \ . \tag{3.25}$$

We now examine the terms involving the $n_{l,v}$ for $1 \leq l \leq r - 1$ in the expression for ΔP_{ij}. These are also obtained from Algorithm 1. Let c_{jl} be the coefficient on n_l for potential P_j. We have from the algorithm that for P_j, the coefficient on $n_{1,v}$ is $c_{j1} = \gamma_{1,0j} + c_{01}$. For P_i, the coefficient of $n_{1,v}$ is $c_{i1} = \gamma_{1,0i} + c_{01}$. Therefore, the coefficient on $n_{1,v}$ in ΔP_{ij} is $\gamma_{1,ij} = \phi_{ij}$. Thus, from Equation (3.20), we have $\gamma_{l,ij} = l\phi_{ij}$ for the coefficient of $n_{l,v}$ in ΔP_{ij}, and over all $n_{l,v}$ we have

$$\text{terms in } n_{l,v} \text{ of } \Delta P_{ij} = \phi_{ij} \sum_{l=1}^{r-1} l n_{l,v} \ . \tag{3.26}$$

From $\phi_{ij}\sigma_v = \phi_{ij}x_v + \phi_{ij}\sum_{l=1}^{r-1} l n_{l,v}$, and Equations (3.26), (3.24) and (3.25), we obtain

$$\Delta P_{ij} = \sum_{l=i}^{j-1} (k_{l,l+1} + k_{l+1,l}) + C_j - C_i + \phi_{ij}\sigma_v - \phi_{ij}x_v. \tag{3.27}$$

We eliminate σ_v using the state transition criterion $\sigma_v \geq k_{ij}$. Since $\phi_{ij} < 0$ for $j > i$, we have $\phi_{ij}\sigma_v \leq \phi_{ij}k_{ij}$. Substituting into the last result yields $\Delta P_{ij} \leq \sum_{l=i}^{j-1}(k_{l,l+1} + k_{l+1,l}) + C_j - C_i + \phi_{ij}k_{ij} - \phi_{ij}x_v$. A decrease in potential for a state transition of a single vertex v means $\Delta P_{ij} \leq -1$, and we obtain an inequality for

fixed points involving only thresholds and constants terms as required, and which is given by Equation (3.22) since $x_v = i$.

Consider next a down-transition $i \to j$ where $i > j$. The foregoing approach holds with only slight modifications. Given transitions $i' \leftrightarrow j'$, we have $\Delta P_{i',j'} = -\Delta P_{j',i'}$, so Equation (3.24) now becomes

$$\begin{aligned}\text{threshold terms in } \Delta P_{ij} &= -(k_{i,i+1} + k_{i+1,i}) - (k_{i+1,i+2} + k_{i+2,i+1}) - \cdots - (k_{j-1,j} + k_{j,j-1}) \\ &= \sum_{l=j}^{i-1} -(k_{l,l+1} + k_{l+1,l}).\end{aligned} \tag{3.28}$$

The constant terms remain unchanged, and the terms in σ_v and x_v do not change sign, as the sign enters through ϕ_{ij}. Hence, we have $\Delta P_{ij} = \sum_{l=j}^{i-1} -(k_{l,l+1} + k_{l+1,l}) + C_j - C_i + \phi_{ij}\sigma_v - \phi_{ij}x_v$. Again we eliminate σ_v by using the transition criterion $\sigma_v \leq k_{ij} - 1$, and so $\phi_{ij}\sigma_v \leq \phi_{ij}(k_{ij} - 1)$ (with $\phi_{ij} > 0$). We have $\Delta P_{ij} \leq \sum_{l=j}^{i-1} -(k_{l,l+1} + k_{l+1,l}) + C_j - C_i + \phi_{ij}(k_{ij} - 1) - \phi_{ij}x_v$. A potential decrease for a state transition of a single vertex v means $\Delta P_{ij} \leq -1$, resulting in the FPC of Equations (3.23), completing the proof. □

In totality, for a specified r, Algorithm 1 provides potentials that are then used in the equations of Theorem 30 to establish the FPCs for a GDS.

3.4.2 Multithreshold Systems That Omit Some State Transitions

We have assumed that all transitions are present in each r-state system, but this need not be the case. When an up-transition is absent, the threshold k_{ij} $(i < j)$ is set to a large integer $L_{ij} \in \mathbb{N}$ such that all $i \to j$ transitions are precluded. Similarly, when a down-transition is absent, the threshold k_{ij} $(i > j)$ is set to a small number $S_{ij} \in \mathbb{N}$ such that all $i \to j$ transitions are eliminated. The constants L_{ij} and S_{ij} are readily determined from the system dynamics. Note that, in general, one cannot merely remove an FPC for a transition that does not exist because a particular threshold may appear in multiple FPCs.

For example, suppose that the transition $1 \to 2$ in Figure 3.1 does not exist. The largest value of σ_v from Equation (3.3) is $\sigma_{12,max} = (r-1)d_{max} + 1 = 2d_{max} + 1$,

where the first term is the maximum contribution from any vertex's neighborhood, which occurs when all neighbors u of v are in state $x_u = 2$, and $x_v = 1$. Therefore, to preclude $1 \to 2$, by ensuring $\sigma \not\geq k_{12}$, we can set $k_{12} = L_{12} = \sigma_{12,max} + 1$.

This approach also reduces our multithreshold systems to other systems, as the following example illustrates. Suppose we have the 3-state system of Figure 3.2, but that only the up-transitions $0 \to 1$ and $1 \to 2$ are permissible. This is the state transition system studied in [56]. Systems such as these are called *progressive* [41], emphasizing that vertices can only move among states in one direction. We set $k_{10} = L_{10} = k_{21} = L_{21} = 0$ to render the two down-transitions infeasible. From Corollary 19, the fixed point conditions become

$$(i)\ \ 0 - k_{01} \leq \min\{-C_1 - 1, C_1 + 3\},$$

$$(ii)\ \ 0 - k_{12} \leq \min\{C_1 - C_2 - 3, -C_1 + C_2 + 5\}\ \ ,$$

where C_1 and C_2 are constants. Since we can set $C_1 = -2$ and $C_2 = -6$ to make the RHSs of both inequalities equal to 1, this means that a fixed point is generated for any combination of k_{01} and k_{12}. With a straight-forward extension from [44], we know that progressive systems have only fixed points as limit sets.

3.5 Summary and Conclusions

We generalized the notion of bi-threshold models from [46] to cover an arbitrary number of vertex states. The analysis has focused on the asynchronous case and gives conditions on thresholds values which guarantee that all ω-limit sets are fixed points. Although we did not address bifurcations that may arise as the thresholds fail to satisfy these conditions, computational experiments analogous to those for the case $r = 3$ show the same type of results.

In closing, we address the synchronous case. The result of Goles [25] for binary threshold systems does generalize to bi-threshold systems as we demonstrated in [46], but with the introduction of more than two vertex states, it seems that their proof cannot be extended easily. Preliminary results from computational experiments do nevertheless demonstrate that there are changes from the Boolean case. We compared the behavior of sequential and synchronous systems across conditions from three propositions from the main text. In some cases, qualitative limit cycle behavior is the same, and sometimes the update schemes produce different dynamics.

Proposition 22 uses $\boldsymbol{k} = (k_{01}, k_{10}, k_{12}, k_{21}, k_{02}, k_{20}) = (1, 4, 4, 6, 2, 5)$ and shows that sequential update on Circ_n ($n \geq 5$) produces limit cycles of length $n - 1$, for the 6-transition system. If we use synchronous update instead, then for $n = 5$ and 10, Circ_n produces maximum cycle lengths of 2. For the 4-transition system on Circ_n ($n \geq 5$), where $\boldsymbol{k} = (k_{01}, k_{10}, k_{12}, k_{21}) = (1, 3, 4, 6)$, sequential update produces cycles of length $n - 1$ (see Proposition 24). The corresponding synchronous system again only produces 2-cycles for $n = 5$ and 10.

According to Proposition 25, for asynchronous systems, $\boldsymbol{k} = (k_{01}, k_{10}, k_{12}, k_{21}, k_{02}, k_{20}) = (2, 3, 6, 6, 4, 5)$ produces only fixed points on Circ_n. However, $\boldsymbol{k} = (1, 3, 6, 6, 4, 5)$ produces cycles of length $n - 1$. The analogous synchronous systems, for the two threshold vectors, both produce cycles of length n for Circ_n, for the cases $n = 5$ and 10. Thus, we no longer have that synchronous systems are limited to cycle sizes ≤ 2. Future work including a formal proof of this fact is certainly warranted.

Chapter 4

Hierarchical Systems

4.1 Introduction

Many researchers model the spread of contagions (e.g., fads, rumors, influence, social movements) [14, 31, 67] as two-state systems where state 0 (resp., 1) means that an agent does not (resp., does) possess a contagion. In a standard or classic threshold model, a vertex contracts a contagion when at least a threshold number of its neighbors already possess it. More formally, a standard Boolean *threshold function* of the form $\tau_{k,m}\colon \{0,1\}^m \longrightarrow \{0,1\}$ is defined by

$$\tau_{k,m}(x_1,\ldots,x_m) = \begin{cases} 1, & \text{if } \sigma(x_1,\ldots,x_m) \geq k \quad \text{and} \\ 0, & \text{otherwise,} \end{cases} \tag{4.1}$$

where $\sigma(x_1,\ldots,x_m) = \big|\{1 \leq i \leq m \mid x_i = 1\}\big|$. A *bithreshold function* is a function $\tau_{i,k^\uparrow,k_\downarrow,m}\colon \{0,1\}^m \longrightarrow \{0,1\}$ defined by

$$\tau_{i,k^\uparrow,k_\downarrow,m}(x_1,\ldots,x_m) = \begin{cases} \tau_{k^\uparrow,m}, & \text{if } x_i = 0, \\ \tau_{k_\downarrow,m}, & \text{if } x_i = 1\ . \end{cases} \tag{4.2}$$

Here i denotes a designated argument; later it will be the index for a vertex or cell. We call $k^\uparrow$ the *up-threshold* and $k_\downarrow$ the *down-threshold*. When $k^\uparrow = k_\downarrow$ the bithreshold function coincides with a standard threshold function. Note that unlike the standard threshold function in Equation (4.1) which is symmetric, the bithreshold function is *quasi-symmetric* (or outer-symmetric) – with the exception of index i, it only depends on its arguments through their sum.

In this study, we integrate threshold systems into hierarchical systems, where the state transition of a vertex v is based not only on the states of its neighbors, but also on the connectivity among the neighbors. Collections of connected vertices form hiearchical structures, and these structures are incorporated into the state transition functions, such as those in Equations (4.1) and (4.2). Hierarchical cellular automata have been formulated and explored experimentally in [4] through computations of space-time diagrams for particular systems. That formulation is very general—to the point that it is difficult to prove anything about the behavior of such a broad class of systems.

Here we take a slightly different approach. We introduce a particular hierarchical model, and prove statements about its dynamics. Our dynamical system is a generalization of a new model [71] that was devised from mining online experimental data that describe how people join Facebook. We summarize informally the Facebook model next.

The Facebook data reveal the notion of *social contexts*. A context for vertex v is a set U of s distance-1 neighbors $U = \{u_1, u_2, \ldots, u_s\}$ of v such that there is a path between u_i and u_j, for all $i, j \in \{1, 2, \ldots, s\}$ using only edges from the original graph whose incident vertices are both in U. For a system in which a vertex v may occupy one of two states in $\{0, 1\}$, a context contributes 1 towards meeting v's threshold if at least one vertex in that context is in state 1. Otherwise a context contributes 0. Note that a context contribution can be modeled as a threshold function, Equation (4.1), with $k = 1$, and then the subsequent state transition of v can be modeled with Equation (4.1) or (4.2).

An example comparing a standard or classic threshold model and the hierarchical model is provided in Figure 4.1, in which we show the relevant subgraph of a graph X to illustrate the ideas. We focus on the state transition of vertex v, which is assumed to be in state $x_v = 0$ initially. Suppose $k_v^{\uparrow} = 3$. A classic threshold model, with no concept of a context, causes v to transition to state 1 because three of its neighbors, namely u_1, u_2, and u_4, are in state 1 (filled symbols). In contrast, for the hierarchical model, there are three contexts, denoted $X_{v,1}$, $X_{v,2}$, and $X_{v,3}$. Context $X_{v,1}$ contributes 1 toward meeting v's threshold because at least one of its vertices, u_1 (the only one), is in state 1. Context $X_{v,2}$ also contributes 1 toward meeting v's threshold because at least one vertex in this context (in fact, two vertices) is in state 1. Context $X_{v,3}$ contributes 0, since no vertex in $X_{v,3}$ is in state 1. Because the total contribution of 2 from all contexts is less than $k_v^{\uparrow}$, v remains in state 0. Thus, the two models yield different next states for v.

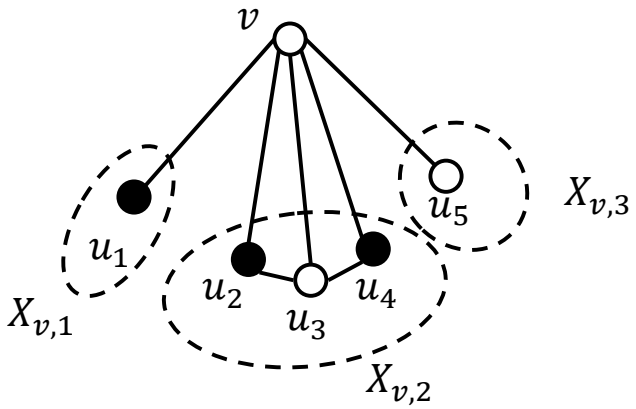

Figure 4.1: A six-vertex subgraph X_v where our focus is vertex v. For arbitrary vertex w, a filled (respectively, open) circle means that $x_w = 1$ (respectively, 0). There are three contexts, $X_{v,1}$, $X_{v,2}$, and $X_{v,3}$. This figure is used to illustrate the difference between a standard or classic threshold model and a hierarchical threshold model. The end result for $k_v^{\uparrow} = 3$ is that the next state x'_v for v is 1 in a standard threshold model, while $x'_v = 0$ for the hierarchical model. See text for details.

In this work, we generalize the hierarchical model and explore its resulting dynamics. We are primarily interested in threshold-governed dynamics, but we also investigate other models.

We note that one can capture the ideas of contexts by adding vertices and edges to the original graph X. We choose not to take this approach, however, since doing so even for small graphs can obscure the relationships among vertices of X. Our formal model development will reflect this choice.

Contributions and Organization. In Section 4.2, we define the hierarchical graph dynamical system (HGDS) and contrast it with a standard or classical GDS (CGDS). In Section 4.3, we specialize the HGDS for the Facebook model of [71]. We provide conditions under which two permutation HGDS maps are equal in Section 4.4. In Section 4.5, we show a result on graph structure that is implied by the equality of two permutation Nor HGDS maps, illustrating that a result for Nor CGDS maps carries over to the HGDS framework. In Section 4.6, we provide the conditions under which Boolean sequential HGDS maps for the model of [71] produce only fixed points as limit sets. Conclusions are in Section 4.7.

4.2 Background and Terminology

4.2.1 Hierarchical GDS

Let X denote an undirected graph with vertex set $\mathrm{v}[X] = \{1, 2, \ldots, n\}$ and edge set $\mathrm{e}[X]$. For each vertex $v \in \mathrm{v}[X]$, there exists a collection of subgraphs $(X_{v,i})_{i=1}^{l_v}$ with vertex sets $\mathrm{v}[X_{v,i}]$ and edge sets $\mathrm{e}[X_{v,i}]$, where $\mathrm{v}[X_{v,i}] \subseteq \mathrm{v}[X]$ and $\mathrm{e}[X_{v,i}] \subseteq \mathrm{e}[X]$.

To each vertex v we assign a state $x_v \in K = \{0, 1\}$ and refer to this as the *vertex state*. Let $n[v]$ denote the sequence of vertices in the 1-neighborhood of v sorted in increasing order, with $n[v](i)$ being the ith element of $n[v]$, and write

$$x[v] = (x_{n[v](1)}, x_{n[v](1)}, \ldots, x_{n[v](d(v)+1)})$$

for the corresponding sequence of vertex states that includes x_v. Here $d(v)$ is the degree of v. We call $x = (x_1, x_2, \ldots, x_n)$ the *system state* and $x[v]$ the *restricted state*. Let $B_{v,i} = \mathrm{v}[X_{v,i}]$ so that the states of vertices in $B_{v,i}$ comprise the sequence

$$x_{B_{v,i}} = (x_j \mid j \in B_{v,i}) \ ,$$

with $x_{B_{v,i}} \in K^{|B_{v,i}|}$, where again the j are arranged in increasing order. The collection of all such sequences is given by

$$x_B[v] = (x_{B_{v,i}} \mid 1 \leq i \leq l_v) \ .$$

The dynamics of vertex states are described by two kinds of *component vertex functions*. Type I component functions describe a single state update for the set $B_{v,i}$. A nested sequence $((f_{v,i}^I)_{i=1}^{l_v})_{v=1}^n$ of maps $f_{v,i}^I \colon K^{|B_{v,i}|} \longrightarrow M$ is defined by

$$z_{v,i} = f_{v,i}^I(x_{B_{v,i}}) \ , \tag{4.3}$$

where M can depend on v and i. Type II component functions form a sequence $(f_v^{II})_{v=1}^n$ of functions $f_v^{II} \colon K^{d(v)+1} \times M^{|l_v|} \longrightarrow K$ defined by

$$x_v = f_v^{II}(x[v], (z_{v,i})_{i=1}^{l_v}) \ . \tag{4.4}$$

We define a list of *vertex functions* $(f_v)_{v=1}^n$, where each $f_v \colon K^{d(v)+1} \longrightarrow K$ is given as

$$f_v(x[v]) = f_v^{II}(x[v], (z_{v,i})_{i=1}^{l_v}) = f_v^{II}(x[v], (f_{v,i}^I(x_{B_{v,i}}))_{i=1}^{l_v}) \ . \tag{4.5}$$

The state x_v of a vertex v is updated at time t by the vertex function operating on the restricted state $x(t)[v]$

$$x_v(t+1) = f_v\big(x(t)[v]\big) \ . \tag{4.6}$$

An *update mechanism* governs how the list of vertex functions assemble to a *graph dynamical system* map (see e.g. [51, 58])

$$\mathbf{F}\colon K^n \longrightarrow K^n \tag{4.7}$$

sending the system state at time t to that at time $t+1$.

For the update mechanism, we use *synchronous* (or *parallel*) and *asynchronous* (or *sequential*) schemes. In the former case we obtain Boolean networks where

$$\mathbf{F}(x_1, \ldots, x_n) = (f_1(x[1]), \ldots, f_n(x[n])) \ .$$

This sub-class of graph dynamical systems is sometimes referred to as *generalized cellular automata*. In the latter case we will consider permutation update sequences. For this we first introduce the notion of *X-local functions*. Here the X-local function $F_v\colon K^n \longrightarrow K^n$ is given by

$$F_v(x_1, \ldots, x_n) = (x_1, x_2, \ldots, f_v(x[v]), \ldots, x_n) \ . \tag{4.8}$$

Using $\pi = (\pi_1, \ldots, \pi_n) \in S_X$ (the set of all permutations of v$[X]$) as an update sequence, the corresponding asynchronous (or sequential) graph dynamical system map $\mathbf{F}_\pi\colon K^n \longrightarrow K^n$ is given by

$$\mathbf{F}_\pi = F_{\pi(n)} \circ F_{\pi(n-1)} \circ \cdots \circ F_{\pi(1)} \ . \tag{4.9}$$

We also refer to this class of asynchronous systems as (permutation) *sequential dynamical systems* (SDSs). The X-local functions are convenient when working with the asynchronous case.

The phase space of the GDS map $\mathbf{F}\colon K^n \longrightarrow K^n$ is the directed graph with vertex set K^n and edge set $\{\big(x, \mathbf{F}(x)\big) \mid x \in K^n\}$. A state x for which there exists a positive integer p such that $\mathbf{F}^p(x) = x$ is a *periodic point*, and the smallest such integer p is the *period* of x. If $p = 1$ we call x a *fixed point* for $\mathbf{F}$. A state that is not periodic is a *transient state*. Classically, the *omega-limit set* of x, denoted by $\omega(x)$, is the set of accumulation points of the sequence $\{\mathbf{F}^k(x)\}_{k\geq 0}$. In the finite case, the omega-limit set is the unique periodic orbit reached from x under $\mathbf{F}$.

We remark that graph dynamical systems generalize concepts such as cellular automata and Boolean networks, and can describe a wide range of distributed, nonlinear phenomena.

4.2.2 Classic or Standard GDS

The classic GDS [51] differs from the foregoing HGDS in only one respect. That is, for the standard GDS, there are no subgraphs $X_{v,i}$ corresponding to a vertex v. Consequently, there are no component vertex functions $f^I_{v,i}$, nor are the f^{II}_v needed. Rather, a vertex function $f_v \colon K^{d(v)+1} \longrightarrow K$ is defined *directly* and maps as Equation (4.6), as before. Examples for f_v include the threshold functions of Equations (4.1) and (4.2); e.g., $f_v = f_{v,k,m} := \tau_{k,m}$. (In contrast, for an HGDS, f_v is defined in terms of $f^I_{v,i}$ and f^{II}_v, and these latter two functions are defined directly; e.g., by Equations (4.1) and (4.2).) From this point, the standard GDS description continues with Equation (4.7) as in Section 4.2.1.

4.2.3 Note on HGDS

There are other HGDS constructions in addition to the one presented here. For example, we could include in the argument of $f^I_{v,i}$ not only the states $x_{B_{v,i}}$ of the vertices of $X_{v,i}$, but also those for each of these vertices' distance-1 neighbors. The chosen approach was driven by the model of [71], and will be specialized in Section 4.3.

4.3 Specialization of the HGDS Formulation for the Context Model

We specialize the HGDS in Section 4.2.1 in two ways: (i) graph structure and function dependencies, and (ii) component vertex functions.

4.3.1 Structure Specialization and Function Dependencies

We now specialize the subgraphs $X_{v,i}$ for an arbitrary vertex v, from Section 4.2.1, based on the description in [71]. We form connected subgraphs, comprised solely of vertices that are distance-1 neighbors of v, and the only permissible edges are those whose incident vertices are both distance-1 neighbors of v. More formally, a *distance-1 connected graph with respect to* v, denoted $X_{v,i}$, is a graph with the following properties

1. vertex set $B_{v,i} = \mathrm{v}[X_{v,i}]$ with $B_{v,i} = \{u_{v,i,1}, u_{v,i,2}, \ldots, u_{v,i,m_{v,i}}\}$, where $\{v, u_{v,i,j}\} \in \mathrm{e}[X]$, $(1 \leq j \leq m_{v,i})$, and $m_{v,i} = |B_{v,i}|$;
2. edge set $\mathrm{e}[X_{v,i}] = \big\{\{u_{v,i,j_1}, u_{v,i,j_2}\} \mid \{u_{v,i,j_1}, u_{v,i,j_2}\} \in \mathrm{e}[X] \text{ where } 1 \leq j_1, j_2 \leq m_{v,i}\big\}$; and
3. there is a path in $X_{v,i}$ between each pair of vertices in $B_{v,i}$.

A *maximal distance-1 connected graph with respect to* v is a distance-1 connected graph such that there is no vertex $w \in \mathrm{v}[X]$ with all of the following characteristics: (i) $\{v, w\} \in \mathrm{e}[X]$, (ii) $\{w, u_{v,i,j}\} \in \mathrm{e}[X]$, and (iii) $u_{v,i,j} \in \mathrm{v}[X_{v,i}]$. We take the subgraphs $X_{v,i}$ of Section 4.2.1 as the maximal distance-1 connected graphs. An example with $l_v = 3$ and $m_{v,1} = 1$, $m_{v,2} = 3$, and $m_{v,3} = 2$ is given in Figure 4.2.

The component vertex function $f^I_{v,i}$ is unchanged. The component vertex function f^{II}_v is refined from Equation (4.4) to depend only on x_v and $(z_{v,i})_{i=1}^{l_v}$ so that $f^{II}_v \colon K \times M^{|l_v|} \longrightarrow K$ may be written as

$$f_v(x[v]) = f^{II}_v(x_v, (z_{v,i})_{i=1}^{l_v}) \; . \tag{4.10}$$

This specific formulation of an HGDS has an analogous formulation as a CGDS. In effect, the contributions from the distance-1 neighbors of v in a standard GDS are replaced by contributions from its induced maximal distance-1 connected subgraphs.

4.3.2 Vertex Function Specialization

In subsequent developments, specialization may stop with Section 4.3.1, or it may also include either of the following. Consistent with [71], $f^I_{v,i}$ is a threshold function given by Equation (4.1) with $k = 1$ (i.e., a 1-threshold function). Secondly, f^{II}_v is the threshold function of either Equation (4.1) or (4.2).

4.4 Equality of GDS Maps

4.4.1 Equality of Permutation HGDS Maps

Two GDS maps $\mathbf{F}_1$ and $\mathbf{F}_2$ are equal (i.e., $\mathbf{F}_1 = \mathbf{F}_2$) if and only if $\mathbf{F}_1(x) = \mathbf{F}_2(x)$ for all x. Let $\pi, \pi' \in S_X$ be two permutations of vertices of X. We write $\pi \approx_X \pi'$ if (i) π

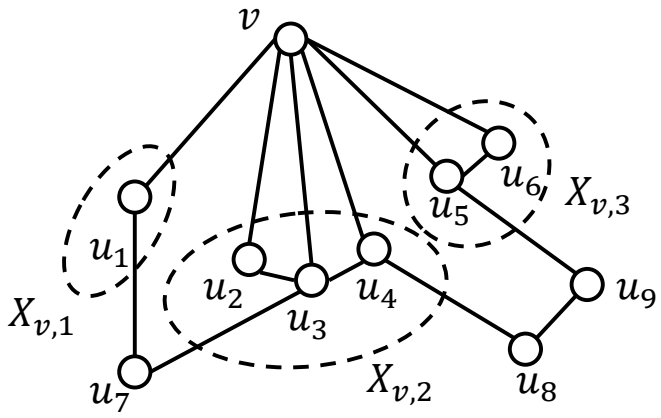

$$B_{v,1} = \{u_1\} \quad B_{v,2} = \{u_2, u_3, u_4\} \quad B_{v,3} = \{u_5, u_6\}$$

$$x_{B_{v,1}} = (x_{u_1}) \quad x_{B_{v,2}} = (x_{u_2}, x_{u_3}, x_{u_4}) \quad x_{B_{v,3}} = (x_{u_5}, x_{u_6})$$

$$x_B[v] = (x_{B_{v,1}}, x_{B_{v,2}}, x_{B_{v,3}})$$

Figure 4.2: A ten-vertex subgraph where our focus is vertex v. There are three subgraphs induced on the distance-1 neighbors of v, namely $X_{v,1}$, $X_{v,2}$, and $X_{v,3}$, which are circled. We have $l_v = 3$ and $m_{v,1} = 1$, $m_{v,2} = 3$, and $m_{v,3} = 2$. These notions of hiearchy are taken from [71].

and π' differ precisely on two consecutive coordinates where (ii) the coordinates are not connected by an edge in X. Define $\sim_X$ on S_X to be the reflexive and transitive closure of $\approx_X$, and hence $\sim_X$ is an equivalence relation. We have the following known result for CGDSs.

Proposition 31. *[58] Given a graph X with $\pi, \pi' \in S_X$. Let $\mathbf{F}'_\pi$ and $\mathbf{F}'_{\pi'}$ be permutation CGDS maps. If $\pi \sim_X \pi'$, then $\mathbf{F}'_\pi = \mathbf{F}'_{\pi'}$.*

We show a similar result for an HGDS, as follows.

Proposition 32. *Given a graph X with $\pi, \pi' \in S_X$. Let $\mathbf{F}_\pi$ and $\mathbf{F}_{\pi'}$ be permutation HGDS maps described in Section 4.2.1, with the specialization of $X_{v,i}$ as described in Section 4.3.1. If $\pi \sim_X \pi'$, then $\mathbf{F}_\pi = \mathbf{F}_{\pi'}$.*

Proof. Consider two permutations π and π' whose only difference is that the vertices u and v are switched, so Equation (4.9) yields $\mathbf{F}_\pi = F_{\pi(n)} \circ F_{\pi(n-1)} \circ \cdots F_v \circ F_u \circ \cdots \circ F_{\pi(1)}$ and $\mathbf{F}_{\pi'} = F_{\pi(n)} \circ F_{\pi(n-1)} \circ \cdots F_u \circ F_v \circ \cdots \circ F_{\pi(1)}$. Consider $F_v \circ F_u$ produced from π. Since $\pi \sim_X \pi'$ means that there is no edge between vertices u and v, we have $v \notin x[u]$ and $u \notin x[v]$. Thus, the state update of u (resp., v), through Equation (4.6), does not depend on v (resp., u). From Equation (4.8), it follows that $F_v \circ F_u = F_u \circ F_v$. The result then follows. □

4.4.2 GDS Map Equality Between CGDS and HGDS Maps

We now prove the condition under which a CGDS and HGDS are functionally equivalent. We are using the specialized form of an HGDS as described in Section 4.3.1, and for only $f^I_{v,i}$ from Section 4.3.2. Our result is for both synchronous and sequential GDS maps. Note that we are not using the special form of f^{II}_v of Section 4.3.2. We take as a given that for sequential systems, the CGDS permuation π' is the same as that for the context HGDS. We also assume that the vertex state sets are the same for the two GDSs. We identify the structural feature of a graph (i.e., its vertex connectivity) that guarantees that the dynamics of a context HGDS are the same as those for the the corresponding CGDS; i.e., a sufficient condition such that an HGDS map and its corresponding CGDS map are equal.

Proposition 33. *Let X be a graph and let $K = \{0, 1\}$. Let $\mathbf{F}'$ be a CGDS map with vertex functions $(f'_v)_v$. Let $\mathbf{F}$ be an HGDS map with specialized $X_{v,i}$ as described in Section 4.3.1, and with $f^I_{v,i}$ being the 1-threshold function (Equation* (4.1) *with*

$k = 1$) per Section 4.3.2. Let f_v^{II} of the HGDS, given by Equation (4.10)*, be the same function as the vertex function for the CGDS; i.e., $f_v^{II} = f'_v$. If there are no triangle subgraphs in X, then $\mathbf{F} = \mathbf{F}'$.*

Proof. Since the CGDS map $\mathbf{F}'$ and HGDS map $\mathbf{F}$ will be equal if f'_v for the CGDS and f_v^{II} for the HGDS evaluate the same for each vertex v, we require that the values of the argument lists for the two functions be the same. We consider the response for both systems for an arbitary v in an arbitrary graph X. We deal with three cases. In case 1, v has no distance-1 neighbors; it is an isolated vertex and therefore is not part of any triangle. Hence, there are no inputs to Equation (4.3), and so there are no $z_{v,i}$ in Equation (4.10); $l_v = 0$. Therefore, the single input to both f'_v and f_v^{II} is x_v and hence the functions will produce the same next state because $f_v^{II} = f'_v$. In case 2, v has one distance-1 neighbor, u, and therefore v is not part of any triangle. For the HGDS, the 1-threshold component vertex function $f_{v,1}^I$, given by Equation (4.3), yields $z_{v,1} = x_u = f_{v,1}^I(x_u)$. This means that the two inputs to f_v^{II} and f'_v are x_v and x_u, and the two functions will produce the same next state value for v. In case 3, v has $s \geq 2$ distance-1 neighbors, u_j, $1 \leq j \leq s$. Consider any two neighboring vertices of v, namely u_1 and u_2. Because there is no triangle incident on v, and because there exists edges $\{v, u_1\}$ and $\{v, u_2\}$, it must be that there is no edge formed between u_1 and u_2. Since u_1 and u_2 are arbitrary, there is no edge between any pair of distance-1 neighbors of v, and so each distance-1 neighbor of v forms a distinct $X_{v,i}$ subgraph. Therefore, $z_{u_j} = x_{u_j} = f_{v,i}^I(x_{u_j})$ for each u_j, $1 \leq j \leq s$. Hence, the restricted states are the same for f'_v and f_v^{II}, and consequently, the functions will give the same next state x_v. Since v is arbitrary, $\mathbf{F}'$ and $\mathbf{F}$ are equal as functions. □

There are many stylized graphs that have no embedded triangles, thus producing the following result.

Corollary 34. *The following graphs possess no triangles and therefore give rise to equal corresponding classic and context GDS maps, irrespective of vertex functions and update schemes:* Circ_n *(for $n > 3$); Path_n; Star_n; any tree (acyclic graph); any Von Neumann lattice* $\text{VNLattice}_{r,c}$ *(the graph with boundaries and also the torus version); Peterson graph (not all graphs in the Peterson family of graphs qualify (e.g., Dürer graph does not conform), but the original Peterson graph does, as does the Möbius-Kantor graph [$G(8,3)$] and $G(9,2)$); multipartite* $\text{MP}_{c,r(c)}$ *and hence* $\text{Bipartite}_{2,r}$*; and regular dodecahedron* RegularDodecahedron.

Many networks possess triangles. Examples of stylized networks include Moore lattices where every non-boundary vertex has degree 8, and fully connected graphs of n

vertices (K_n), $n \geq 3$. For example, K_n contains $\binom{n}{3}$ triangles. The following provides examples of real networks possessing triangles.

Example 35. *In practice, many networks have triangle subgraphs. For example, an Epinions social network [63] with 75879 vertices contains 1.6 million triangles; a Twitter network [55] of 81306 vertices possesses 13 million triangles; and a LiveJournal social network [5] of 4847571 nodes contains 285 million triangles. Social networks often have large numbers of triangles because they often possess high clustering.*

4.5 Nor **HGDS Map**

Let K be the Boolean vertex state set $\{0, 1\}$. The Nor GDS map on K is given by the sequence of vertex functions $(f_v)_v$ where each f_v is nor: $K^m \longrightarrow K$ defined by $\mathrm{nor}_m = \prod_{i=1}^{m}(1 + x_i)$. The function nor evaluates to 1 only when all inputs are zero. In general, the converse of Proposition 31 is not true; i.e., $\mathbf{F}'_\pi = \mathbf{F}'_{\pi'} \not\Longrightarrow \pi \sim_X \pi'$. For Nor, however, we have the following known result for CGDSs.

Proposition 36. *[58] Given a graph X with $\pi, \pi' \in S_X$. Let $\mathbf{F}'_\pi$ and $\mathbf{F}'_{\pi'}$ be permutation* Nor *CGDS maps. Then $\mathbf{F}_\pi = \mathbf{F}_{\pi'} \implies \pi \sim_X \pi'$.*

We have a similar result for the HGDS conforming to [71], where $X_{v,i}$ are specialized according to Section 4.3.1, $f^I_{v,i}$ is specialized according to Section 4.3.2, and f^{II}_v is given by the nor function.

Proposition 37. *Given an undirected graph X with $\pi, \pi' \in S_X$. Let $\mathbf{F}_\pi$ and $\mathbf{F}_{\pi'}$ be permutation HGDS maps with vertex functions f_v given by Equation* (4.10)*, where $f^I_{v,i}$ is a threshold function (Equation* (4.1)*) with $k = 1$ and f^{II}_v is the* nor *function. Then $\mathbf{F}_\pi = \mathbf{F}_{\pi'} \implies \pi \sim_X \pi'$.*

Proof. Let π and π' be two permutations whose only difference is the order of two consecutive vertices, u and v. Let $\pi = (\pi(1), \pi(2), \ldots, u, v, \ldots, \pi(n))$ and let $\pi' = (\pi'(1), \pi'(2), \ldots, v, u, \ldots, \pi'(n))$. Since $\mathbf{F}_\pi = \mathbf{F}_{\pi'}$, this equality holds for all states x, including state x^* in which the state of each vertex in the permutation from $\pi(1)$ through u is 1, and the state of each vertex in the permutation from vertex v through $\pi(n)$ is 0. Let s be the position of u in the permutation π. The state of each of the first s vertices in π will change to 0 in the state $\mathbf{F}_\pi(x^*)$, because regardless of the states of $x_{B_{w,i}}$, for vertex w in this list, $x_w = 1$ and so the Nor X-local function

will evaluate 0. Since all vertex states are 0 for the evaluation of F_v, the 1-threshold functions $f^I_{v,i}$ evaluate 0, and the Nor X-local function will evaluate 1. Thus, the next states for the two vertices of interest are $x'_u = 0$ and $x'_v = 1$ for permutation π.

Consider the same initial state x^*, and the new state $F_{\pi'}(x^*)$, where now v is evaluated before u. The first $s-1$ vertices are evaluated the same as before, so their states become 0. The next vertex state evaluated is x_v. When F_v is evaluated, there is only one vertex of X in state 1, which is u. There are two cases: in the first case, u and v form an edge, and in the second case they do not. Consider Case 1. There exists an edge $\{u, v\}$, so the next state of v is $x'_v = 0$ because the $X_{v,i}$ to which u belongs will produce state 1 (because $x_u = 1$), and the Nor X-local function will produce the stated result. Then F_u will produce $x'_u = 0$ because $x_u = 1$. These two vertex states ($x'_u = 0$ and $x'_v = 0$) do not match those generated with π, so we violate the hypothesis that the two maps are equal. Now consider Case 2, where there is no edge between u and v, and address the state update of v. Since $x_v = 0$ and every vertex forming an edge with v is in state 0, $x'_v = 1$. Now u is evaluated and $x'_u = 0$ because $x_u = 1$. In Case 2, the two vertex next states for π' are the same as those for π. The remaining corresponding vertices of the two permutations will have the same state updates. Therefore, if $\mathbf{F}_\pi = \mathbf{F}_{\pi'}$, then there is no edge between u and v, and hence $\pi \sim_X \pi'$. □

A consequence of this result is that the number of acyclic orientations of X, denoted $|\mathrm{Acyc}(X)|$, is an upper bound for the number of distinct permutation HGDS maps that can be constructed for fixed functions.

4.6 Fixed Point Conditions in Sequential Bithreshold HGDS

We now identify the conditions for which sequential bithreshold HGDSs produce only fixed points as limit sets. We use the model of [71] and the specialized HGDS of Section 4.3, and we specify f^{II}_v as the bithreshold function of Equation (4.2).

Proposition 38. *Let X be a graph, let $K = \{0, 1\}$, let $\pi \in S_X$, and let $(f_v)_v$ be bithreshold vertex functions of an HGDS that are specialized according to Section 4.3. The vertex functions are comprised of component vertex functions as follows: (i) $f^I_{v,i}$ being a 1-threshold function corresponding to Equation* (4.1) *with $k = 1$; and (ii) f^{II}_v being the bithreshold function of Equation* (4.2) *with $k^\uparrow$ and $k_\downarrow$, whose arguments are*

given by Equation (4.10)*. Let all* f_v *satisfy* $\Delta(v) = k_\downarrow - k^\uparrow \leq 1$*. The sequential dynamical system map* $\mathbf{F}_\pi$ *has only fixed points as limit sets.*

Proof. The proof uses a potential function based on a construction in [6], but see also [29, 46]. For a given state $x \in K^n$ we assign to each vertex the potential

$$P(v,x) = \begin{cases} k_{\downarrow_v}, & x_v = 1 \\ d_c(v) + 2 - k_v^\uparrow, & x_v = 0 \ . \end{cases}$$

Here, $d_c(v) = l_v$. Note that the quantity $d_c(v) + 2 - k_v^\uparrow$ is the smallest number of subgraphs $X_{v,i}$ where the states of all vertices must be zero, plus one (for x_v). We define a super-vertex $p_{v,i}$ to represent all vertices in $B_{v,i}$. We can define a corresponding super-edge $e = \{v, p_{v,i}\}$ and assign to it a potential

$$P(e = \{v, p_{v,i}\}, x) = \begin{cases} 1, & x_v \neq z_{v,i} \\ 0, & x_v = z_{v,i} \ . \end{cases}$$

We let $n_i = n_i(v; x)$ denote the number of super-vertices adjacent to v in state i for $i = 0, 1$ and note that $n_0 + n_1 = d_c$. The *system potential* $P(x)$ at the state x is the sum of all the vertex and all the edge potentials. For the theorem statement it is clearly sufficient to show that each application of a vertex function that leads to a change in a vertex state causes the system potential to drop.

Consider first the case where x_v is mapped from 0 to 1 which implies that $n_1 \geq k_v^\uparrow$. Since a change in system potential only occurs for vertex v and super-edges incident on v, we may disregard the other potentials when determining this change. Denoting the system potential before and after the update by P and P', we have $P = d_c + 2 - {k^\uparrow}_v + n_1$ and $P' = k_{\downarrow_v} + n_0$ which implies that

$$\begin{aligned} P' - P &= k_{\downarrow_v} + n_0 - d_c - 2 + {k^\uparrow}_v - n_1 = k_{\downarrow_v} + {k^\uparrow}_v - 2n_1 - 2 \\ &\leq -({k^\uparrow}_v - k_{\downarrow_v}) - 2 = \Delta(v) - 2 \ , \end{aligned}$$

and this is strictly negative whenever $\Delta = k_\downarrow - k^\uparrow \leq 1$. Similarly, for the transition where x_v maps from 1 to 0, one must have $n_1 + 1 \leq k_{\downarrow_v} - 1$ or $n_1 \leq k_{\downarrow_v} - 2$. In this case we have

$$\begin{aligned} P' - P &= [d_c + 2 - {k^\uparrow}_v + n_1] - [k_{\downarrow_v} + n_0] = 2n_1 + 2 - k_{\downarrow_v} - {k^\uparrow}_v \\ &\leq 2k_{\downarrow_v} - 4 + 2 - {k^\uparrow}_v - k_{\downarrow_v} = \Delta(v) - 2 \end{aligned}$$

as before, concluding the proof. □

We immediately have the following for the model of [71], if $k^{\uparrow} = k_{\downarrow} = k$.

Corollary 39. *The sequential HGDS defined in Section 4.3, which describes the model in [71], where we take f_v^{II} to be the classic threshold function, has only fixed points as limit sets.*

4.7 Summary and Conclusions

We introduced a hierarchical GDS based on recent findings of the behavior of individuals joining Facebook [71]. We generalized the experimentally-determined model, and showed that the more general HGDS produces maps that are equal when switching two consecutive vertices in two otherwise identical permutations, if the two vertices do not form an edge in X. This behavior is also found in standard GDS. We also identified the absence of triangles in a graph X as a sufficient condition to ensure that an HGDS map and its corresponding standard GDS map are equal. We also demonstrated a property of Nor maps that holds for HGDS as well as standard GDS. Finally, we identified the conditions under which a Boolean sequential HGDS map will only generate fixed points as limit sets. This work is ongoing. Open issues include the extension of the fixed point conditions to multithreshold systems, exploration of limit sets of synchronous systems, and other formulations of HGDSs.

Chapter 5

Conclusion

Our work extends threshold GDSs in three ways: (i) by utilizing separate up- and down-thresholds to govern transitions $0 \to 1$ and $1 \to 0$, respectively, in Boolean networks; (ii) by extending Boolean state GDSs to multistate, multithreshold systems, where any number r of vertex states may be used; and (iii) by analyzing hierarchical Boolean GDSs. We state, prove, and analyze conditions characterizing long-term dynamics of all of these models. Ongoing and future work was provided in the respective chapters. While our motivations come from the social sciences, these results may be useful in the study of other fields, such as biology.

Bibliography

[1] Steffen Angenendt, Muriel Asseburg, Andre Bank, Asiem El Difraoui, Ulrike Freitag, Iris Glosemeyer, Wofram Lacher, Katja Niethammer, Volker Perthes, Walter Posch, Stephan Roll, Johannes Thimm, and Kirsten Westphal. Protest, revolt, and regime change in the arab world 2012. Technical report, German Institute for International and Security Affairs, 2012.

[2] Luca Dall Asta and Claudio Castellano. Effective Surface-Tension in the Noise-Reduced Voter Model. *Europhys. Lett.*, 77(12):60005p1–60005p6, 2011.

[3] R. Atkinson, W. Dietz, J. Foreyt, N. Goodwin, J. Hill, J. Hirsch, F. Pi-Sunyer, R. Weinsier, R. Wing, J. Hoofnagle, J. Everhart, V. Hubbard, and S. Yanovski. Weight Cycling. *Journal of the American Medical Association*, 272(15):1196–1202, 1994.

[4] Nils A. Baas and Torbjörn Helvik. Higher order cellular automata. *Advances in Complex Systems*, 8:169–192, 2005.

[5] L. Backstrom, D. Huttenlocher, J. Kleinberg, and X. Lan. Group Formation in Larges Social Networks: Membership, Growth, and Evolution. In *ACM International Conference on Data Mining and Knowledge Discovery (KDD 2006)*, 2006.

[6] Christopher L. Barrett, Harry B. Hunt III, Madhav V. Marathe, S. S. Ravi, Daniel J. Rosenkrantz, and Richard E. Stearns. Complexity of reachability problems for finite discrete sequential dynamical systems. *Journal of Computer and System Sciences*, 72:1317–1345, 2006.

[7] G. Bischi and U. Merlone. Global Dynamics in Binary Choice Models with Social Influence. *J. Math. Sociology*, 33:277–302, 2009.

[8] G. V. Bodenhausen, L. Sheppard, and G. Kramer. Negative Affect and Social Judgment: The Differential Impact of of Anger and Sadness. *European Journal of Social Psychology*, 24:45–62, 1994.

[9] Melvyn Bragg. *The Adventure of English*. Arcade Publishing, 2003.

[10] Halvard Buhaug and Kristian Skrede Gleditsch. Congation or Confusion? Why Conflicts Cluster in Space. *International Studies Quarterly*, 52:215–233, 2008.

[11] N. Bulger, A. DeLongis, R. Kessler, and E. Wethington. The Contagion of Stress Across Multiple Roles. *Journal of Marriage and the Family*, 51:175–183, 1989.

[12] Colin Campbell, Suann Yang, Rka Albert, and Katriona Sheab. A network model for plantpollinator community assembly. *Proceedings of the National Academy of Sciences*, 108(1):197–202, 2011.

[13] C. Castillo-Chavez and B. Song. Models for the transmission dynamics of fanatic behaviors. In H. Banks and C. Castill-Chavez, editors, *Bioterrorism: Mathematical Modeling Applications in Homeland Security; in SIAM Frontiers in Applied Mathematics*, pages 155–172. SIAM, 2003.

[14] D. Centola and M. Macy. Complex Contagions and the Weakness of Long Ties. *American Journal of Sociology*, 113(3):702–734, 2007.

[15] Wei Chen, Chi Wang, and Yajun Wang. Scalable Influence Maximization for Prevalent Viral Marketing in Large-Scale Social Networks. In *Proc. ACM Intl. Conf. on Data Mining and Knowledge Discovery (KDD 2010)*, pages 1029–1038, 2010.

[16] N. Christakis and J. Fowler. The Spread of Obesity in a Large Social Network Over 32 Years. *New England Journal of Medicine*, pages 370–379, 2007.

[17] Mario Diani. Social Movements and Collective Action. In John Scott and Peter J. Carrington, editors, *The SAGE Handbook of Social Network Analysis*, pages 223–235. SAGE, 2011.

[18] R. William Doherty. The Emotional Contagion Scale: A Measure of Individual Differences. *Journal of Nonverbal Behavior*, 21:131–154, 1997.

[19] P. Dreyer and F. Roberts. Irreversible k-Threshold Processes: Graph-Theoretical Threshold Models of the Spread of Disease and Opinion. *Discrete Applied Mathematics*, 157:1615–1627, 2009.

[20] D. Easley and J. Kleinberg. *Networks, Crowds and Markets: Reasoning About A Highly Connected World*. Cambridge University Press, New York, NY, 2010.

[21] Jon Elster. *The Cement of Society*. Cambridge University Press, 1989.

[22] J. Epstein. Modeling civil violence: An agent-based computational approach. *PNAS*, 99:7243–7250, 2002.

[23] Erika Forsberg. *Neighbors at Risk: A Quantitative Study of Civil War Contagion*. PhD thesis, Uppsala Universitet, 2009.

[24] James H. Fowler and Nicholas A. Christakis. Dynamic spread of happiness in a large social network: longitudinal analysis over 20 years in the Framingham Heart Study. *BMJ*, 337, 2008.

[25] E. Goles and J. Olivos. Periodic behavior in generalized threshold functions. *Discrete Mathematics*, 30:187–189, 1980.

[26] E. Goles and J. Olivos. Comportement periodique des fonctions a seuil binaires et applications. *Discrete Applied Mathematics*, 3:93–105, 1981.

[27] Eric Goles and Servet Martinez. *Neural and Automata Networks*. Kluwer Academic Publishers, 1 edition, 1990.

[28] E. Goles-Chacc, F. Fogelman-Soulie, and D. Pellegrin. Decreasing energy functions as a tool for studying threshold networks. *Discrete Applied Mathematics*, 12:261–277, 1985.

[29] Eric Goles-Chacc, Franọise Fogelman-Soulie, and Didier Pellegrin. Decreasing energy functions as a tool for studying threshold networks. *Discrete Applied Mathematics*, 12:261–277, 1985.

[30] Sandra Gonzalez-Bailon, Javier Borge-Holthoefer, Alejandro Rivero, and Yamir Moreno. The Dynamics of Protest Recruitment Through an Online Network. *Nature Scientific Reports*, pages 1–7, 2011. DOI: 10.1038/srep00197.

[31] M. Granovetter. Threshold models of collective behavior. *American Journal of Sociology*, 83(6):1420–1443, 1978.

[32] K. Harris. The National Longitudinal Study of Adolescent Health (Add Health), Waves I and II, 1994-1996; Wave III, 2001-2002 [machine-readable data file and documentation], 2008. Chapel Hill, NC: Carolina Population Center, University of North Carolina at Chapel Hill 2008.

[33] E. Hatfield, J. Cacioppo, and R. Rapson. *Emotional Contagion*. Cambridge University Press, 1994.

[34] Beth R. Hoffman, Steve Sussman, Jennifer B. Unger, and Thomas W. Valente. Peer influences on adolescent cigarette smoking: A theoretical review of the literature. *Substance Use and Misuse*, 41:103–155, 2006.

[35] M. Hoogendoorn, J. Treur, C. N van der Wal, and A. van Wissen. An agent-based model for the interplay of information and emotion in social diffusion. In *Proceedings of the 10th IEEE/WIC/ACM International Conference on Intelligent Agent Technology (IAT 2010)*, pages 439–444, 2010. An 8-page version is accessible through the internet.

[36] Carol Huang. Facebook and Twitter key to Arab Spring uprisings: report. In *The National*. 2011.

[37] Ira M. Longini Jr., Azhar Nizam, Shufu Xu, Kumnuan Ungchusak, Wanna Hanshaoworakul, Derek A. T. Cummings, and M. Elizabeth Halloran. Containing pandemic influenza at the source. *Science*, 309:1083–1087, 2005.

[38] Ulas Karaoz, T.M. Murali, Stan Letovsky, Yu Zheng, Chunming Ding, Charles R. Cantor, and Simon Kasif. Whole-genome annotation by using evidence integration in functional-linkage networks. *Proceedings of the National Academy of Sciences*, 101(9):2888–2893, 2004.

[39] S. A. Kauffman. Metabolic stability and epigenesis in randomly constructed genetic nets. *Journal of Theoretical Biology*, 22:437–467, 1969.

[40] Kazuki Kawachi, Motohide Seki, Hiraku Yoshida, Yohei Otake, Katsuhide Warashina, and Hiroshi Ueda. A rumor transmission model with various contact interactions. *Journal of Theoretical Biology*, 253:55–60, 2008.

[41] D. Kempe, J. Kleinberg, and E. Tardos. Maximizing the Spread of Influence Through a Social Network. In *Proc. ACM Intl. Conf. on Data Mining and Knowledge Discovery (KDD 2003)*, pages 137–146, 2003.

[42] J. Kleinberg. Cascading Behavior in Networks: Algorithmic and Economic Issues. In N. Nissan, T. Roughgarden, E. Tardos, and V. Vazirani, editors, *Algorithmic Game Theory*, chapter 24, pages 613–632. Cambridge University Press, New York, NY, 2007.

[43] P. L. Krapivsky, S. Redner, and D. Volovik. Reinforcement-Driven Spread of Innovations and Fads. *Journal of Statistical Mechanics: Theory and Experiment*, 2011(12):P12003–1–P12003–12, 2011.

[44] Chris J. Kuhlman, V. S. Anil Kumar, Madhav V. Marathe, S. S. Ravi, and Daniel J. Rosenkrantz. Finding Critical Nodes for Inhibiting Diffusion of Complex Contagions in Social Networks. In *Proceedings of the European Conference on Machine Learning and Principles and Practice of Knowledge Discovery in Databases (PKDD 2010)*, pages 111–127, 2010.

[45] Chris J. Kuhlman, V. S. Anil Kumar, Madhav V. Marathe, S. S. Ravi, Daniel J. Rosenkrantz, Samarth Swarup, and Gaurav Tuli. A Bithreshold Model of Complex Contagion and its Application to the Spread of Smoking Behavior. In *Proceedings of the Workshop on Social Network Mining and Analysis (SNA-KDD 2011)*, August 2011.

[46] Chris J. Kuhlman, Henning S. Mortveit, David Murrugarra, and V. S. Anil Kumar. Bifurcations in boolean networks. *Automata 2011*, pages 29–46, 2011.

[47] J. Leskovec, L. Adamic, and B. Huberman. The Dynamics of Viral Marketing. *ACM Transactions on the Web*, 1(1), 2007.

[48] Jianghong Li, Margaret R. Weeks, Stephen P. Borgatti, Scott Clair, and Julia Dickson-Gomez. A Social Network Approach to Demonstrate the Diffusion and Change Process of Intervention From Peer Health Advocates to the Drug Using Community. *Substance Use & Misuse*, 47:474–490, 2012.

[49] Vittorio Loreto, Andrea Baronchelli, Animesh Mukherjee, Andrea Puglisi, and Francesca Tria. Statistical physics of language dynamics. *Journal of Statistical Physics*, pages P04006–1–P04006–29, 2011.

[50] Matthew Macauley and Henning S. Mortveit. On enumeration of conjugacy classes of Coxeter elements. *Proceedings of the American Mathematical Society*, 136(12):4157–4165, 2008. math.CO/0711.1140.

[51] Matthew Macauley and Henning S. Mortveit. Cycle equivalence of graph dynamical systems. *Nonlinearity*, 22(2):421–436, 2009. math.DS/0709.0291.

[52] Michael Macy. Chains of Cooperation: Threshold Effects in Collective Action. *American Sociological Review*, 56(6):730–747, 1991.

[53] Thijs Markwat, Erik Kole, and Dick van Dijk. Contagion as a domino effect in global stock markets. *Journal of Banking & Finance*, 33:1996–2012, 2009.

[54] Doug McAdam. Tactical Innovation and the Pace of Insurgency. *American Sociological Review*, 48:735–754, 1983.

[55] J. McAuley and J. Leskovec. Learning to Discover Social Circles in Ego Networks. In *Conference on Neural Information Processing Systems Foundation (NIPS 2012)*, 2012.

[56] Sergey Melnik, Jonathan A. Ward, James P. Gleeson, and Mason A. Porter. Multi-Stage Complex Contagions, 2011. appears as ArXiv arXiv:1111.1596.

[57] H. S. Mortveit and C. M. Reidys. Discrete, sequential dynamical systems. *Discrete Mathematics*, 226:281–295, 2001.

[58] Henning S. Mortveit and Christian M. Reidys. *An Introduction to Sequential Dynamical Systems*. Universitext. Springer Verlag, 2007.

[59] Daniel J. Myers and Pamela E. Oliver. The opposing forces diffusion model: the initiation and repression of collective violence. *Dynamics of Asymmetric Conflict*, 1:164–189, 2008.

[60] Robin L. Nabi. Anger, Fear, Uncertainty, and Attitude: A Test of the Cognitive-Functional Model. *Communication Monographs*, 69:204–216, 2002.

[61] P. Oliver, G. Marwell, and R. Teixeira. A Theory of the Critical Mass. I. Interdependence, Group Heterogeneity, and the Production of Collective Action. *American Journal of Sociology*, 91(3):522–556, 1985.

[62] Pamela E. Oliver and Daniel J. Myers. Networks, Diffusion, and Cycles of Collective Action. In Mario Diani and Doug McAdam, editors, *Comparative Politics: Social Movements and Networks*, pages 173–203. Oxford University Press, 2003.

[63] M. Richardson, R. Agrawal, and P. Domingos. Trust Management for the Semantic Web. In *Second International Semantic Web Conference (ISWC 2003)*, pages 351–368, 2003.

[64] T. Schelling. *Micromotives and Macrobehavior*. W. W. Norton and Company, 1978.

[65] Susan G. Sherman, Donald S. Ganna, Karin E. Tobin, Carl A. Latkin, Christopher Welsh, and Peter Bielenson. The life they save may be mine: Diffusion of overdose prevention information from a city sponsored programme. *International Journal of Drug Policy*, 20:137–142, 2009.

[66] Robert J. Shiller and John Pound. Survey Evidence on Diffusion of Interest and Information Among Investors. *Journal of Economic Behavior and Organization*, 12:47–66, 1989.

[67] D. Siegel. Social networks and collective action. *Americal Journal of Political Science*, 53:122–138, 2009.

[68] D. Stauffer and M. Sahimi. Discrete Simulations of the Dynamics of Spread of Extreme Opinions in a Society. *Physica A*, 364:537–543, 2006.

[69] D. Stauffer and M. Sahimi. Can a Few Fanatics Influence the Opinion of a Large Segment of a Society? *European Phys. J. B*, 57:146–152, 2007.

[70] Jason Tsai, Emma Bowring, Stacy Marsella, and Milind Tambe. Empirical evaluation of computational emotional contagion models. In *Proceedings of the 11th International Conference on Intelligent Virtual Agents (IVA 2011)*, 2011.

[71] Johan Ugander, Lars Backstrom, Cameron Marlow, and Jon Kleinberg. Structural Diversity in Social Contagion. *Proceedings of the National Academy of Sciences (PNAS 2012)*, 109(9):5962–5966, 2012.

[72] Alessandro Vespignani. Modelling dynamical processes in complex socio-technical systems. *Nature Physics*, 8:32–39, 2012.

[73] D. Volovik and S. Redner. Dynamics of Confident Voting. *Journal of Statistical Mechanics: Theory and Experiment*, 2012:P04003–1–P04003–12, 2012.

[74] D. Watts. A Simple Model of Global Cascades on Random Networks. *Proceedings of the National Academy of Sciences (PNAS)*, 99:5766–5771, 2002.

[75] Stan Wilson. Riot anniversary tour surveys progress and economic challenges in Los Angeles. In *Cable New Network (CNN)*. 2012.

[76] Amos Yadlin, Oded Eran, Shimon Stein, Zvi Magen, Yoram Schweitzer, Shlomo Brom, Ephraim Kam, Yeol Guzansky, Benedetta Berti, Gallia Lindenstrauss, David Friedman, Ephraim Asculai, Emily B. Landau, Anat Kurz, Gabi Siboni, and Mark Heller. One year of the arab spring: Global and regional implications. Technical report, The Institute for National Security Studies, 2012.